Drivers of burn severity in the northern Cascade Range, Washington, USA

C. Alina Cansler

A thesis
submitted in partial fulfillment of the
requirements for the degree of

Master of Science

University of Washington

2011

Program Authorized to Offer Degree:
School of Forest Resources

University of Washington
Graduate School

This is to certify that I have examined this copy of a master's thesis by

C. Alina Cansler

and have found that it is complete and satisfactory in all respects,
and that any and all revisions required by the final
examining committee have been made.

Committee Members:

_____
Donald McKenzie

_____
L. Monika Moskal

_____
Dave L. Peterson

Date:_____

TABLE OF CONTENTS

CHAPTER 3: CLIMATE AND TOPOGRAPHICAL INFLUENCES ON BURN SEVERITY IN THE NORTHERN CASCADE RANGE, WASHINGTON, USA

LIST OF FIGURES

LIST OF TABLES

CHAPTER 1: DEVELOPMENT OF THE NORTHERN CASCADE RANGE BURN SEVERITY ATLAS

ABSTRACT

Remotely sensed indices of burn severity are now commonly used by researchers and fire managers to assess post-fire effects, but their relationship to field measurements of burn severity has not been evaluated in all ecosystems. In order to develop a geospatial atlas of burn severity for a 25 year period (1984-2008) in the northern Cascade Range, of Washington, USA, the accuracy of two remotely sensed indices of burn severity, the differenced Normalized Burn Ratio (dNBR) and the Relative differenced Normalized Burn Ratio (RdNBR), was assessed using field data from 639 plots located across four fires.

In the process of comparing the two indexes, two methods of assessing field-based burn severity were compared: the Composite Burn Index (CBI) (Key and Benson 2006) and a newer version of the CBI that weighs severity scores by percentage cover (De Santis and Chuvieco 2009). The new weighted version of the CBI performed worse than the original unweighted version. Three methods of sub-sampling dNBR and RdNBR pixel values at field plot locations were compared, and bilinear interpolation, which uses the four nearest neighbors to determine pixel values, performed best.

Four different statistical models of the relationship between field-based and remotely sensed burn severity were evaluated. The relative strengths of the dNBR and RdNBR indices were evaluated based on the R^2 and the categorization accuracy of each model, and the best-fit model for each index was used to develop classification thresholds for categorical burn-severity images. The dNBR model had a higher R^2 than the RdNBR model ($R^2 = 0.50$ and $R^2 = 0.47$,

respectively), but categorization based on the dNBR model (overall accuracy =59%, Kappa= 0.36) was lower than the RdNBR model (overall accuracy =59%, Kappa= 0.36).

Both dNBR and RdNBR performed similarly and would be suitable for producing classified burn severity images in the northern Cascade Range, but RdNBR performed better and was used as the basis for categorical images of burn severity for all 125 fires in the northern Cascade Range burn-severity atlas. The slightly better performance of RdNBR falls in between the results of Miller and Thode (2007), in which RdNBR performed better than dNBR in the Sierra Nevada, and the results of Soverel et al. (2010), in which dNBR had higher classification accuracy than RdNBR in the Canadian boreal forest and the Canadian Rockies, possibly because variable pre-fire reflectance does not present as much of a challenge in the northern Cascade Range as in the Sierra Nevada.

INTRODUCTION

Fire regimes with variable severity are less tractable to field-based study methods than fire regimes that burn predominantly with low or high severity. Conventional methods of studying fire regimes, such as fire-history studies, use fire scars from individual recorder trees or stand ages to reconstruct fire frequency and landscape fire pattern (Agee 1993). These data sets are temporally deep but require assumptions about how fires burn in mixed-severity areas (Hessburg et al. 2007). Remote sensing of burn severity can augment fire-history studies by describing, quantifying, and analyzing aspects of the fire regime that are otherwise difficult to quantify. Specifically, remote sensing of burn severity can be used (1) examine large and relatively inaccessible areas that pose logistical challenges to field studies, (2) link data gathered in the field with spatially continuous data, and (3) measure and quantify the landscape pattern created by fire. These benefits are particularly strong in mixed-severity fire regimes, in which the variation of the within-fire severity pattern creates and maintains a complex landscape pattern.

I describe the development of a geospatial atlas of burn severity covering 25 years of fire occurrence in the northern Cascade Range, of Washington, USA (Figure 1). Fire plays an important role throughout the Cascade Range in influencing species composition, forest structure, and resource availability (Agee 1993). Fire regimes also vary across the study area along a climatic gradient from the moist maritime climate in the west to a dry interior climate in the Columbia River basin in the east. In the northern Cascade Range, fire regimes are typically mixed or high severity, and severity patterns are spatially complex. The northern Cascade Range is therefore an area where the benefits of using remote sensing to quantify the severity and spatial pattern of fires are particularly strong. Field-based study of the fire regimes is logistically challenging due to the rugged terrain and limited accessibility by roads.

Remotely sensed burn severity indices

To develop the geospatial atlas of burn severity for the northern Cascade Range I evaluated the accuracy of two remotely sensed indices of burn severity, the differenced Normalized Burn Ratio (dNBR) (Key and Benson 2006) and the Relative differenced Normalized Burn Ratio (RdNBR) (Miller and Thode 2007). Both dNBR and RdNBR are based on the NBR, which is calculated as follows:

$$NBR = \frac{(R4 - R7)}{(R4 + R7)}$$

where R4 and R7 are the intensity of per-pixel surface spectral reflectance of Landsat bands 4 (0.76–0.90 μm, near-infrared) and 7 (2.08–2.35 μm, mid-infrared). Band 4 is sensitive to leaf area index and plant productivity, and decreases with higher burn severity. Band 7 is sensitive to the difference between non-photosynthetically active dry vegetation and non-organic surface cover and increases with higher burn severity (Key and Benson 2006). Recent burns have negative NBR values (R4 < R7) whereas nearby unburned vegetated has strongly positive values NBR values (R4 > R7).

The dNBR is the change from pre-fire to post-fire NBR:

$$dNBR = NBR_{prefire} - NBR_{postfire}$$

Increasingly positive values of dNBR indicate increasing burn severity. The Relative differenced Normalized Burn Ratio (RdNBR) was developed by Miller and Thode (2007) in order to improve accuracy of burn-severity assessment in mixed forest and shrubland in California. To account for spatial variation in pre-fire leaf area index the RdNBR normalizes the dNBR by the initial image reflectance:

$$RdNBR = \frac{dNBR - dNBR_{offset}}{\sqrt{|NBR_{prefire}/1000|}}$$

The "$dNBR_{offset}$" value in the equation above corrects the RdNBR images for mismatches in phenologies. The $dNBR_{offset}$ value is the average dNBR value of a nearby area of unburned vegetation (of a type that is similar to the vegetation that did burn). In theory, the $dNBR_{offset} = 0$ when the phenologies of the pre-fire and post-fire image are perfectly matched. By subtracting the $dNBR_{offset}$ from the dNBR, RdNBR values are more consistent across image sets, facilitating the comparison of different fires (Miller and Thode 2007).

Both indices have been used to assess burn severity across a wide variety of ecosystems. The dNBR index was first proposed by López-Garcia and Caselles (1991) to identify burned areas in Spain. Subsequently, it was implemented to map historical burn severity across a number of national parks in the USA (Key 2006). Because both indices use Landsat imagery, which has relatively high resolution (30 m), is readily available, and now free to the public, they have been widely used (Lentile et al. 2006). Both indices were adopted by the Monitoring Trends in Burn Severity project (MTBS), which in 2006 began mapping burn severity of all fires since 1984 that were >404 ha in the western US and >202 ha in the eastern US (Eidenshink et al. 2007). MTBS uses the dNBR index to produce five-class categorical burn severity images, but unclassified dNBR and RdNBR images are also produced for all fires (Eidenshink et al. 2007).

In temperate conifer forests in western North America, dNBR and RdNBR provide more accurate measurements of burn severity than other indices (van Wagtendonk et al. 2004, Brewer et al. 2005, Zhu et al. 2006) and are correlated with field-based measurements of burn severity (Key and Benson 2006, Zhu et al. 2006, Miller and Thode 2007, French et al. 2008, Hudak et al. 2008, Miller et al. 2009, Soverel et al. 2010). When tested in mixed-conifer forests of the Sierra

Nevada with the 224 spectral bands available from the AVIRIS sensor, the bands used in the dNBR calculation were among the four most sensitive bands to changes in surface spectral reflectance after fire (van Wagtendonk et al. 2004). Brewer et al. (2005) compared six approaches of classifying and mapping fire severity in the Rocky Mountains (USA) with Landsat TM data to a "control" method of photo-interpretation and field data, and found the dNBR to be the most accurate and consistent index.

Studies in the Sierra Nevada have shown RdNBR to be a more accurate index of burn severity than dNBR, but the relative accuracy of each index has not been evaluated in all systems. Based on a large field data set from 25 fires in the Sierra Nevada and Klamath mountains of California, Miller et al. (2009) found that RdNBR was better than dNBR when burn-severity thresholds were extrapolated to fires not included in the original calibration. The RdNBR is also considered a more robust index than dNBR when multiple fires are compared, particularly when fires occur in different vegetation types, such as comparing Rocky Mountains and Cascade-Sierra conifer forest types, or comparing heavily vegetated to sparsely vegetated areas (Zhu et al. 2006, Miller and Thode 2007, Miller et al. 2009). In the Sierra Nevada, Miller and Thode (2007) found that in locations where pre-fire vegetation is highly variable, RdNBR has similar or slightly lower classification accuracy than dNBR in the low-severity class, but higher overall accuracy. RdNBR also had greater classification accuracy in the high-severity class; severely burned patches are often of greater interest to scientists and managers than the low-severity class since these areas often have greater change in vegetation species composition, slower vegetation responses, greater susceptibility to invasive species establishment, and higher erosion potential. It is not clear if RdNBR is more accurate than dNBR in all systems. A recent study in the Canadian Rocky Mountains and the western boreal forests of Canada, using field

data from six fires, found higher correlation and better classification accuracy with dNBR (72.2%) than RdNBR (65.2%), concluding that classification based on RdNBR was similar to dNBR when based on pooled data from multiple fires or on individual fire data (Soverel et al. 2010).

Accuracies of dNBR and RdNBR vary among ecosystems. French et al. (2008) reviewed 26 studies that compared the dNBR with field-based measures of burn severity, and found an average accuracy of 73% but that accuracies varied from 50 to 95%. Comparisons of RdNBR to dNBR showed that RdNBR generally has a stronger correlation with field data then dNBR and higher classification accuracy vegetation types with a mix of grass and shrubland or with a mix of forest and non-forest (Zhu et al. 2006). Higher regional correlations between dNBR and field data were also found, but RdNBR produced more consistent regression curves across multiple regions (Zhu et al. 2006). This suggests that the relative merits of each index depend on the system in which they are used and the range of ecological variation among fires included in a given analysis.

Study objectives

The goals of this study are to develop an empirical relationship between the two remotely sensed indices of burn severity and field data, assess the relative merits of dNBR and RdNBR for creating burn-severity classifications, and use the most accurate index to produce empirically based categorical burn-severity images for all fires in the northern Cascade Range burn severity atlas. Based on previous research, categorized images of burn severity based on RdNBR were expected to have higher accuracy than those based on dNBR (Miller and Thode 2007, Miller et al. 2009). The results of this study provide empirical validation of the two burn severity indices in a new region; little empirical validation of the two burn severity indices has been conducted in

the northern Cascade Range compared to other regions of North America. This is a necessary step, because previous research shows that the relationship of the two remotely sensed burn-severity indexes with field-based measurements of burn severity may vary between regions (Zhu et al. 2006), and local field-based burn-severity data are needed to fine-turn burn severity classifications of dNBR or RdNBR (Key and Benson 2006, Lentile et al. 2006). In the process of modelling the relationship between field-based and remotely sensed burn severity, I also evaluated different methods for 1) computing burn-severity from field data, 2) interpolating pixel values of burn severity from the remotely sensed images of burn severity, and 3) modelling the relationship between field-based and remotely sensed burn-severity values.

METHODS

Burn severity atlas development

To create a burn severity atlas for the northern Cascade Range, I used geospatial fire-occurrence layers from federal land-management agencies to identify all 125 wildland fires >10 ha that occurred in the study area from 1984 through 2008. Prescribed fires were not included. The MTBS project has streamlined production of geospatial burn-severity images for fires >121 hectares in the western US (Eidenshink et al. 2007), but until 2008 few fires < 121 hectares were processed. I downloaded burn-severity image packages, which contain geospatial layers of fire perimeters, dNBR images, 5-class burn-severity images derived from the dNBR images, and RdNBR images, from the Monitoring Trends in Burn Severity (MTBS) website (Monitoring Trends in Burn Severity 2008 <http://mtbs.gov/dataquery/individualfiredata.html>) for the 35 fires that had images available. For the 89 fires that were not available online, I identified cloud-free Landsat image pairs with matching phenology to create burn-severity images. Image pairs

were from the year immediately before and immediately after the fire, except in a few cases in which clouds or mismatched phenology required that images from a wider time period be used. I sent spreadsheets of the selected Landsat images and GIS layers of fire polygons or point locations to the US Geological Survey National Center for Earth Resources Observation and Science (EROS). They processed selected scenes according to existing USGS-EROS protocols: image data were geometrically corrected (including terrain correction) and radiometrically corrected, the NBR index was calculated for pre-fire and post-fire images, and these were inspected for co-registration accuracy and corrected if spatial differences were excessive and extensive (> 30 meters), NBR images were differenced for each fire-scene pair to generate the dNBR, the RdNBR was created from the pre-fire NBR and the dNBR images, and fire perimeters were updated based on the burn-severity images, although in many cases little or no change from agency-derived perimeters was necessary. The boundaries of burn-severity images were based on the updated perimeters, because fire perimeters produced by the land management agencies are developed with inconsistent methods and have been found to be of variable accuracy, particularly in complex terrain (Kolden and Weisberg 2007).

I reviewed the entire burn-severity atlas for quality and completeness. Nine fires included in the original request were not found in the LANDSAT images and therefore were not processed. To verify that no fires were missed, I reviewed LANDSAT images from other years at the fire location and aerial photography, available on Google Earth. Six missing fires could be confidently dropped from the data set, and I created dNBR and RdNBR images for the three for which I found evidence. During the development of the dNBR and RdNBR images EROS personnel identified nine additional fires not included in the data request. I included four of these fires in the final data set because they matched a fire location and date in agency-provided GIS

layers, but had been excluded from the initial request because their size was listed as being below the 10 ha minimum fire size cutoff. I also included one other fire because the fire size and location precluded it from being prescribed fire and the location corresponded with a large missing fire from a previous year.

I reviewed the final fire boundaries for accuracy and final image pairs to be sure they came from similar phenological periods. The images pairs were well matched. I corrected additional minor inaccuracies in perimeters and created RdNBR layers for a few fires that had only dNBR images because they were produced under USGS/NPS burn-severity mapping protocols that predated MTBS protocols. The final burn-severity atlas included perimeters, dNBR, and RdNBR images for 125 fires (Appendix I).

Field methods

Field data were collected from four fires in the study area to determine 1) which index of burn severity, dNBR or RdNBR, was more accurate, and 2) which numeric thresholds to use between four burn-severity classes: unchanged, low, moderate, and high. Collection of field validation data on the 2006 Tripod fire and the 2006 Flick Creek fire was coordinated by S. Prichard and K. Kopper, respectively, in conjunction with two other studies focusing on the specific effects of those individual fires. I collected field data on two additional fires that took place in 2008, the Arctic fire and Camel Humps fire. These four fires were well separated across the study area and had different dominant tree species (Table 1).

The primary field-based measurement of burn severity used in this study was the Composite Burn Index (CBI), which combines ecologically significant variables related to burn severity into one numeric site index (Key and Benson 2006). Burn severity is rated from 0 (unchanged) to 3 (high severity) for three to five individual factors, for each stratum present on a

plot (substrate, herbs and low shrubs, tall shrubs, subcanopy trees, and dominant trees); the CBI score is the average score for all factors (Figure 2). The CBI method may not adequately characterize important burn-severity characteristics in some systems, such as boreal forests (Kasischke et al. 2008) and chaparral (Keeley et al. 2008), but in conifer forests in the western U.S. it corresponds well with field-based measurements of plant injury, fuel consumption, and tree mortality (Key and Benson 2006, Miller et al. 2009).

The CBI was used to assess burn severity on all four fires with field plots (Key and Benson 2006). Collection of CBI data followed the rating factors on the standard data sheet (2006) and was overseen by personnel who had experience with fire ecology in the northern Cascade Range. Field plot locations were collected on the Arctic and Camel Humps fires with WASS-enabled Garmin handheld GPS units. All accuracies for these two fires were better than 6 m, and average accuracy was 3.3 m.

In addition to the 251 CBI plots, I used data from 388 "forest plots" from a study of the Tripod fire. These plots included physical measurements of overstory tree canopy scorch, char height, tree mortality, and surface fuel consumption, which were converted into CBI scores. Numerical scores for three different strata (substrate, subcanopy trees, and dominant trees) were calculated from soil scorch, char, and consumption; tree scorch height, tree char height, and tree mortality; and a CBI score for each plot was calculated by averaging the scores for the three strata, just as with five strata for the CBI index (Prichard 2009).

On the two larger fires CBI plot locations were selected via stratified random sampling; plots were stratified by burn severity, forest cover, accessibility, and on the Tripod fire, physiography. In order to maximize the number of plots in the two smaller fires, I created plot locations by transferring the raster grid into a grid of points and a random sample of the points,

spaced at least 60 meters apart, was selected (Figure 3). I entered field data from the Arctic, Camel Humps, and Flick Creek fires twice, and compared the two entries for accuracy. Data from the Tripod fire were entered previously. I calculated the CBI following Key and Benson (2006).

A third method of evaluating burn severity in the field used the same data from the CBI plots, but employed an alternative method of calculating plot CBI. De Santis and Chuvieco (2009) found that at low burn severity, the percentage of cover of vegetation in each stratum, as shown on the CBI data sheet (Figure 2), influenced the reflectance of both bands used in the NBR calculation. They found that by weighting the score for each stratum by the percentage cover of each stratum and then averaging these scores to calculate the plot CBI score, there was a stronger relationship between field-based and remotely sensed burn severity on plots where the burn severity and fraction of cover of the overstory and the understory differ between strata. I compare a "weighted" and the un-weighted version of CBI on the 146 plots for which percentage cover was recorded for each stratum. A weighted version of the CBI could not be calculated on all plots because the percentage cover of each stratum was not consistently recorded on the Flick Creek and Tripod fires; CBI data collection on these fires occurred prior to the introduction of a weighted version of the CBI in the literature.

Determining the best data set

I developed and assessed models in the statistical programming language R (R Core Development Team 2010). My first step was to determine which versions of the field data to use in the final models. In order to determine if both the forest plots and the regular CBI plots could be used in the same model I tested to see if data from the two field methods had the same relationship with the remotely sensed burn-severity indices. This was done with the Tripod fire

data, because that was the only fire on which forest plots were installed. A polynomial model form predicting dNBR or RdNBR as a function of CBI with plot type as a cofactor were produced. A second set of models without plot type as a cofactor were also produced. ANOVA was used to test between the two models to determine if removing the plot type as an interaction term significantly reduced explanatory power. If there was no significant loss of explanatory power, both forest plots and CBI plots could be used simultaneously.

I tested the explanatory power of the weighted and unweighted CBI values to see if there was any advantage to the weighted version of the CBI. Only the subset of 146 plots for which weighted values could be calculated was used in this test. I also evaluated three methods of interpolating the values of dNBR and RdNBR images that corresponded with CBI plot locations. All CBI plots (i.e. the un-weighted CBI values) and all forest plots were used. The three sub-sampling methods, all available in ArcGIS, were nearest neighbor, bilinear interpolation (weighted value based on the four nearest neighbors), and cubic convolution (weighted value using the 8 nearest neighbors).

The highest correlations between dNBR and RdNBR with CBI have been found when non-linear model forms were used (French et al. 2008). Originally a second degree polynomial model (van Wagtendonk et al. 2004, Key 2006) was used to model burn severity, but those studies predicted CBI as a function of dNBR, producing a model with a peak near dNBR = 750, with decreasing values of CBI predicted with increasing dNBR values above that. Subsequently, polynomial model forms have been used as I used them here, to predict dNBR or RdNBR as a function of CBI, which within the scope of the model, predicts a continued increase in dNBR or RdNBR values with CBI (Soverel et al. 2010, Soverel et al. in press). Various other non-linear models have been used (Zhu et al. 2006, Miller and Thode 2007, Hall et al. 2008, Miller et al.

2009). For this study, three model forms were then assessed to model dNBR or RdNBR (x) as a function of CBI (y):

$$\text{Model 1:} \quad y = a + bx + cx^2$$

$$\text{Model 2:} \quad y = a + be^{cx}$$

$$\text{Model 3:} \quad y = a + bx^c$$

These models were tested using the final data set (bilinear interpolation, unweighted CBI values along with CBI values based on forest plots). Models were assessed based on overall model significance, R^2, visual assessment of model fit, plots of residuals, the significance of model coefficients, and the classification accuracies of each model (described below).

Comparison of burn severity indices

Using the final data set (bilinear interpolation, unweighted CBI values, and CBI values based on forest plots), and the best-fit model (Model 3), dNBR and RdNBR were compared based on R^2 and classification accuracy. To determine the different burn-severity classes, CBI threshold values were used to predict dNBR and RdNBR threshold values. The thresholds between four severity classes—unchanged, low, moderate, and high—were based on the same CBI values that were used by Miller and Thode (2007) and Soverel et al. (2010) (Table 2) to facilitate comparisons of classification thresholds and burn-severity levels between different study areas. CBI threshold values were the same, but dNBR and RdNBR values at the thresholds between the classes differed from these other studies because they were predicted using the model parameters from local field data, resulting in an empirically based classification scheme for the northern Cascade Range.

The classification accuracy was calculated from a confusion matrix showing the classification of field plots (columns) and remotely sensed pixels (rows) of each model

(Lillesand et al. 2007). Confusion matrices were used to compute (1) the producer's accuracy (percentage of CBI plots classified correctly in each class), (2) the user's accuracy (percentage of pixel values classified correctly in each class), (3) the overall accuracy (percentage of correct classifications across all classes) (Lillesand et al. 2007), and the kappa statistic ($\hat{k}$), a measure of overall accuracy compared to random classification, which was calculated following Lillesand et al. (2007):

$$\hat{k} = \frac{N\sum_{i=1}^{r} x_{ii} - \sum_{i=1}^{r}(x_{i+} \cdot x_{+i})}{N^2 - \sum_{i=1}^{r}(x_{i+} \cdot x_{+i})}$$

where:
r = number of rows in the confusion matrix
x_{ii} = number of observation in row i and column i
x_{i+} = total of observations in row i
x_{+i} = total of observations in column i
N = total number of observations in the matrix

Kappa values ≤ 0 indicate that a classification is no better than chance. Positive kappa values (0,1) can be interpreted as the proportional improvement of the actual classification over a random classification.

RESULTS

Determining the best data set

Results for ANOVA showed no significant difference between models with and without plot type as a cofactor (P = 0.787 for dNBR model, P = 0.569 for RdNBR model). Therefore, CBI values from both the forest plots and regular CBI plots were used in final validation models. Weighted CBI values showed no improvement over the original unweighted CBI values (Figure 4). As mentioned above, weighted CBI values could not be calculated on all plots. Therefore, the full plot data set of un-weighted CBI values was used in all subsequent models. R^2 values for

different pixel subsample methods were similar, but models based on bilinear interpolation consistently had highest R^2, and models based on cubic convolution had the lowest R^2 (Table 3). Therefore, DNBR and RdNBR values based on bilinear interpolation were used as response variables. The similarity between the three different pixel subsample methods was probably due to both reflectance from neighboring pixels and spatial auto-correlation of burn severity at small scales.

Model 1, a quadratic form, had better fit and greater explanatory power than a linear model. Model 2 (the models used by Miller and Thode 2007) and Model 3 (the model I developed) had better overall model fit than the polynomial model, and better classification accuracy. Both had similar shape and similar R^2, Model 3 explained slightly less variance than Model 2 (Figures 5 and 6), but the individual parameter terms of Model 3 were all significant, whereas the parameters of Model 2 were not all significant. The parameters of Model 3 were also more interpretable and reflected an expected asymptote as the maximum CBI value of 3 was reached. Lastly, Model 3 had the best classification accuracy of the 3 models (Table 5). Therefore I used Model 3, instead of Miller and Thode's model form (Model 2) to evaluate the difference between the two remotely sensed burn severity indices.

Comparison of burn severity indices

The final models for dNBR and RdNBR explained similar amounts of variance. The dNBR model had a slightly higher R^2 than the RdNBR model ($R^2 = 0.50$ for dNBR and $R^2 = 0.47$ RdNBR, Figure 6). Conversely, RdNBR had better classification accuracy then dNBR. The dNBR model had lower overall accuracy and kappa values than RdNBR (Tables 4 and 5). RdNBR had higher producer's accuracy in all classes but the unchanged class, and higher user's accuracy in all classes but the high class. Because the primary purpose of this analysis was to

produce classified burn severity images, I considered RdNBR, with its higher classification accuracy, to be the best index for that purpose.

DISCUSSION

Unweighted vs. weighted CBI values

The lack of improvement showed by the weighted version of the CBI compared to the un-weighted version was surprising. The weighted version of CBI proposed by De Santis and Chevieco (2009) is consistent with remote sensing theory and is intuitive, but there are a number of explanations for its lower accuracy. The weighted CBI method may be less accurate because it undervalues the influence of the overstory on the plot CBI score. The dominant tree strata may have a stronger influence on reflectance than lower strata: plots with a higher pre-fire tree cover can have a stronger correlation between field-based and remotely sensed burn severity (Zhu et al. 2006, Miller et al. 2009). In my study, substrate, herbs and low shrubs, and tall shrubs often had a greater percentage cover than the intermediate and dominant trees (Table 6). Therefore, the weighted version of the CBI decreased the effect of the overstory and intermediate strata on the CBI score of the plot because. To account for the greater influence of the dominant tree strata on plot reflectance Soverel et al. (2010) weighted the dominant tree stratum twice as strongly as the other strata. An alternative explanation for the lower correlation of weighted CBI is that plot strata all burn with similar severities; therefore differences between the two indices were inconsequential, reflecting only random variation in the data set. Consistently recording percentage cover by stratum on plots in the future will improve evaluation of the different methods to calculate CBI.

Statistical model form

The relationship between field-based and remotely sensed measurements of burn severity was best fit by a non-linear model, which supports the findings of other recent studies (Zhu et al. 2006, Miller and Thode 2007, Hall et al. 2008, Miller et al. 2009, Soverel et al. 2010, Soverel et al. in press). Of the three models tested Model 3 performed best: it had the higher R^2 and best classification accuracy for both dNBR and RdNBR. Evaluating a variety of non-linear models, (Hall et al. 2008) identified a single non-linear model for all future classifications in temperate conifer forests of western North America. This would streamline the process of determining severity-class thresholds and make future classifications more comparable.

Production of categorical burn severity images

The final model that used RdNBR had better classification accuracy than the model based on dNBR. Also, breakpoints based on RdNBR are generally more robust to extrapolation to fires not in the original classification (Miller and Thode 2007, Miller et al. 2009). Therefore, I used RdNBR, and the class thresholds based on the RdNBR model, to classify burn-severity images of fires in the northern Cascade Range burn-severity atlas (Figure 7). Nevertheless, classification accuracies for dNBR and RdNBR are within the range found by similar studies in California and Canada (Miller and Thode 2007, Miller et al. 2009, Soverel et al. 2010) (Table 7), and therefore both indices should be considered suitable for producing categorical burn-severity images in the northern Cascade Range.

Comparison of the results of this study to others shows that burn-severity class thresholds vary between regions. The RdNBR class thresholds are higher than those found by Miller and Thode (2007) and those based on a single fire used to classify burn-severity images in the Gila National Forest, New Mexico (Holden et al. 2009) (Table 8). Thresholds using the same model

with dNBR data were higher than dNBR thresholds from the Sierra Nevada presented in Miller and Thode (2007) but lower than those developed for Canada (Soverel et al. in press), and most similar to the dNBR thresholds of Key and Benson (2006) that were developed primarily from field data gathered in Glacier National Park (Table 8). The slightly better performance of RdNBR falls in between the results of Miller and Thode (2007), in which RdNBR performed better than dNBR in the Sierra Nevada, and the results of Soverel et al. (2010), in which dNBR had higher classification accuracy than RdNBR in the Canadian boreal forest and the Canadian Rockies. One possible explanation for similarity between dNBR and RdNBR in the northern Cascade Range is that variable pre-fire reflectance does not present as much of a challenge in the northern Cascade Range as in the Sierra Nevada.

Future research needs

This study provided an empirical basis for producing categorical burn severity images in the northern Cascade Range, but more research is warranted. Additional research needs for the Cascade Range include installing plots on more fires, and developing classification thresholds based on a random training data set and then using an explicit test of the extrapolation of dNBR and RdNBR thresholds to fires not included in the original training data (Miller et al. 2009). The collection of additional field data to validate burn severity should emphasize fires in vegetation types not covered in this study. The collection of CBI data on more fires, covering locations with a wider variety of dominant species, vegetation structure, and soil types would refine the placement of burn-severity classification thresholds in this region. In particular, data from a greater number of fires where pre-fire reflectance is variable, such as ponderosa pine woodlands, may elucidate larger differences between the two remotely sensed burn-severity indices in the northern Cascade Range.

REFERENCES

Agee, J. K. 1993. Fire ecology of Pacific Northwest forests. 1 edition. Island Press, Washington, D.C.

Brewer, C. K., J. C. Winne, R. L. Redmond, D. W. Opitz, and M. V. Mangrich. 2005. Classifying and mapping wildfire severity: A comparison of methods. Photogrammetric Engineering and Remote Sensing **71**:1311-1320.

De Santis, A. and E. Chuvieco. 2009. GeoCBI: A modified version of the Composite Burn Index for the initial assessment of the short-term burn severity from remotely sensed data. Remote Sensing of Environment **113**:554-562.

Eidenshink, J., B. Schwind, K. Brewer, Z.-L. Zhu1, B. Quayle, and S. Howard. 2007. A Project for Monitoring Trends in Burn Severity. Fire Ecology Special Issue **3**:3-21.

French, N. H. F., E. S. Kasischke, R. J. Hall, K. A. Murphy, D. L. Verbyla, E. E. Hoy, and J. L. Allen. 2008. Using Landsat data to assess fire and burn severity in the North American boreal forest region: an overview and summary of results. International Journal of Wildland Fire **17**:443-462.

Hall, R. J., J. T. Freeburn, W. J. de Groot, J. M. Pritchard, T. J. Lynham, and R. Landry. 2008. Remote sensing of burn severity: experience from western Canada boreal fires. International Journal of Wildland Fire **17**:476-489.

Hessburg, P. F., R. B. Salter, and K. M. James. 2007. Re-examining fire severity relations in pre-management era mixed conifer forests: inferences from landscape patterns of forest structure. Landscape Ecology **22**:5-24.

Holden, Z. A., P. Morgan, and J. S. Evans. 2009. A predictive model of burn severity based on 20-year satellite-inferred burn severity data in a large southwestern US wilderness area. Forest Ecology and Management **258**:2399-2406.

Hudak, A. T., P. Morgan, M. J. Bobbitt, A. M. S. Smith, S. A. Lewis, L. B. Lentile, P. R. Robichaud, J. T. Clark, and R. A. McKinley. 2008. The relationship of multispectral satellite imagery to immediate fire effects. Journal of Fire Ecology **3**:64-90.

Kasischke, E. S., M. R. Turetsky, R. D. Ottmar, N. H. F. French, E. E. Hoy, and E. S. Kane. 2008. Evaluation of the composite burn index for assessing fire severity in Alaskan black spruce forests. International Journal of Wildland Fire **17**:515-526.

Keeley, J. E., T. Brennan, and A. H. Pfaff. 2008. Fire severity and ecosystem responses following crown fires in California shrublands. Ecological Applications **18**:1530-1546.

Key, C. H. 2006. Ecological and sampling constraints on defining landscape fire severity. Fire Ecology **2**:34-59.

Key, C. H. and N. C. Benson. 2006. Landscape Assessment (LA). In Pages LA-1-55 *in* D. C. Lutes, R. E. Keane, J. F. Caratti, C. H. Key, N. C. Benson, S. Sutherland, and G. L.J., editors. FIREMON: Fire Effects Monitoring and Inventory System. USDA Forest Service, Rocky Mountain Research Station, Fort Collins, CO.

Kolden, C. A. and P. J. Weisberg. 2007. Assessing accuracy of manually-mapped wildfire perimeters in topographically dissected areas. Fire Ecology Special Issue **3**:22-31.

Lentile, L. B., Z. A. Holden, A. M. S. Smith, M. J. Falkowski, A. T. Hudak, P. Morgan, S. A. Lewis, P. E. Gessler, and N. C. Benson. 2006. Remote sensing techniques to assess active fire characteristics and post-fire effects. International Journal of Wildland Fire **15**:319-345.

Lillesand, T. M., R. W. Kiefer, and J. W. Chipman. 2007. Remote sensing and image interpretation. 6th edition. John Wiley & Sons, Hoboken, NJ.

López-Garcia, M. J. L. and V. Caselles. 1991. Mapping burns and natural reforestation using Thematic Mapper data. Geocarto International **1**:31-37.

Miller, J. D., E. E. Knapp, C. H. Key, C. N. Skinner, C. J. Isbell, R. M. Creasy, and J. W. Sherlock. 2009. Calibration and validation of the relative differenced Normalized Burn Ratio (RdNBR) to three measures of fire severity in the Sierra Nevada and Klamath Mountains, California, USA. Remote Sensing of Environment **113**:645-656.

Miller, J. D. and A. E. Thode. 2007. Quantifying burn severity in a heterogeneous landscape with a relative version of the delta Normalized Burn Ratio (dNBR). Remote Sensing of Environment **109**:66-80.

Monitoring Trends in Burn Severity. 2008. Individual Fire-Level Geospatial Data - Monitoring Trends in Burn Severity (MTBS)<http://mtbs.gov/dataquery/individualfiredata.html> accessed: 3-01-2008.

Prichard, S. J. 2009. Unpublished data.

R Development Core Team. 2010. R: A language and environment for statistical computing. R Foundation for Statistical Computing, Vienna, Austria. ISBN 3-900051-07-0, URL http://www.R-project.org/.

Soverel, N. O., N. C. Coops, D. D. B. Perrakis, L. D. Daniels, and S. E. Gergel. in press. The transferability of a dNBR derived model to predict burn severity across ten wildland fires in western Canada International Journal of Wildland Fire.

Soverel, N. O., D. D. B. Perrakis, and N. C. Coops. 2010. Estimating burn severity from Landsat dNBR and RdNBR indices across western Canada. Remote Sensing of Environment **114**:1896-1909.

van Wagtendonk, J. W., R. R. Root, and C. H. Key. 2004. Comparison of AVIRIS and Landsat ETM+ detection capabilities for burn severity. Remote Sensing of Environment **92**:397-408.

Zhu, Z., C. H. Key, D. Ohlen, and N. C. Benson. 2006. Evaluate sensitivities of burn severity mapping algorithms for different ecosystems and fire histories in the United States. Final Report to the Joint Fire Science Program. Project: JFSP 01-1-4-12.

TABLES

Table 1. Field validation plots were located on four fires in different vegetation types across the study area.

Fire Name	Dominant Tree Species	Ecological Subsection*	Fire Year	Year of CBI Data Collection	Number of CBI Plots	Number of Veg. Plots	Fire Size (ha)
Flick Creek	Douglas fir, ponderosa pine, grand fir, alpine larch	Wenatchee-Chelan Highlands	2006	2007	100		2856
Tripod	Ponderosa pine/Douglas-fir, lodgepole pine, western larch, subalpine fir, Engelmann spruce	Pasayten-Sawtooth Highlands	2006	2007		388	70753
				2008	43		
				2009	56		
Arctic	Subalpine fir, mountain hemlock, silver fir	North Cascades Highland Forests	2008	2009	24		35
Camel Humps	Subalpine fir, Engelmann spruce	Pasayten-Sawtooth Highlands	2008	2009	28		53
Total Plots = 639					251	388	

* Ecological subsections are described in Chapter 2, and are listed here for reference.

Table 2. CBI severity category definitions*

Severity category	CBI threshold	Definitions
Unchanged	0-0.1	One year after the fire the area was indistinguishable from pre-fire conditions. This does not always indicate the area did not burn.
Low	0-1.25	Areas of surface fire occurred with little change in cover and little mortality of the structurally dominant vegetation
Moderate	1.26-2.25	The area exhibits a mixture of effects ranging from unchanged to high
High	2.25-3.0	Vegetation has high to 100% mortality

*Table follows definitions and severity categories given by Miller and Thode (2007).

Table 3. Comparison of different pixel sub-sampling methods. R^2 are for a polynomial model where dNBR or RdNBR is predicted from CBI.

Burn severity index	Pixel sub-sampling method	R^2
dNBR	nearest neighbor	0.47
dNBR	bilinear interpolation	0.50
dNBR	cubic convolution	0.49
RdNBR	nearest neighbor	0.45
RdNBR	bilinear interpolation	0.47
RdNBR	cubic convolution	0.46

Table 4 Confusion matrix for field data (columns) and dNBR values at field plot locations (rows) for Models 1-3.

	Overall Accuracy =	60.3		Kappa =	0.376	
	Unchanged	Low	Moderate	High	Total	User's Accuracy
Unchanged	23	26	9	1	59	39.0
Low	1	34	74	3	112	30.4
Moderate	1	43	225	40	309	72.8
High	0	4	52	103	159	64.8
Total	25	107	360	147	639	
Producer's Accuracy	92.0	31.8	62.5	70.1		

Model 2

	Overall Accuracy =	59.0		Kappa =	0.366	
	Unchanged	Low	Moderate	High	Total	User's Accuracy
Unchanged	24	30	11	1	66	36.4
Low	0	32	73	3	108	29.6
Moderate	1	40	216	38	295	73.2
High	0	5	60	105	170	61.8
Total	25	107	360	147	639	
Producer's Accuracy	96.0	29.9	60.0	71.4		

Model 3

	Overall Accuracy =	59.0		Kappa =	0.361	
	Unchanged	Low	Moderate	High	Total	User's Accuracy
Unchanged	24	34	16	1	75	32.0
Low	0	26	64	3	93	28.0
Moderate	1	42	224	40	307	73.0
High	0	5	56	103	164	62.8
Total	25	107	360	147	639	
Producer's Accuracy	96.0	24.3	62.2	70.1		

Table 5. Confusion matrix for field data (columns) and RdNBR values at field plot locations (rows) for Models 1-3.

Model 1

	Overall Accuracy = 0.61			Kappa = 0.391		
	Unchanged	Low	Moderate	High	Total	User's Accuracy
Unchanged	21	21	10	1	53	39.6
Low	4	36	67	5	112	32.1
Moderate	0	41	226	34	301	75.1
High	0	9	57	107	173	61.8
Total	25	107	360	147	639	
Producer's Accuracy	84.0	33.6	62.8	72.8		

Model 2

	Overall Accuracy = 0.612			Kappa = 0.395		
	Unchanged	Low	Moderate	High	Total	User's Accuracy
Unchanged	22	23	14	2	61	36.1
Low	3	34	60	4	101	33.7
Moderate	0	41	227	33	301	75.4
High	0	9	59	108	176	61.4
Total	25	107	360	147	639	
Producer's Accuracy	88.0	31.8	63.1	73.5		

Model 3

	Overall Accuracy = 0.617			Kappa = 0.398		
	Unchanged	Low	Moderate	High	Total	User's Accuracy
Unchanged	22	24	14	2	62	35.5
Low	3	32	56	4	95	33.7
Moderate	0	42	233	34	309	75.4
High	0	9	57	107	173	61.8
Total	25	107	360	147	639	
Producer's Accuracy	88.0	29.9	64.7	72.8		

Table 6. Proportional cover of each stratum assessed to calculated the weighted CBI

	Mean proportion of cover of each stratum					
Fire	Substrate	Herbs and low shrubs	Tall shrubs	Subcanopy trees	dominant trees	Number of plots
Arctic	1.00	0.72	0.19	0.29	0.11	24
Camel Humps	1.00	0.63	0.16	0.09	0.06	28
Flick Creek	1.00	0.23	0.05	0.13	0.44	39
Tripod	1.00	0.53	0.11	0.27	0.17	55
All fires	1.00	0.50	0.12	0.20	0.21	146

Table 7. Classification results for the northern Cascade Range compared to classification accuracy of other studies the used RdNBR

Study	Location	Number of plots	Number of fires	Overall accuracy	Kappa	R^2
This study	Northern Cascade Range, WA, USA	639	4	61.7	0.398	0.47
Miller and Thode (2007)	Sierra Nevada, CA, US	741	14	59.8	0.411	0.61
Miller et al. (2009)	Sierra Nevada and Klamath, CA, US	295	25		0.461	0.68
Soverel et al. (2010)	Canadian Rockies	110	3	68.2	0.52	0.71
Soverel et al. (2010)	Western boreal forests	125	3	60.3	0.37	0.70

Table 8. Classification results for the northern Cascade Range compared to class thresholds of other studies for both RdNBR and dNBR

Study	CBI class thresholds				Remotely sensed class thresholds		
	unchanged-low	low-moderate	moderate-high	Index	unchanged-low	low-moderate	moderate-high
This study	0.1	1.25	2.25	RdNBR	189	372	703
Miller and Thode (2007)	0.1	1.25	2.25	RdNBR	69	316	641
Holden et al. (2009)	NA	NA	2.2	RdNBR	NA	NA	665
This study	0.1	1.25	2.25	dNBR	106	218	456
Key and Benson (2006)				dNBR	100	270	440*
Miller and Thode (2007)	0.1	1.25	2.25	dNBR	41	177	367
Soverel et al. *(in press)*	NA	1.25	2.25	dNBR	NA	311	568

* Key and Benson (2006) actually used a 7 class system. This is the thresholds between the moderate-low and moderate-high severity class. The threshold for the highest severity class is 600.

FIGURES

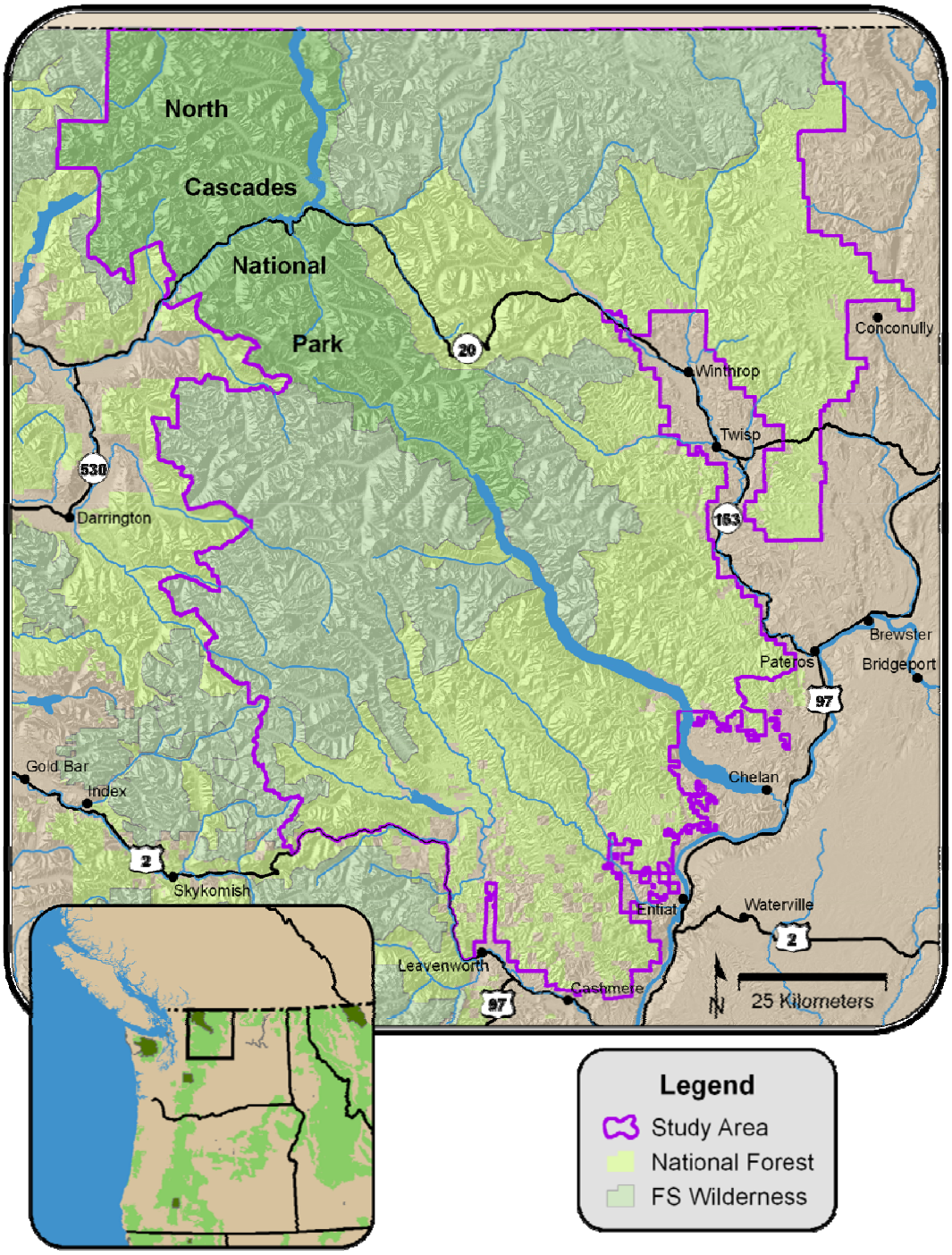

Figure 1. The study area extends from the western boundaries of North Cascades National Park and Glacier Peak Wilderness, to the eastern boundaries of Okanogan-Wenatchee National Forest. The US-Canadian border is the northern boundary, and Washington State Highway 2 is the southern boundary.

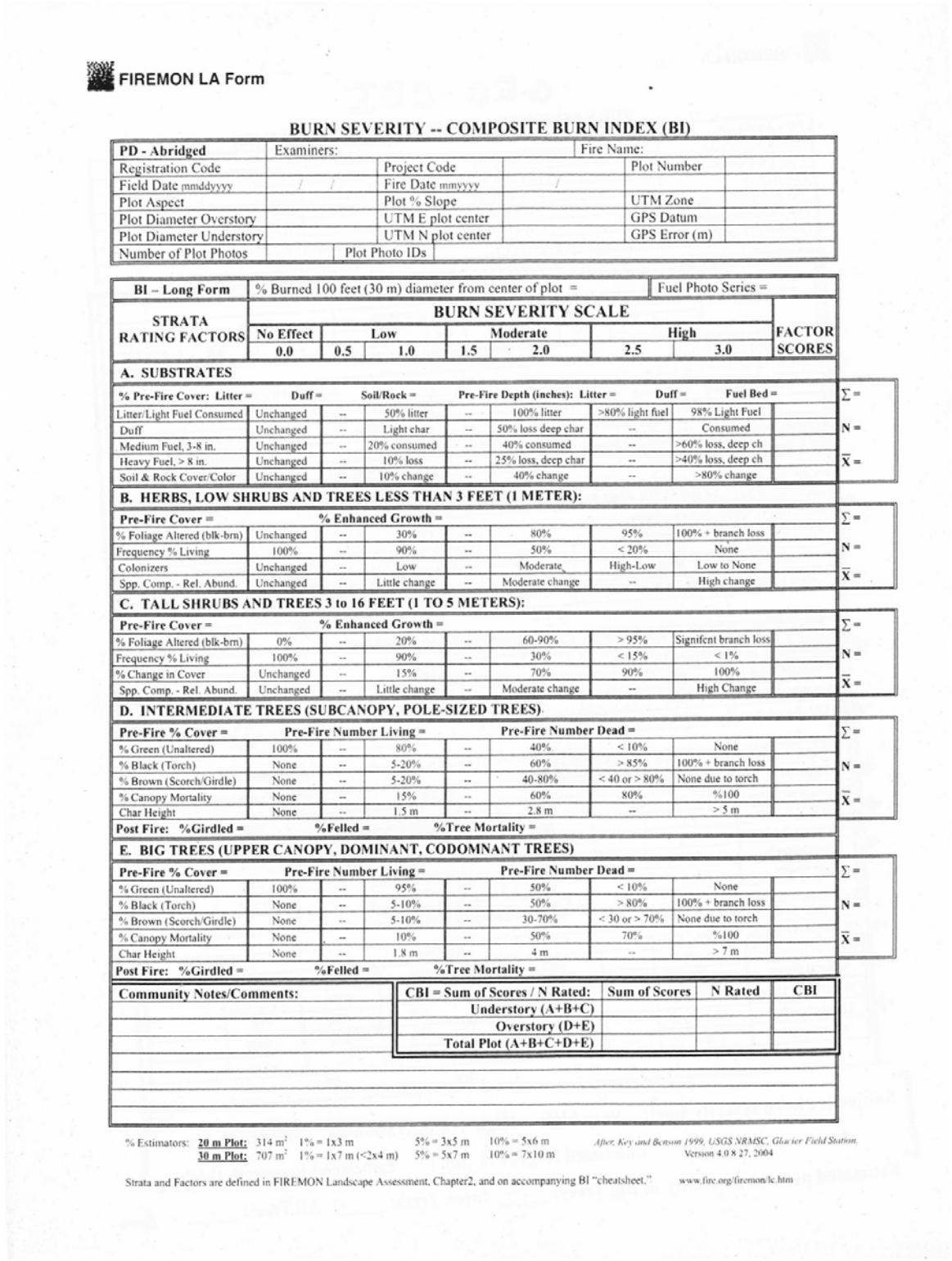

FIREMON LA Form

BURN SEVERITY -- COMPOSITE BURN INDEX (BI)

PD - Abridged	Examiners:		Fire Name:	
Registration Code		Project Code	Plot Number	
Field Date mmddyyyy	/ /	Fire Date mmyyyy	/	
Plot Aspect		Plot % Slope	UTM Zone	
Plot Diameter Overstory		UTM E plot center	GPS Datum	
Plot Diameter Understory		UTM N plot center	GPS Error (m)	
Number of Plot Photos		Plot Photo IDs		

BI – Long Form	% Burned 100 feet (30 m) diameter from center of plot =	Fuel Photo Series =

STRATA RATING FACTORS	BURN SEVERITY SCALE							FACTOR SCORES
	No Effect	Low		Moderate		High		
	0.0	0.5	1.0	1.5	2.0	2.5	3.0	
A. SUBSTRATES								
% Pre-Fire Cover: Litter =	**Duff =**		**Soil/Rock =**	**Pre-Fire Depth (inches): Litter =**		**Duff =**	**Fuel Bed =**	Σ =
Litter/Light Fuel Consumed	Unchanged	--	50% litter	--	100% litter	>80% light fuel	98% Light Fuel	
Duff	Unchanged	--	Light char	--	50% loss deep char	--	Consumed	N =
Medium Fuel, 3-8 in.	Unchanged	--	20% consumed	--	40% consumed	--	>60% loss, deep ch	
Heavy Fuel, > 8 in.	Unchanged	--	10% loss	--	25% loss, deep char	--	>40% loss, deep ch	$\bar{X}$ =
Soil & Rock Cover/Color	Unchanged	--	10% change	--	40% change	--	>80% change	
B. HERBS, LOW SHRUBS AND TREES LESS THAN 3 FEET (1 METER):								
Pre-Fire Cover =			**% Enhanced Growth =**					Σ =
% Foliage Altered (blk-brn)	Unchanged	--	30%	--	80%	95%	100% + branch loss	
Frequency % Living	100%	--	90%	--	50%	< 20%	None	N =
Colonizers	Unchanged	--	Low	--	Moderate	High-Low	Low to None	
Spp. Comp. - Rel. Abund.	Unchanged	--	Little change	--	Moderate change	--	High change	$\bar{X}$ =
C. TALL SHRUBS AND TREES 3 to 16 FEET (1 TO 5 METERS):								
Pre-Fire Cover =			**% Enhanced Growth =**					Σ =
% Foliage Altered (blk-brn)	0%	--	20%	--	60-90%	> 95%	Signifcnt branch loss	
Frequency % Living	100%	--	90%	--	30%	< 15%	< 1%	N =
% Change in Cover	Unchanged	--	15%	--	70%	90%	100%	
Spp. Comp. - Rel. Abund.	Unchanged	--	Little change	--	Moderate change	--	High Change	$\bar{X}$ =
D. INTERMEDIATE TREES (SUBCANOPY, POLE-SIZED TREES).								
Pre-Fire % Cover =	**Pre-Fire Number Living =**				**Pre-Fire Number Dead =**			Σ =
% Green (Unaltered)	100%	--	80%	--	40%	< 10%	None	
% Black (Torch)	None	--	5-20%	--	60%	> 85%	100% + branch loss	N =
% Brown (Scorch/Girdle)	None	--	5-20%	--	40-80%	< 40 or > 80%	None due to torch	
% Canopy Mortality	None	--	15%	--	60%	80%	%100	$\bar{X}$ =
Char Height	None	--	1.5 m	--	2.8 m	--	> 5 m	
Post Fire: %Girdled =			**%Felled =**		**%Tree Mortality =**			
E. BIG TREES (UPPER CANOPY, DOMINANT, CODOMNANT TREES)								
Pre-Fire % Cover =	**Pre-Fire Number Living =**				**Pre-Fire Number Dead =**			Σ =
% Green (Unaltered)	100%	--	95%	--	50%	< 10%	None	
% Black (Torch)	None	--	5-10%	--	50%	> 80%	100% + branch loss	N =
% Brown (Scorch/Girdle)	None	--	5-10%	--	30-70%	< 30 or > 70%	None due to torch	
% Canopy Mortality	None	--	10%	--	50%	70%	%100	$\bar{X}$ =
Char Height	None	--	1.8 m	--	4 m	--	> 7 m	
Post Fire: %Girdled =			**%Felled =**		**%Tree Mortality =**			

Community Notes/Comments:	CBI = Sum of Scores / N Rated:	Sum of Scores	N Rated	CBI
	Understory (A+B+C)			
	Overstory (D+E)			
	Total Plot (A+B+C+D+E)			

% Estimators: **20 m Plot:** 314 m^2 1% = 1x3 m 5% = 3x5 m 10% = 5x6 m
30 m Plot: 707 m^2 1% = 1x7 m (<2x4 m) 5% = 5x7 m 10% = 7x10 m

After, Key and Benson 1999, USGS NRMSC, Glacier Field Station.
Version 4.0 8 27, 2004

Strata and Factors are defined in FIREMON Landscape Assessment, Chapter2, and on accompanying BI "cheatsheet." www.fire.org/firemon/lc.htm

Figure 2: CBI data sheet.

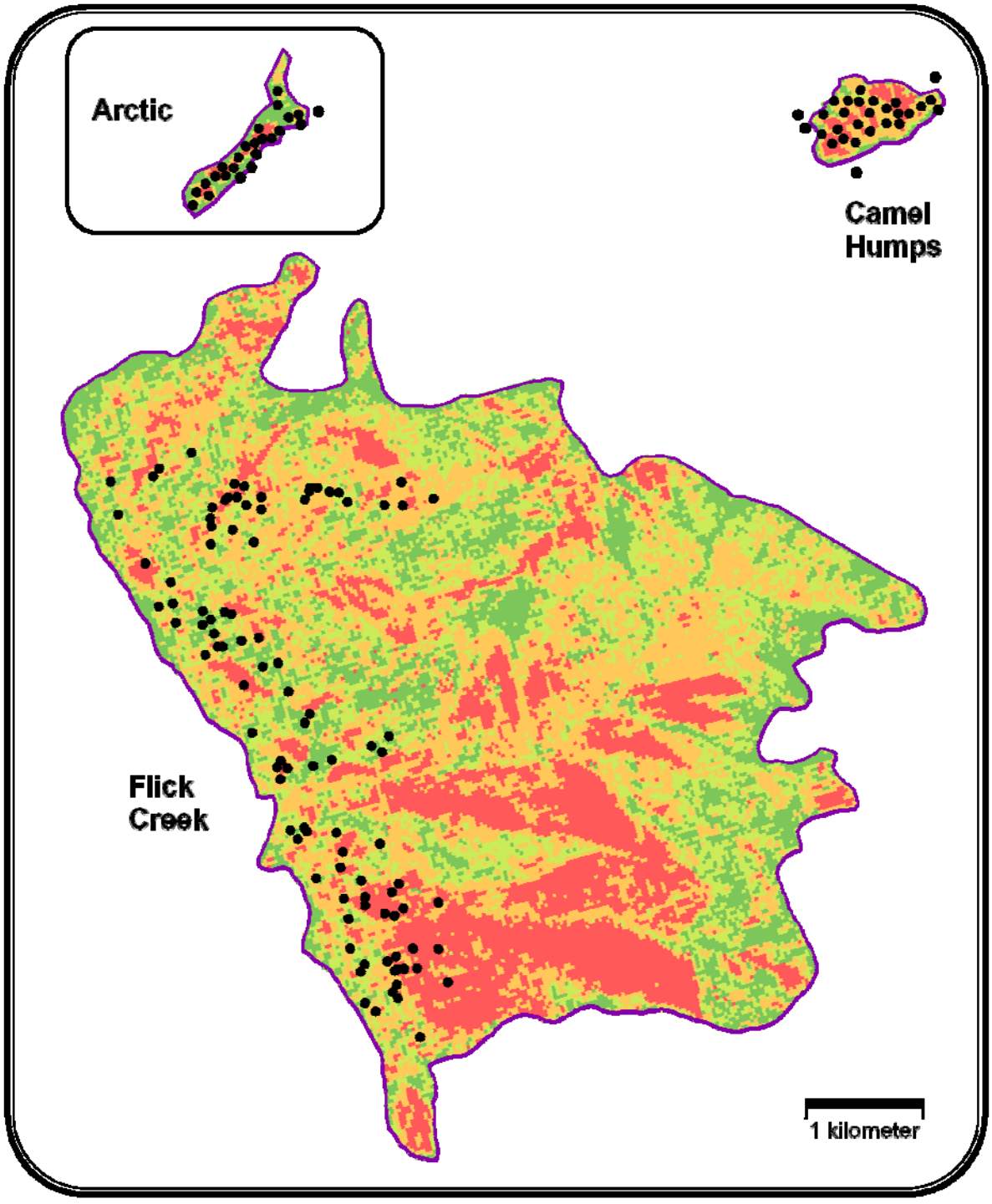

Figure 3. Plot locations in the 2006 Arctic and Camel Humps fires, and the 2006 Flick Creek and Tripod fires. In the Tripod fire, CBI plots are more dispersed across the fire and forest plots were arranged in networks. Despite their seemingly close proximity forest plots were located in different pixels. Some plots on the Arctic and Camel Humps fires were located outside fire perimeters in order to sample unburned areas. Plots were located on the low elevation western portion of the Flick Creek fire, because high elevation eastern portions were inaccessible or sparsely vegetated.

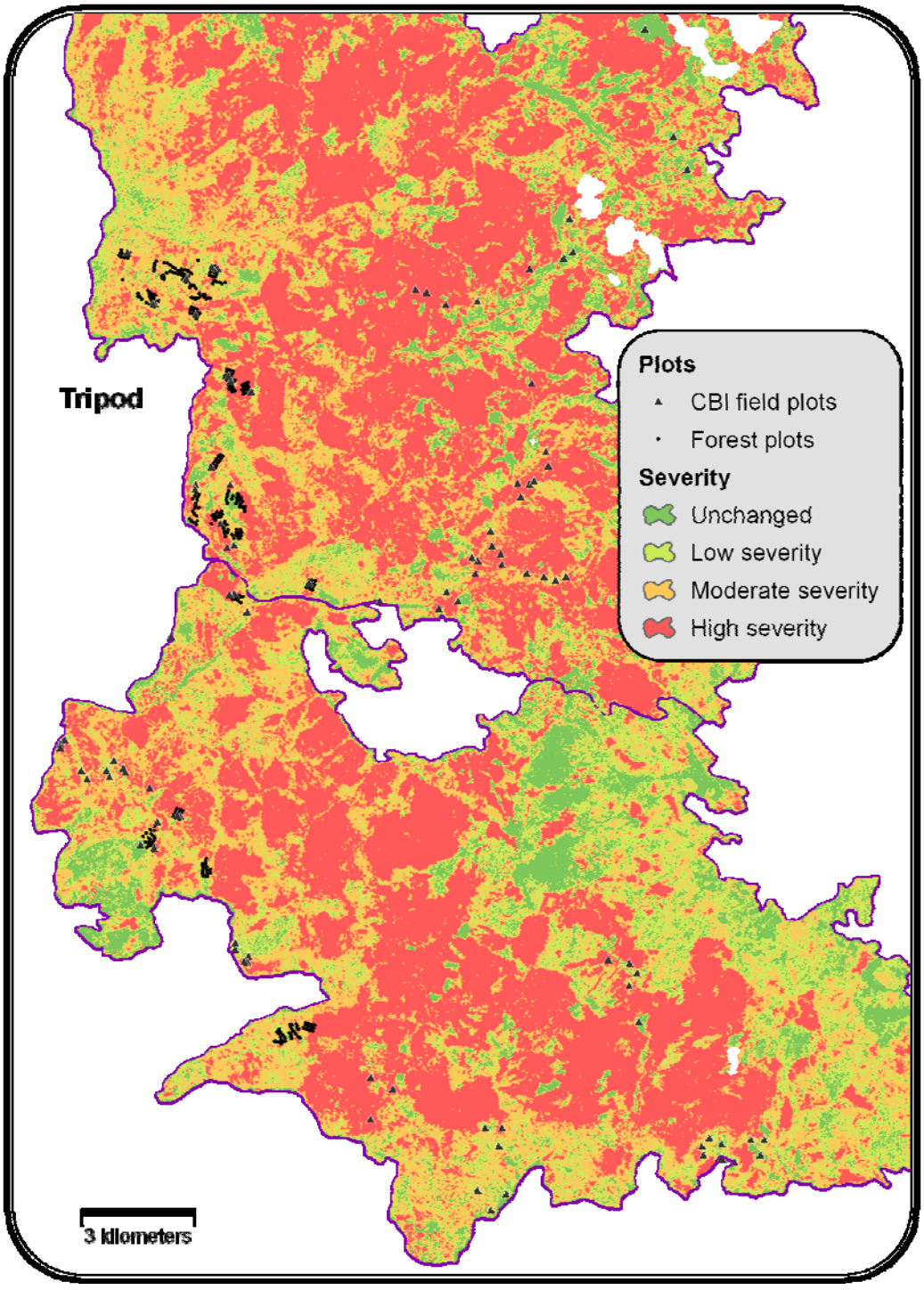

Figure 3 (extended).

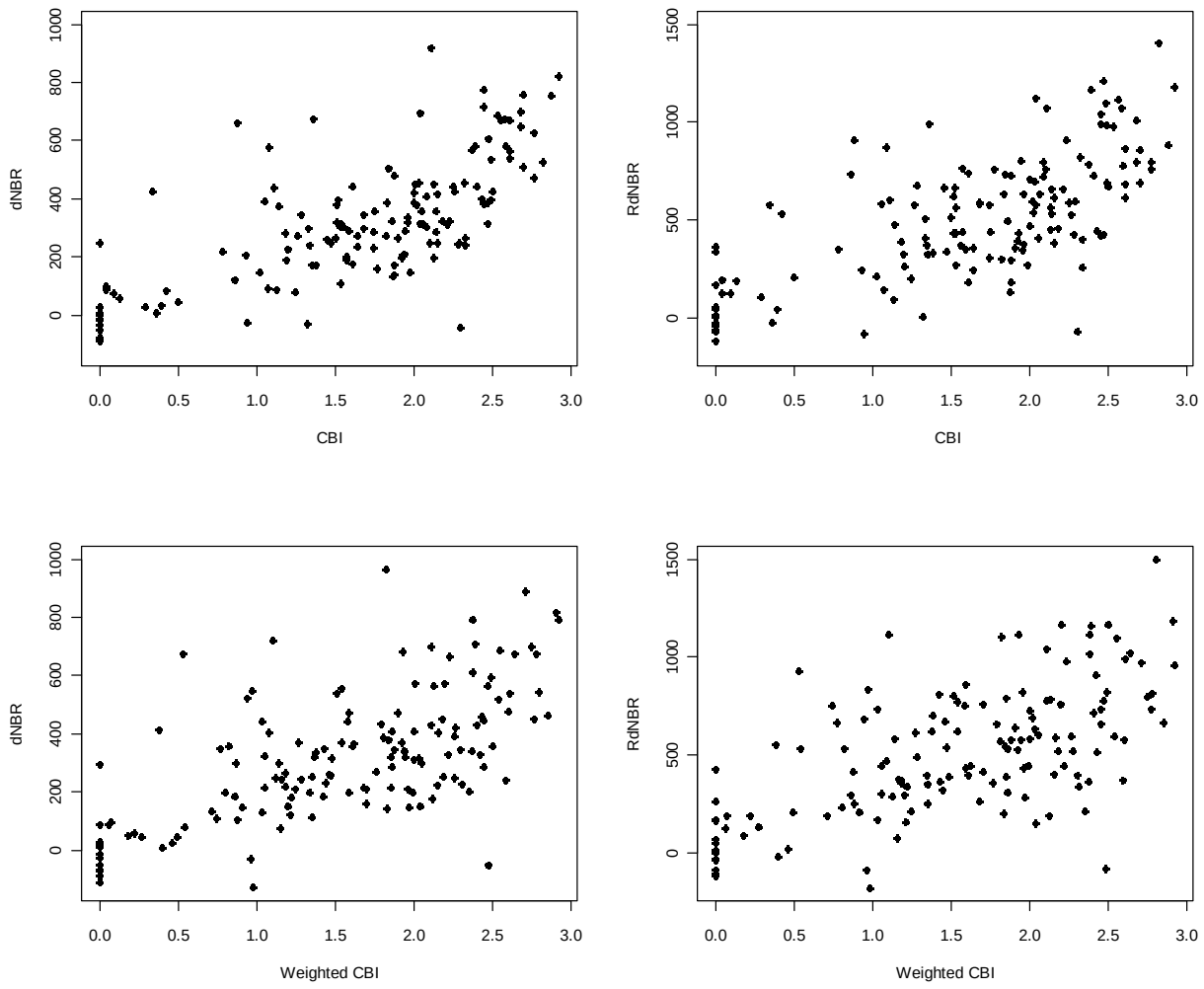

Figure 4. A comparison of unweighted and weighted CBI values, on the subset of plots for which a weighted version of the CBI could be calculated. Compare top scatter plots of unweighted CBI and dNBR (left) and unweighted CBI and RdNBR (right) with bottom scatter plots of weighted CBI and dNBR (left) and weighted CBI and RdNBR (right). In both cases the scatter of the weighted CBI values is much greater than the unweighted version.

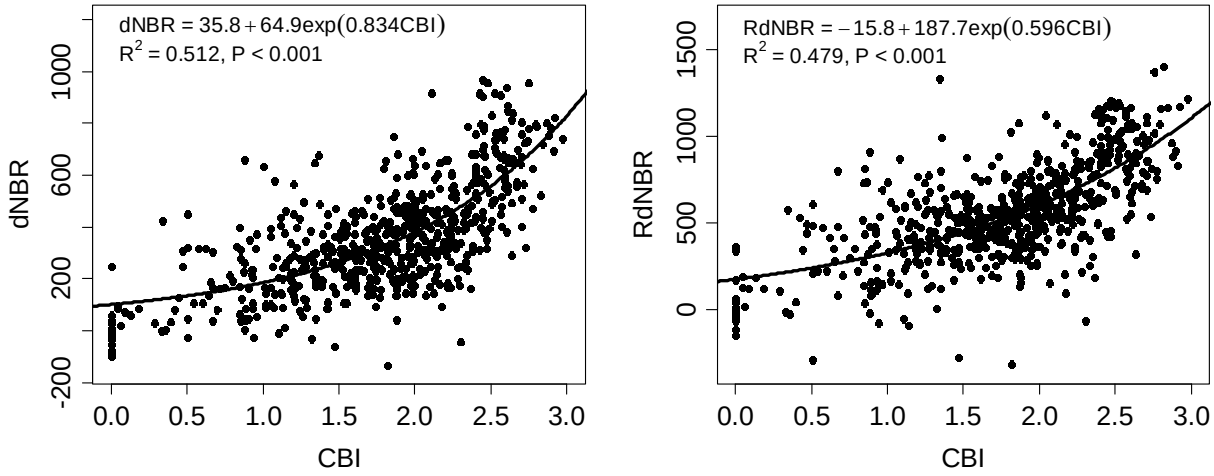

Figure 5. DNBR and RdNBR as a function of CBI using Model 2, the same model from used by Miller and Thode (2007) and Miller et al. (2009).

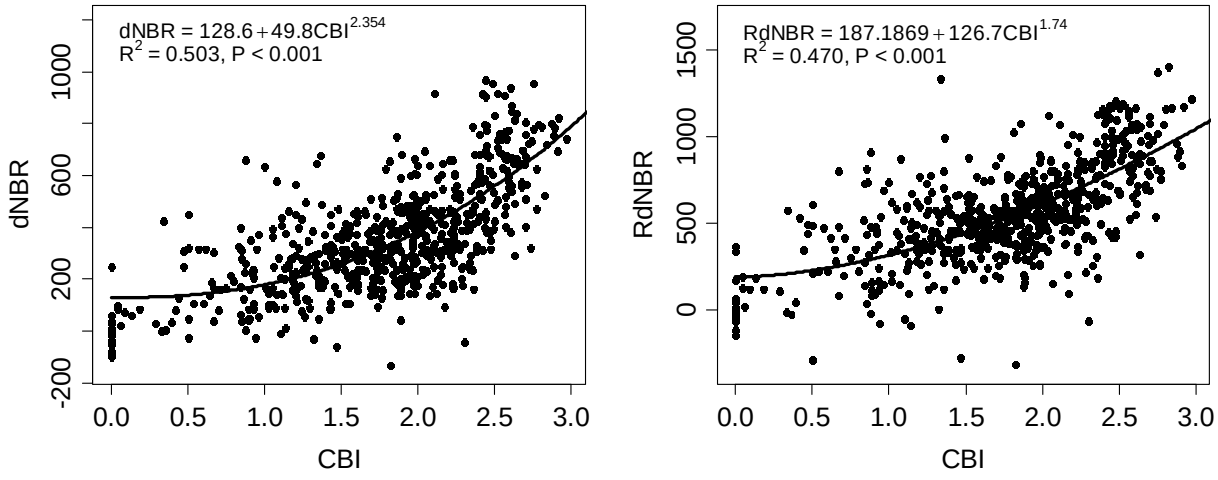

Figure 6. DNBR and RdNBR as a function of CBI using Model 3.

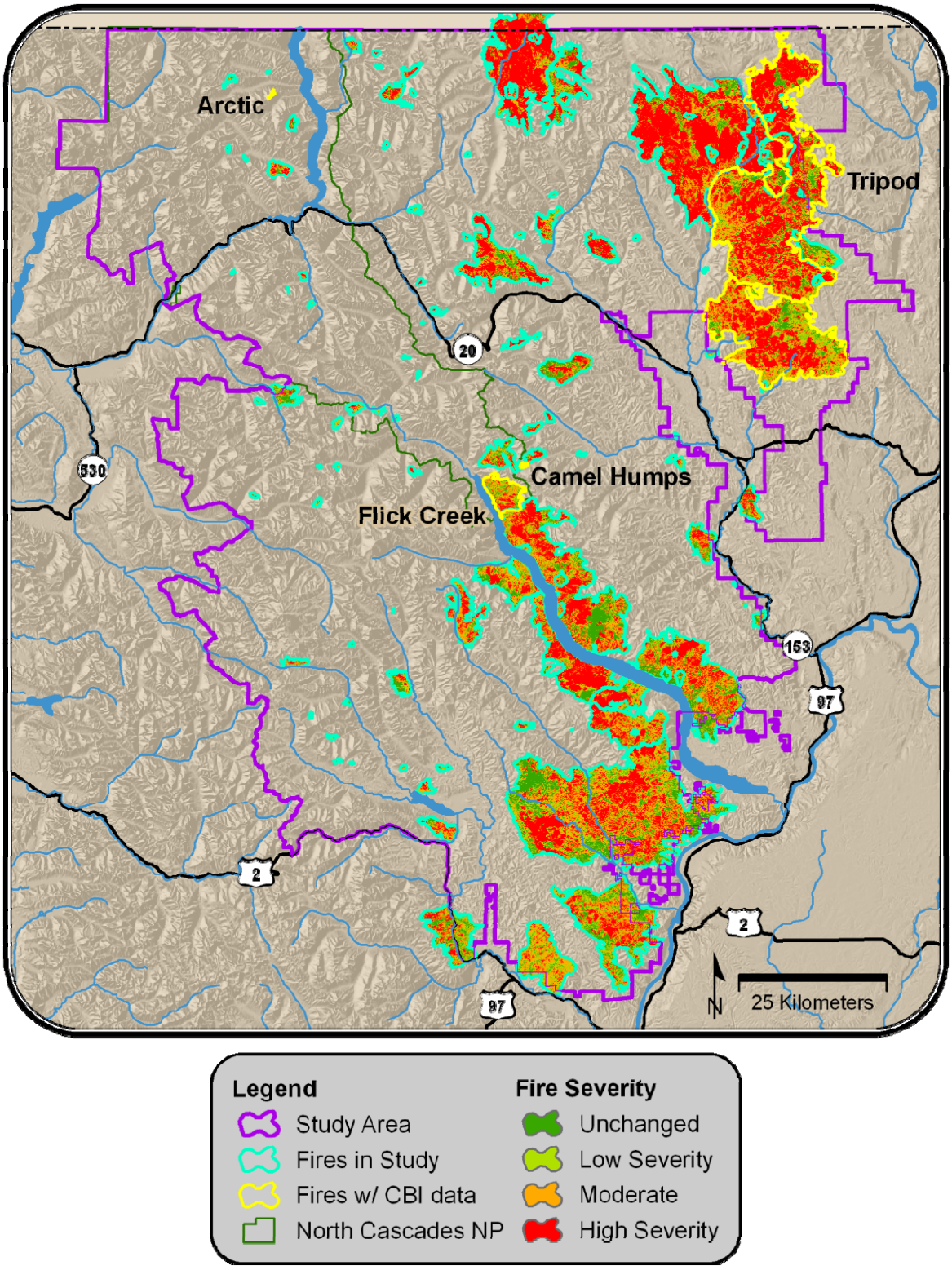

Figure 7. Fire locations and classified burn-severity images for all fires. The four fires on which CBI data were collected are labeled and outlined in yellow. Note the increase in fire size from west to east across the study area.

CHAPTER 2: THE FIRE REGIME OF THE NORTHERN CASCADE RANGE, WASHINGTON, USA: A SPATIALLY EXPLICIT ELABORATION OF THE FIRE REGIME CONCEPT

ABSTRACT

Quantifying attributes of mixed-severity fire regimes is challenging due to their high temporal and spatial variability. Traditionally, fire regimes have been described in terms of their predominant severity, frequency, and fire type. Increased availability of spatially explicit data and analysis tools and the use of natural fire regime characteristics as benchmarks for land management have led researchers and managers to take a more nuanced view of fire regimes. This view encompasses additional fire regime attributes, such as the seasonality, size, and spatial complexity of fires. This research quantifies patterns of severity and spatial pattern in the northern Cascade Range, WA, USA, compares variation in severity and spatial pattern within the larger study area, and examines how severity and spatial pattern vary with fire size.

Geospatial fire occurrence records and a remotely sensed index of burn severity (Relative differenced Normalized Burn Ratio), were used to map fire severity for all fires greater than 10 ha (n = 125) that occurred during a 25 year period (1984-2008) in the northern Cascade Range, Washington, USA. Patterns of fire size, burn severity, patch size, the size hierarchy of the patch distribution, patch interior (area > 90 m from edge of patch), and spatial complexity were quantified for each fire. Results were summarized for four ecological subsections within the study area. Linear regression was used to test the relationship between fire size and burn severity, patch size, patch interior, and spatial complexity. ANCOVA was used to test if these relationships differed among subsections.

The low elevation mixed-conifer forest in the eastern Cascades burned with less high severity, more moderate severity, smaller patches, and greater spatial complexity than the other

subsections. The north-east section of the study area, which has vegetation more similar to the northern Rocky Mountains, was dominated by large high-severity fires with very large patch sizes. Fires in the high-elevation forests along the Cascade Crest were smaller and were relatively evenly distributed between high severity, moderate severity, and unchanged areas. Burn severity, patch size, and the inequality of the patch size distribution (as measured by the Gini coefficient) increased with fire size. Severity, patch size, and patch interior increase more quickly with fire size in north-east section of the study area.

This study found positive relationships between fire size and the proportion of area burned at high severity, and between fire size and the size and core area of high severity patches. These results suggest that under future climate fire may not only be larger in size but also may produce more high-severity fire with a different, more aggregated burn-severity pattern. Results also indicate that the strength of the relationships between fire size and severity and fire size and spatial pattern are dependent on the local ecological context; differences in fire severity and spatial pattern within the northern Cascade Range reflect differences between each subsection's vegetation, fuels, and topography. Future research focus on variation in burn severity, as opposed to fire size or area burned, will further elucidate the influence of fire on landscape spatial pattern.

INTRODUCTION

Fire affects the structure, composition, and function of the physical and biological elements of natural ecosystems on multiple scales. Wildfire creates and maintains landscape pattern in many ecological systems across western North America (Agee 1993, Morgan et al. 2001, Turner 2010). The role of multiple fires throughout an ecosystem can be described by the temporal, spatial, and magnitude of its fire regime; attributes commonly considered to be important to ecosystem function are seasonality, fire return interval, size, spatial complexity, fireline intensity, severity, and fire type (Sugihara et al. 2006). These attributes reflect variability in the fire behavior of individual fires and the distribution of repeating patterns of fire occurrence.

Mixed-severity fire regimes usually exhibit high spatial complexity and variable burn severity which poses a challenge when trying to study these fire regimes using traditional methods. Traditional methods of studying fire's influence on ecosystems with dendrochronological fire-history data have the strength of being temporally deep, but require assumptions about fire behavior in areas where there are neither individual fire-scarred trees nor even-aged stands (Baker and Ehle 2001, Hessburg et al. 2007). Fire atlases based on mapped fire perimeters allow the distribution of some spatial attributes of individual fires, such as fire size and fire shape, to be examined (Baker 1992, Rollins et al. 2001) and reveal associations between fire occurrence and area burned and climate at a regional scale (Morgan 2008, Littell et al. 2009, Lutz et al. 2009).

The landscape pattern created by fire cannot be understood just based on the boundaries of the fire; variation of severity within the fire also creates and maintains landscape pattern (Agee 1993, Baker 2009, Turner 2010). Recent availability of remote-sensing burn-severity data,

such as the burn severity images produced by the Monitoring Trends in Burn Severity (MTBS) project (Zhu et al. 2006, Monitoring Trends in Burn Severity 2008), facilitates the examination factors that influence the severity at the level of the individual fire (Finney et al. 2005, Lentile et al. 2005, Collins et al. 2007) and across ecosystems or regions (van Wagtendonk et al. 2004, Thode 2005, Duffy et al. 2007, Lentile et al. 2007, Lutz et al. 2009). This allows for the quantification of the spatial patterns of burn severity created by fires (Thode 2005, Keane et al. 2008, Haire and McGarigal 2009, Lutz et al. 2009, Collins and Stephens 2010).

Quantifying burn severity and the spatial pattern of burn severity is important because these fire-regime attributes directly influence many ecological functions. Site-specific fire severity influences the severity and timing of future disturbances, wildlife habitat suitability, and the composition and timing of post-fire succession (Romme et al. 1995, Turner et al. 1997, Turner et al. 1999, Saab et al. 2004, Baker et al. 2007, Lentile et al. 2007, Keane et al. 2008). In landscapes with long ecological memory (Peterson 2002, McKenzie et al. 2011), the severity and spatial pattern of previous disturbances affect subsequent disturbances. For example, in pre-settlement dry forests in the eastern Cascade Range the heterogeneous spatial pattern of vegetation and fuels created by mixed-severity fire affects the occurrence and size of subsequent disturbances (Everett et al. 2000, Hessburg et al. 2005). In larger patches of high severity, seed sources from wind- and animal-dispersed species may be more limited, influencing the timing and composition of subsequent vegetation establishment and nutrient availability (Turner et al. 1994). Heterogeneous patterns of fire severity may also facilitate regeneration in fire regimes with frequent low-severity fire (Baker and Ehle 2001), allowing trees to avoid mortality long enough to express fire-resistant traits, such as thick bark. Animal species are also influenced by burn severity and the spatial pattern of severity: cavity-nesting bird species in the northern Rocky

Mountains have been shown to be sensitive to the burn severity and distance to edge of high-severity patches (Saab et al. 2004) and small mammals were shown to respond to both burn severity and the spatial complexity of burn severity in Sierra mixed-conifer forests (Roberts et al. 2008).

Examining how severity and spatial pattern vary between ecological systems in complicated because severity and the spatial pattern (1) are highly variable between fires and (2) are correlated with the size of the fire in some systems. Keane et al. (2008) compared 11 large fires (>10500 ha) to 25 small fires (<3300 ha) and found that large fires burned with a greater proportion of high and moderately high severity, a lower proportion of unburned area, and had larger patches (as seen by their lower patch density) and less edge. Burn severity increased with area burned across 24 fires in boreal forests of interior Alaska (Duffy et al. 2007). In an analysis of 103 fires in Yosemite National Park, Lutz et al. (2009) also found that the proportion of area burned at high severity increases with annual area burned, but found that patches become more complex as annual area burned increases. Because of these relationships, to characterize the severity and spatial pattern of a fire regime requires either knowledge of the fire-size distribution or a large enough data set so that the scaling relationship between these attributes and fire size can be examined.

This relationship between fire size, severity, and severity pattern is of particular interest because larger fires and greater area burned are positively correlated with warm and dry climate (Westerling et al. 2006, Heyerdahl et al. 2008, Morgan 2008, Littell et al. 2009, Lutz et al. 2009). Under future climate a significant increase in area burned is expected (Littell et al. 2010). If the increase in fire size co-occurs with an increase in severity and greater spatial aggregation of

high-severity areas, then future fires will produce different landscape spatial pattern and modify ecosystem processes.

Despite the wide availability of remotely sensed burn-severity data, they have mostly been used in case studies of individual fires (Collins et al. 2007, Collins and Stephens 2010) or in relatively small data sets (<25 fires) (Duffy et al. 2007, Lentile et al. 2007, Haire and McGarigal 2009), primarily due to a lack of field validation, which is needed to set burn-severity classes accurately for a particular ecosystem (Key and Benson 2006, Lentile et al. 2006, French et al. 2008, Keeley et al. 2008). An exception to the small sample size is work in the Sierra Nevada (Thode 2005, van Wagtendonk and Lutz 2007, Lutz et al. 2009), where extensive field validation has been conducted (Miller and Thode 2007, Miller et al. 2009).

This study examines the variation in burn severity and spatial pattern within the northern Cascade Range of Washington State, USA. Specifically, I use an index of burn severity, the Relative differenced Normalized Burn Ratio (RdNBR) (Miller and Thode 2007), derived from Landsat Thematic Mapper (LTM) data, to map burn severity over a 25-year period. The objectives of this study were threefold: (1) to quantify patterns in fire regime attributes—fire size, burn severity, patch size, the size hierarchy of the patch distribution, and the spatial complexity of the within-fire severity pattern—across the study area, (2) to determine if fire regime attributes differ between four ecological subsections within the larger study area, and (3) to determine if fire size showed the same relationships with burn severity, patch size, and the spatial complexity of burn severity among subsections. If the latter is the case, then we would expect severity and spatial patterns created future climate to depend on ecological context.

METHODS

STUDY AREA AND ECOLOGICAL SUBSECTIONS

The study area encompasses 1,445,500 hectares of federally managed land in the northern Cascade Range of Washington State, USA (Figure 1, Table 9). The US-Canadian border is the northern boundary and WA State Highway 2 is the southern boundary. The study area extends from the western boundaries of North Cascades National Park and Glacier Peak Wilderness to the eastern boundary of Okanogan-Wenatchee National Forest. The distribution of vegetation within the study area changes gradually from moist forests on the west side of the Cascade Crest to dry forests on the east side, reflecting gradients in climate, soil types, and elevation (Franklin and Dyrness 1988). In most of the study area the fire regimes are of high or mixed severity, although at low elevations on the eastern side some areas had a low-severity fire regime during the pre-settlement era. Fires are actively suppressed on most of the national forests in the study area but many fires have been allowed to burn under wildland fire use guidelines in North Cascades National Park since 1991. Also, since 2001, wildland fire use has also been allowed on National Park Service (NPS) and U.S. Forest Service (USFS) managed land near the northern end of Lake Chelan (National Park Service 2007), but few fires have been managed under these guidelines thus far.

In order to examine variation in fire-regime attributes within the study area ecological subsections were used to delineate ecologically similar areas. Ecological subsections represent the smallest hierarchical mapping unit identified under the USDA Forest Service's National Hierarchical Framework; larger ecosections have been in use for over 30 years and refined through subsequent peer review (Bailey 1976, Cleland et al. 1997, ECOMAP 2007). Subsection boundaries were developed by local and national interdisciplinary teams, and were delineated

based on climatic gradients, physiographic and geologic substrate, patterns in potential vegetation, soil groups, and hydrography (ECOMAP 2007). As the study-area boundary follows federal land management agency boundaries, only small portions of the ecological subsections on the western and eastern boundaries of the study area were included. Therefore, after visually evaluating geospatial layers of vegetation, fuels, and climate in relation to subsection boundaries, the two western-most subsections were combined into one group, and the low-elevation dry subsections were combined into another group, (Figure 8, Table 10). The Pasayten-Sawtooth Highlands and the Wenatchee-Chelan Highlands were maintained as separate subsections (Figure 8, Table 10). This allowed for a large enough sample size of fires in each group (hereafter "subsection") for fire-regime attributes to be compared statistically.

The North Cascades subsection comprises areas where fire has strongly influenced species composition and pattern and areas where fire has been either extremely infrequent or absent. Topography is steep and rugged and barriers to fire spread are common here. Lower-elevation forest include those dominated by western hemlock (*Tsuga heterophylla*), Douglas-fir (*Pseudotsuga menziesii*), and Pacific silver fir (*Abies amabilis*). Fire-return intervals in these forest are centuries long (Hemstrom and Franklin 1982) but infrequent fire has played a role throughout the Holocene (Cwynar 1987). Subalpine vegetation in the westernmost portion of the North Cascades subsection is dominated by parkland with mountain hemlock (*Tsuga mertensiana*) and subalpine fir (*Abies lasiocarpa*) the principal tree species (Agee and Pickford 1985, Franklin and Dyrness 1988). These subalpine areas likely have fire-return intervals similar to those found at Mt. Rainer, where some fire-return intervals in subalpine-fir forests exceeded 275 years (Hemstrom and Franklin 1982).

The North Cascades subsection also encompasses a unique ecological community along Ross Lake in North Cascades National Park, which contains a mix of forest types from the west side and east side of the Cascade Range (Agee et al. 1990). Open ponderosa pine (*Pinus ponderosa*) parklands are found at lower elevations. Forests contain lodgepole pine (*Pinus contorta*), grand fir (*Abies grandis*) and Douglas-fir at middle elevations, and Pacific silver fir, mountain hemlock, and subalpine fir at high elevations and on north aspects. Fire plays an important role here by maintaining fine-scale heterogeneity of shade-tolerant and shade-intolerant species (Franklin and Dyrness 1988, Agee et al. 1990, Prichard 2003). Mean fire-return intervals ranged from 52 to 137 years at mid-elevations and from 109-137 years for subalpine fir (Agee et al. 1990). Forests with similar composition found to the west or east have longer or shorter return intervals, respectively (Agee et al. 1990).

Fire regimes in the Pasayten-Sawtooth Highlands subsection may be more analogous to those in northern Rocky Mountain than to subalpine areas in the Cascade Range, reflecting dryer interior climate and the mixture of interior tree species (Fahnestock 1976, Franklin and Dyrness 1988). Mid-elevation forests in the Pasayten-Sawtooth Highlands include subalpine fir and a co-dominant component of Engelmann spruce (*Picea engelmannii*), although Pacific silver fir, western larch (*Larix occidentalis*), and lodgepole pine are also common (Fahnestock 1976). The subalpine fir/Engelmann spruce forests extend into subalpine areas and subalpine larch (*Larix lyallii*) and whitebark pine (*Pinus albicaulis*) are common at timberline. Western larch and lodgepole pine become more common in the eastern portion of this subsection. Previous large fire episodes in the Pasayten Wilderness occurred during multi-year droughts in the 1920s (Fahnestock 1976). Fire-free intervals of 250 years, with a range from 50-400 years, were found in the portion of the Pasayten Wilderness east of the Cascade Crest (Fahnestock 1976).

The Wenatchee Chelan Highlands subsection includes mid-elevation mixed-conifer forests, with a mix of Douglas-fir and grand fir, subalpine forests, and alpine areas. Little fire-history research has been done in this area, but fire regimes likely reflect these forest types, with high-severity fire at high elevation, similar to the North Cascades subsection to the west, and mixed-severity fire in lower-elevation mixed-conifer forests. Ongoing fire-history research near the north end of Lake Chelan in the southeast corner of North Cascades National Park Complex supports the existence of a mixed-severity fire regime, not a low-severity fire regime, in the mixed-conifer (Douglas-fir/ponderosa pine/grand fir) forest there (Kopper 2009, personal communication).

The Okanogan-Chelan Hills subsection comprises lower-elevation areas that have low to little winter snow pack and high summer temperatures. Low-severity fire probably typified the open grasslands and ponderosa pine parkland present at low elevations, while mixed-severity fire was common throughout the mid-elevation mixed-conifer forests (Agee 1993). One study found mean fire return intervals in ponderosa pine/Douglas-fir forests in the eastern Cascade Range of approximately 7 years during the pre-settlement period (1700 – 1860), and 39 and 48 years during the suppression period (1910-1996) (Everett et al. 2000). Multiple fire events with different boundaries over time created heterogeneity at fine scales, but occasional homogenous patches of vegetation, reflecting past stand replacing events, also occurred (Everett et al. 2000). A study using photo interpretation of stand structure from the 1930-1940s supports that both dry (Douglas-fir/ponderosa pine) and wet (grand fir) mixed-conifer forest in the eastern Cascades had a predominantly mixed-severity fire regime (Hessburg et al. 2007).

Fire is not present in all parts of the study area. Non-flammable areas, such as lakes, glaciers, permanent snow fields, and barren rocky areas are present in all the subsections and

make up over 10% of the area in the North Cascades subsection (Table 10). Not included in these calculations of non-flammable area are other areas where fire may be virtually absent due to continuously high fuel moisture, such as wet subalpine herb communities, heather meadows, hardwood-dominated avalanche tracks, and river bottoms (Agee and Pickford 1985).

DEVELOPMENT OF BURN-SEVERITY ATLAS

To build a burn-severity atlas for the northern Cascade Range, geospatial fire-occurrence data from federal land management agencies were used to identify all fires over ten hectares that occurred in the study area from 1984 through 2008. Burn severity was measured with the Relative differenced Normalized Burn Ratio (RdNBR) (Miller and Thode 2007), which measures the change in reflectance from pre-fire to post-fire of the near- and mid-infrared bands of Landsat Thematic Mapper (LTM) data. Unclassified RdNBR images and fire perimeters were downloaded from the Monitoring Trends in Burn Severity (MTBS) website (Monitoring Trends in Burn Severity. 2008) for the 35 fires that had images available. For 89 fires that were not available online, I identified Landsat image pairs with matching phenology, usually from 1 year pre and post-fire, to create burn-severity images. Selected scenes were processed according to existing MTBS protocols by the US Geological Survey National Center for Earth Resources Observation and Science (EROS).

Burn-severity class thresholds for the RdNBR images were developed based on field data from 639 field plots located across four fires (Chapter 1, Figure 7). Four categorical burn-severity classes—high, moderate, low, and unchanged—were used, following those defined by Miller and Thode (2007). To create four-class burn severity images from the continuous RdNBR, a non-linear model was used to regress RdNBR on field data in R (R Development Core Team

2010). RdNBR values that would serve as numerical thresholds for burn severity classes were predicted from that model. Overall classification accuracy was 62% and classification was 40% better than a random classification (Chapter 1, Table 5). These accuracies are within the range found by similar studies in California and Canada, which had overall accuracies of 60% and 68% respectively (Miller and Thode 2007, Soverel et al. 2010). Classification accuracies of the high severity class, emphasized in this study, was better or equal to the overall classification, with a user's accuracy of 62% and a producer's accuracy of 72%, and misclassified high severity was predominantly classified as moderate severity, with <5% of plots misclassified as low or unchanged severity. Derived classification thresholds were then used to create four-class categorical burn-severity images for all fires included in the study. The completed burn severity data set contains categorical images for 125 fires.

QUANTIFYING AND SUMMARIZING FIRE REGIME ATTRIBUTES

FRAGSTATS (McGarigal et al. 2002) was used to measure the total area of fires and the proportion of area at each severity, calculate spatial pattern metrics, and produce a list of individual patches and their associated sizes. I used a landscape border, as described in the FRAGSTATS user's manual, in order to compensate for minor inaccuracies (of 30 meters) in fire perimeters and to minimize inaccuracies when fires were spilt along subsection boundaries or when they overlapped the study area boundary.

Severity and spatial pattern were calculated at three different hierarchal levels: the study area, the subsection, and the individual fire. Calculation of spatial metrics based on one image mosaic that included all fires in the study area ("study-wide") or all burned area in a subsection ("subsection-wide") provides a snapshot of the landscape pattern. In cases where multiple fires

burned in the same place in different years images from the most recent fire were used. Multiple overlapping fires had little impact on the severity and spatial results, as only 6170 ha, or less than 1% of the total area burned in any subsection, burned twice or more during the study period. Tables summarizing results for severity and spatial pattern for each subsection were based on the "subsection-wide" burn severity images.

Calculation of spatial metrics for each individual fire was used to analyze the relationship between fire size and spatial aggregation. ANCOVA was used to test for differences in severity and spatial pattern between subsections, with fire size as a cofactor. To model the proportion of area burned at a given severity an arcsine/square-root transformation was applied to the response variable, *sensu* (Kutner et al. 2005):

$$2 * arcsine\sqrt{proportional\ severity}$$

All statistical tests were conducted in the statistical programming language R (R Core Development Team 2010).

Spatial pattern metrics used in this analysis were chosen to (1) quantify different aspects of spatial pattern, such as landscape composition, patch sizes, and spatial aggregation, or (2) examine spatial pattern at the grain of the patch and the grain of the pixel (30 meters). Spatial metrics used in this study, the aspect(s) of landscape pattern they measure, the grain of the calculation (patch or pixel), their formula, a description of what they measure, their strengths, and their limitations are listed in Tables 11-12.

Patch size distributions

The mean and maximum patch sizes were calculated study-wide and subsection-wide. Mean patch size was calculated for each individual fire and regressed against fire size with subsection as a cofactor in ANOVA. To assess differences between subsections fire-size

distributions and severity-patch distributions were calculated for each subsection. Patches were assigned to subsections based on the fires they were in, because individual patch sizes would be biased if they were split along subsection boundaries, and because this method would allow patch sizes to be related to fire sizes.

The shapes of the severity patch distribution for individual fires and individual subsections were quantified with the Gini coefficient. The Gini coefficient measures size inequality and was adapted from the economics literature (Atkinson 1970) to address ecological questions regarding size hierarchies in plant communities (Weiner and Solbrig 1984, Weiner and Thomas 1986). I use it here as a relative measure of the size inequality of the patch distribution, i.e. the extent to which large patches dominate the landscape. The Gini coefficient is based on the Lorenz curve (Lorenz 1905), which plots the cumulative size of an object (here a patch) against the cumulative proportion of the population of objects. The Gini coefficient is a relative measure of the patch distribution, with values ranges from 0 to 1. Here, values approaching 1 indicate that larger patches make up a larger cumulative proportion of the area affected by fire. The list of individual patches and their associated sizes produced in FRAGSTATS was used to calculate the Gini coefficient using the "reldist" package (Hadndcock and Morris 2003).

Spatial aggregation

Core area, defined here as the area greater than 90 meters from the edge of a patch, was calculated for each severity class. Large patches that are simple in shape have greater amounts of core area while small patches, or patches with convoluted edges or interior of different severity, have lower core area. Therefore, high-severity core area might be a better indicator of slowed succession (due to limited sources of wind dispersed seeds) than high-severity patch size. The 90-meter distance also allows for comparison to a previous study (Haire and McGarigal 2009).

Pixel-based spatial complexity metrics were calculate at the two different levels defined in the FRAGSTATS manual; the "landscape level", at which all burn severity classes are analyzed at once (i.e. spatial arrangement and interspersion of classes), and the "class level", at which only one burn severity class is analyzed (i.e. only spatial arrangement) (McGarigal et al. 2002). Two metrics that calculated spatial complexity at the grain of the pixel were included at both the landscape level and class level, to ensure that patterns relating to spatial complexity were distinguished. At the landscape level the Contagion Index and the Aggregation Index were used; both range from 0-100 and increase with greater spatial aggregation. At the severity class level the Clumpiness Index, which increases as spatial aggregation increases, and the Normalized Landscape Shape Index (NLSI), which decreases as spatial aggregation increases, were used.

RESULTS

SUBSECTIONS DIFFERENCES IN BURN SEVERITY AND SEVERITY PATTERN

Fire occurrence and area burned

Ecological subsections showed differing pattern of fire occurrence, area burned, and proportion of area burned in a severity class (Tables 13-14**)**. The North Cascades subsection had the highest number of fires, but only 2% of the flammable area burned during the 25-year study period. In the other subsections 31-36% of the flammable area burned. Large fires make up most of the total burned area, with fires over 50,000 hectares almost 40% and the 7 largest fires large almost 70% (Figure 9). The maximum fire size and the size distributions differed between subsections (Figure 10). The range of fire sizes was smallest in the North Cascades subsection, with a maximum of 1000-2500 ha, while the majority of the area burned in the Pasayten-Sawtooth Highlands subsection was in fires over 1000 ha.

Fire severity

Fire severity differed between subsections (Figure 11, Table 14). In the Pasayten-Sawtooth Highlands and the Wenatchee-Chelan Highlands high severity dominated the severity distribution, with 56% and 36% of the total burn area at high severity, respectively. The Okanogan Chelan Hills subsection burned predominantly with moderate severity (35%). The North Cascades subsection had the most even distribution of burn severity, and the greatest amount of unchanged areas within burns (28%).

Patch size distributions

The greatest mean and maximum patch sizes occurred in the high-severity class, but large patches of unchanged area were also common (Table 15). Low severity and moderate severity are difficult to compare between subsections because of their extremely small size. Unsurprisingly, the Pasayten-Sawtooth Highlands, which had the greatest amount and proportion of area burned at high severity, also had the greatest mean high-severity patch size (5.7 ha), but mean high-severity patch sizes for the other subsections were very similar to each other (2.2, 1.9, and 2.1 ha), despite having relatively different amounts and proportions of high severity. Minimum patch sizes for all classes and subsections was 0.09 ha, the size of a single pixel.

The patch size distributions in Figure 12 show the proportion of total area burned by patches in a given size classes. This is different than a frequency distribution, and better reflects how patches of a given size impact landscape pattern. The patch distributions for high severity and unchanged severity shows that larger high-severity and unchanged patches made up a greater proportion of the total area burned. In the Okanogan-Chelan Hills and the North Cascades subsections, where moderate severity made up more of the area burned across the landscape than

high severity or unchanged severity (Figure 11), the maximum sizes of high-severity and unchanged-severity patches were still larger than those of the moderate severity (Figure 12).

In the Pasayten-Sawtooth Highlands, recent large fires have created large homogenous areas of high severity. The Pasayten-Sawtooth Highlands had almost 40% of the area burned made up of high-severity patches that were over 1000 ha and one extremely large high-severity patch making up 14.5% of area burned (Table 15). These large high-severity patches are noticeable in the three large northernmost fires on the map of burn-severity images (Figure 7), and reflect the large proportion of area burned by fires >50,000 ha (Figure 10) in the Pasayten-Sawtooth Highlands. For comparison, the Okanogan-Chelan Hills had almost the same proportion of area burned by fires >50,000 ha, but had no patches larger than 10,000 ha.

The size inequalities of the patch distributions, as measured by the Gini coefficient (Table 15), reflect the differences in the patch-size distributions described above. The high-severity patch distribution had the greatest size inequality, with Gini coefficients ranging from 0.88 in the North Cascades to 0.97 in the Pasayten-Sawtooth Highlands. The unchanged severity class also showed strong inequality in the patch size distribution, ranging from 0.82 to 0.84. The results for the Gini coefficient for the high-severity class correspond with the severity classes and ecological subsections with the largest mean patch sizes and maximum patch sizes. For example, the Pasayten-Sawtooth Highlands had the greatest inequality in the high-severity class and across all classes combined. This pattern did not hold for the moderate, low, and unchanged severity classes: the Okanogan-Chelan Hills had the greatest inequality in these classes, but did not have consistently larger mean or maximum patch sizes in these classes.

Spatial aggregation

The results for core area most clearly display the spatial aggregation of (1) the high-severity class, and (2) the greater spatial aggregation of high-severity patches in the Pasayten-Sawtooth subsection. The Pasayten-Sawtooth Highlands had four times as much high-severity core area as any of the other subsections, and core area made up 24% of the area burned at high severity (Table 15). There was little to no core area in the moderate- and low-severity classes, even when there was a high proportion of area burned in these classes. For example, the Okanogan-Chelan Hills and North Cascades subsections had similar area burned at moderate severity and high severity, but little moderate-severity core area. This indicates that the large patches of moderate severity had high perimeter-to-area ratios, and often may have had other severity classes interspersed inside the moderate-severity patches.

Overall, differences in spatial aggregation between subsections were not as evident when measured with pixel-based spatial complexity metrics as when measured via core area. When calculated across all severity classes, the Contagion Index and Aggregation Index showed that the Pasayten-Sawtooth Highlands had a more spatially aggregated pattern than other subsections (Table 15). When calculated on a severity class basis, spatial aggregation of high severity was greatest in the Pasayten-Sawtooth Highlands, followed by the Wenatchee-Chelan Highlands (Table 15), and unchanged severity was most aggregated in the Wenatchee-Chelan Highlands.

FIRE SIZE, BURN SEVERITY, AND SEVERITY PATTERN

Fire severity

The relationship between fire size and burn severity was evident when examined across all fires in the study area (Figure 13). The proportion of area burned at high severity increased as fire size increased ($R^2 = 0.22$, $P < 0.001$) and the proportion of area unchanged area decreased ($R^2 = 0.19$, $P < 0.001$), but there was a lot of unexplained variance. Based on ANCOVA, with fire size as a cofactor, the proportion of area burned at high severity was significantly lower in the Okanogan Chelan Hills than the North Cascades subsection or the Pasayten-Sawtooth Highlands subsection but no significant interaction effect between fire size and subsection for high severity was found. Fire size interacted differently with moderate severity in the Pasayten-Sawtooth Highlands than in other subsections; the proportion of area burned at moderate severity decreases as fire size increased ($P = 0.008$), while in other subsections it increases slightly ($P = 0.012$). The Wenatchee Chelan Highlands had a greater proportion of low severity than other subsections ($P = 0.022$). These results for moderate and low severity should be interpreted cautiously as there was decreasing variance in severity with fire size.

Patch size distributions

The fire-size distribution and the severity distribution were generally related to the patch-size distribution, with larger patches of a given severity when fires were larger and when a greater proportion of the area burned at a given severity (Figures 10 and 12). Unsurprisingly, subsections with larger fires had a greater proportion of area burned by larger patches. In the Pasayten-Sawtooth Highlands subsection, where the largest fires occurred, 37% of the area burned was in high-severity patches over 1000 ha, and 19% of the area burned in high-severity

patches over 10,000 ha. The size inequality of the patch distribution of individual fires increased with fire size in the high-severity, moderate-severity, and unchanged classes (Figure 14), with the strongest increase with fire size in the high-severity class.

The influence of the fire-size distribution on the patch-size distribution is particularly evident in the high-severity class (Figure 15). For example, the North Cascades subsection was dominated by small fires (<1000 ha), and had relatively more area burned in small high-severity patches (10-100 ha). There were exceptions to this general trend, though. The Okanogan Chelan Hills and the Pasayten-Sawtooth Highlands subsections both had substantial area burned in fires over 10,000 ha, but the high-severity patch distribution for the Pasayten-Sawtooth Highlands was more strongly skewed toward larger patch sizes. The Okanogan-Chelan Hills and the Pasayten-Sawtooth Highlands had nearly equal amounts of low and unchanged severity, but low-severity patches were much smaller than unchanged-severity patches in both those subsections.

Spatial aggregation

High-severity core area had a significant positive relationship with fire size ($P<0.001$) (Figure 16). When tested with ANCOVA using fire size as a cofactor, the Pasayten-Sawtooth Highlands subsection had significant greater high-severity core area than the North Cascades subsection ($P<0.001$) or the Okanogan Chelan Hills subsection ($P<0.001$), but there was no significant interaction with fire size in subsections. Because there was little moderate-severity and low-severity core area (Table 15) those classes were not tested. There was no significant difference between subsections in the amounts of unchanged core area.

When examined using ANCOVA with fire size as a cofactor, the Contagion index was positively correlated with fire size in the Pasayten-Sawtooth Highlands ($P < 0.001$), and negatively correlated with fire size in all other subsections ($P < 0.001$). Variance in the

Contagion Index decreased with fire size across the other three subsections, so the significance of the latter relationship should be interpreted with caution (Figure 17). Results for the Aggregation Index were similar, showing an increase with fire size in the Pasayten-Sawtooth Highlands ($P = 0.005$), but no significant relationship in the other subsections ($P > 0.1$) (Figure 18). There was no significant difference between other subsections for either the Contagion Index or the Aggregation Index.

Over all fires, high severity NLSI decreased (meaning spatial aggregation increased) significantly with fire size ($P = 0.009$, $R^2 = 0.06$) (Figure 16), as did unchanged severity NLSI ($R^2 = 0.05$, $P = 0.01$). Tested with ANCOVA, with fire size as a cofactor, high severity NLSI was also higher for the Okanogan-Chelan Hills ($P< 0.001$) than in the North Cascades and the Pasayten-Sawtooth Highlands, but there was no significant difference between slopes of different subsections (Figure 19). Differences between subsections were driven by the five small fires in the Okanogan-Chelan Hills subsection with very high NLSI. If these fires are dropped from the analysis differences are not significant (Figure 19). No significant differences were found between subsections for moderate, low, and unchanged severity NLSI.

Unlike NLSI, high-severity clumpiness did not vary significantly with fire size, but there was a similar visual pattern of decreasing variance with fire size (Figure 20). With the exception of the smallest fire in the data set, which was removed from the analysis of the Clumpiness Index as an outlier, all clumpiness values for all severity classes calculated in this study were positive, indicating aggregation greater than random. The clumpiness of the unchanged severity class increased with fire size ($P < 0.001$), (Figure 20). Low-severity clumpiness did significantly increase with fire size ($P <0.001$), but the data showed decreasing variance with fire size, so the significance of this relationship should be interpreted with caution (Figure 20). ANCOVA results

for high severity clumpiness showed the same differences between subsections as with NLSI: Okanogan-Chelan Hills had significantly lower clumpiness than the North Cascades and Pasayten-Sawtooth Highlands ($P < 0.001$), but there was no significant interaction with fire size within individual subsections. Moderate, low, and unchanged severity clumpiness did not differ significantly among subsections.

DISCUSSION

SUBSECTION DIFFERENCES

Fire size was correlated with burn severity and within-fire severity pattern, but the differences between subsection indicate that the local ecological context matters. Differences in fire-regime attributes between the subsections reflect differences in vegetation, topography and climate. There was a lower proportion of high severity and a greater proportion of moderate severity in the Okanogan-Chelan Hills, the lowest-elevation subsection, where fire-tolerant tree species such as ponderosa pine and Douglas-fir were present. The greater spatial complexity found with pixel-based pattern metrics in the Okanogan-Chelan Hills likely reflects the finer-grain mosaic of vegetation and stand structure in low- and mid-elevation forest, compared to the subalpine forests of other subsections. The Wenatchee-Chelan Highlands comprises lower-elevation areas along Lake Chelan and higher-elevation areas with less fire-tolerant tree species. This subsection had larger fires, a greater proportion of high severity, and more spatially aggregated landscape pattern than the North Cascades or Okanogan-Chelan Hills subsections, but smaller fires, less high severity, and more spatial complexity than the Pasayten-Sawtooth Highlands.

The Pasayten-Sawtooth Highlands was the most strikingly different from other subsections. It had the most area burned, and over half the area burned was at high severity. Very large high-severity patches made up a significant proportion of the landscape. Greater contagion of fuels, fewer topographical barriers, and fire-intolerant tree species likely contributed to the formation of large high-severity patches, causing this subsection to exhibit a high-severity fire regime with a high-contrast patchy mosaic more typical of the Northern Rockies than the Cascades. These results correspond with research that has shown that fire scar formation is synchronous over longer distances, and has a weaker relationship with local topography, when bottom-up controls, such as topographic complexity or barriers to fire spread, are weaker (Heyerdahl et al. 2001, Kellogg et al. 2008, Kennedy and McKenzie 2010). Therefore, top-down controls, such as climate, have a stronger influence on the development of large fires and contagious burn-severity patterns in areas where local controls are weak.

The fire tolerance of vegetation alone does not explain the burn severity and spatial patterns displayed by different subsections. For example, the North Cascades subsection had a relatively even distribution of high, moderate, and unchanged severity fire, but many higher elevation tree species in the subsection are very intolerant of fire. The smaller fire sizes, smaller patch sizes, lower core area, less hierarchical patch distributions, and greater spatial complexity in the North Cascades subsection relative to other subsections are probably due to more natural barriers to fire spread. In the mountainous terrain of the North Cascades subsection fuel moisture may be more spatially variable, and ridgelines, avalanche chutes, talus fields, and wet meadows all likely limit fire spread. Similarly, the less complex more rolling terrain in the Pasayten-Sawtooth Highlands, where the largest fires in the data set burned, probably allows for greater fire spread and a more homogenous burn-severity pattern.

FIRE SIZE AND SPATIAL PATTERNS

Fire severity and spatial aggregation increased with fire size. Both burn severity and high-severity core area were positively correlated with fire size, and the high-severity patch-size distribution shifted toward larger patch sizes as fires size increased. These results indicate that in the northern Cascade Range larger fires make landscape pattern more homogenous than do smaller fires. Smaller fires create landscape heterogeneity via both their size and their more complex within-fire burn severity pattern. Larger fires burn with higher severity than smaller fires, leading to decreased variation in species survival at the sub-pixel scale.

Based on observations of severity and spatial pattern of the 1988 fire in Yellowstone National Park and simulation modeling, Turner and Romme (1994) hypothesized that during extreme weather conducive to fire spread, fire escapes the influence of local controls such as topography and fuels. The increases in severity, mean patch size, and high-severity core area with increased fire size found in this study indicate that larger fires do not respond to local controls. Conversely, large fires still create more area in smaller patch sizes than smaller fires do, even though large patches make up a greater proportion of their area. Also, the lack of a strong relationship between pixel-based metrics measuring spatial aggregation and fire size does not support the theory that larger fires override local heterogeneous controls.

The creation of heterogeneous areas in some parts of a fire simultaneously with the creation of very large patches in other parts of the fire may explain why the pixel-based metrics did not show as strong a relationship with fire size as the patch-based metrics. Contagion Index and Aggregation Index increased significantly with fire size in the gentle terrain of the Pasayten-Sawtooth Highlands, but did not increase as expected in the other subsections. Class-level pixel-

based metrics also showed an increase in spatial aggregation with fire size, particularly at high and unchanged severity, but the relationship was weaker than expected and was largely driven by the very low spatial aggregation of some fires under 1000 ha in size. It is difficult to determine if the disparity between patch and pixel-based methods is because pixel-based metrics are not as sensitive to changes in spatial pattern as the patch-based metrics due to being normalized to maximum and minimum possible value, or if the disparity stems from differences in what patch-based and pixel-based metrics are actually measuring.

The most unexpected trend relating to fire size found in this study is that of decreasing variance in severity and spatial pattern with fire size. This pattern is particularly noticeable in the unchanged, moderate, and low burn-severity classes and in the class-level pixel-based metrics. This pattern was also noted in a study of 20 fires in the southwestern U.S. for high-severity clumpiness (Haire and McGarigal 2009). There are three potential explanations for this heteroscedasticity. The pattern may be an artifact of the spatial statistics; they may more sensitive to changes in pattern when a smaller landscape is analyzed when a larger landscape is analyzed. The pattern may reflect the scales of observation; smaller areas within large fires may be just as variable as fires of the same small size. Alternatively, the process of burning on moderate and large sized fires may be more active than small fires, causing the severity pattern to better reflect the local fuel, topography, and diurnal weather conditions, thereby creating severity patterns on large fires that are more similar to each other.

Local controls may continue to be important in mixed-severity fire regimes even under conditions conducive to large fire growth. In the Southwest, even under extreme fire weather, local controls still influenced burn severity and spatial pattern, at least to some extent (Haire and McGarigal 2009). Research in the Sierra Nevada found that spatial complexity increases when

weather (Collins et al. 2007) or climate (Lutz et al. 2009) are conducive to large fire occurrence. Fire is less able to override local controls in low and mixed-severity systems (the Okanogan-Chelan Hills or the Sierra Nevada) than in high-severity systems with continuous fuels (the Pasayten-Sawtooth Highlands or in Yellowstone National Park, where the theory was first formulated). Therefore, instead of "overriding" or removing the influence of fuels and topography, climate may increase the scale at which those local controls influence burn-severity pattern. In other words, in some systems both bottom-up controls and top-down controls may influence pattern simultaneously, and the shift between the two may be gradual instead of sudden. Also, the strength of local controls is likely stronger where topography is extremely rugged and fuels are highly variable (Kellogg et al. 2008, Kennedy and McKenzie 2010).

COMPARISON TO OTHER REGIONS

Comparison of burn severity between studies is difficult due to the high variation between fires, differing methods, and small sample sizes. The most comparable data set is from the mixed-severity fire regime of Yosemite National Park. In that system van Wagtendonk and Lutz (2007) found less high severity and more low severity than I found in the northern Cascade Range: approximate percentage severities for high, moderate, low and unchanged severities were 15, 35, 30, and 21% respectively for wildfires, and 5, 25, 37, 32% for wildland fire-use fires. I expected the Okanogan-Chelan Hills to have similar spatial patterns and severity to other dry-to-mesic mixed conifer forests with a mix of true fir, Douglas-fir, and ponderosa pine. The Okanogan-Chelan Hills, which had high, moderate, low, and unchanged severity at 29, 35, 18, and 19% respectively, had lower severity than the other subsections in this study but more high and mixed severity than that found in Yosemite National Park.

Other studies in mixed-severity systems also found less high severity and more moderate and low severity than in the northern Cascade Range, although their results should be interpreted cautiously due to their small sample size. Across six fires in the Northern Rocky Mountains of Montana, high burn severity ranged from 3.7 to 33.5% of the landscape (Rodriguez 2005). In the Black Hills of South Dakota the severity distribution from one large fire was 27% high severity, 48% moderate severity, and 25% low severity (Lentile et al. 2005). Burn severity of fires on the Klamath National Forest assessed based on color infrared post-burn aerial photography had 12% high severity, 30% moderate severity, and 59% low severity (Odion et al. 2004).

Similar increases with fire size in the proportion of area burned at high severity and the percentage of individual patches made up of high-severity core area ("Core Area Index", defined as > 100m from the edge of a patch) were found in a study of 20 fires in the southwestern USA (Haire and McGarigal 2009). A study in Yosemite National Park found the same positive relationship with area burned and the proportion of area burned at high severity as I did, but differed in that patches become more complex with fire size (Lutz et al. 2009). The different relationships between fire size and spatial complexity in the northern Cascades Range vs. Yosemite National Park probably reflect the shorter fire rotations in Yosemite National Park, which create heterogeneity in fuels on a finer scale than in most of the northern Cascade Range.

When compared to studies that reported patch sizes based on dNBR or RdNBR burn-severity data, patch sizes were within the ranges reported by other studies. In ponderosa pine forests in the Black Hills of South Dakota, Lentile et al. (2005) found mean patch sizes on one large fire of 8 ha, 24 ha, and 10 ha for high, moderate, and low burn severity, respectively (Lentile et al. 2005). Wildland fires in Yosemite National Park had mean patches sizes of approximately 7 ha, 13 ha, 6 ha, and 5 ha for high, moderate, low, and unchanged burn severity

(van Wagtendonk and Lutz 2007). The northern Cascade Range had smaller patches of high severity than found in these studies, and unchanged severity patches were larger than reported by these other studies. The differences between these other studies and mine may be because severity in Yosemite was predominantly unchanged, low, and moderate; theses severity classes tend to be less spatially aggregated than the high-severity class that was more prevalent in the northern Cascade Range.

IMPLICATIONS OF TEMPORAL SCOPE OF THE STUDY

Because availability of remotely sensed data is limited to the last quarter century, the fire-size distribution, severity distribution, and spatial patterns found in this study can only be viewed as a proxy for the true distributions and patterns that would develop over a full fire rotation (the length of time necessary for an area equal to the size of the study area to burn). Severity and within-fire burn severity patterns have likely been influenced by fire suppression and land use that occurred prior to and during the study period. Fire suppression is most effective during moderate and wet climate; large fires, which spread during extreme weather, are not so successfully suppressed. Therefore, fire suppression predominantly decreases the area burned by small and moderate-sized fires, which have a more complex spatial pattern, due to lower severity and a more complex within-fire severity pattern. Conversely, these small and moderate-sized fires, by definition, influence a smaller proportion of the landscape, but without knowledge of the effectiveness of fire suppression efforts it is difficult to know what their combined influence on landscape pattern would be over a full fire rotation. Fire suppression and subsequent changes in fuel structure are thought to increase fire severity and fire size (Hessburg et al. 2005). This is not just true in low-elevation dry forests, but may also have occurred in higher-severity

subsections, such as the Pasayten-Sawtooth Highlands, where previous fires have acted as barriers to fire spread for at least 30 years and previous fuel treatments that include prescribed fire decrease fire severity within large severe fires (Prichard et al. 2010). Lastly, for areas with longer fire rotations, such as the North Cascades subsection, the study period may have been simply too short to capture large infrequent fire events. There is evidence that larger fires do occur in the North Cascades subsection; the Big Beaver fire of 1926 burned 20,000 ha along what is now Ross Lake, and at least two other fires in 1573 and 1851 covered most of a 3500 ha fire history study area at Desolation Peak (Agee et al. 1990).

The study period centers over an upswing in annual area burned across the western USA that occurred from the mid-1980s through the present (Westerling et al. 2006, Littell et al. 2009) and is reflected in the prevalence of large fires in all the subsections except the North Cascades subsection. From the mid 1930s through the mid 1980s, the annual areas burned in the western US was much lower, and fire sizes were likely much smaller (Littell et al. 2009). This corresponds with records from the study area. The last episode of large fire occurrence in the Pasayten area was during the drought of the 1920s when almost 70,000 ha in the section of the Pasayten wilderness east of the Cascade crest burned (Fahnestock 1976). Between that time and the present there were few large extensive fires; from 1930-1969 only 6475 ha of the same area burned (Fahnestock 1976). Because climate conducive to large fires occurs relatively infrequently (Heyerdahl et al. 2008), small and mid-sized fires may have made up more of the total area burned historically than is represented in the relatively short window of this study.

If the study period had covered the middle part of the century, for example, where cool wet conditions limited large fire growth, the overall landscape spatial pattern might have been more spatially complex, due to the increased proportion of small fires compared to large fires.

Nevertheless, even if small and mid-sized fires occur more often than represented by this study, they still may not add up to enough area to appreciably influence landscape pattern. For example, although fires under 1000 ha made up 72% of the area burned in the North Cascades subsection, they only made up 2-4% of the area burned in the other subsections, and only 4.4% of the total area burned over the whole study area. Even assuming that fires under 1000 ha occurred four times as often as was captured by the study period—one quarter of the century followed the fire size distribution seen here, and in the other three quarters there were no large fires but the same distribution of fires under 1000 ha—the total percentage of area burned by fires under 1000ha in subsections other than North Cascades would be only 10 to 14 percent. The results of this study indicate that very large fires drive the spatial pattern on the landscape, but a detailed distribution of fire sizes over a much longer time period would be valuable for refining our understanding of the causes and differences across landscapes.

CONCLUSIONS

This study found positive relationships between fire size and the proportion of area burned at high severity, and between fire size and the size and core area of high-severity patches. These results suggest that under future climate fire may not only be larger in size (Littell et al. 2010) but also may produce more high-severity patches with a different more aggregated burn-severity pattern. Nevertheless, large spatially aggregated fires cannot be seen simply as ecological catastrophes. The weak correlations between fire size and pixel-based spatial pattern metrics and patch-size distributions indicate that large fires also create spatially heterogeneous areas at the same time as creating large high-severity patches. Furthermore, differences in fire severity and spatial pattern within the northern Cascade Range reflect differences between each

subsection's vegetation, fuels, topography, and climate, and therefore the strength of the relationships between fire size and severity, and fire size and spatial pattern, are dependent on the local ecological context.

The highly variable patterns of burn severity found in this study of the northern Cascade Range imply that variation in burn severity within a fire has a more direct influence on the post-fire landscape pattern than fire size alone. These fire-regime attributes and their impact on other ecological functions must be addressed in order for high- and mixed-severity fire regimes to be understood. Continued use of remote sensing of burn severity and quantification of burn-severity patterns in other systems can help us better define which aspects of fire spatial pattern provide the best basis for differentiating ecologically relevant aspects of fire regimes within larger categories of mixed- and high-severity fire.

REFERENCES

Agee, J. K. 1993. Fire ecology of Pacific Northwest forests. 1 edition. Island Press, Washington, D.C.

Agee, J. K., M. Finney, and R. D. Gouvenain. 1990. Forest fire history of Desolation Peak, Washington. Canadian Journal of Forest Research **20**:350-356.

Agee, J. K. and S. G. Pickford. 1985. Vegetation and fuel mapping of North Cascades National Park Service complex: final report. National Park Service, Cooperative Park Studies Unit, College of Forest Resources, University of Washington, Seattle, WA.

Atkinson, A. B. 1970. On the measurement of inequality. Journal of Economic Theory **2** 244-263.

Bailey, R. G. 1976. Ecoregions of the United States (map). USDA Forest Service, Intermountain Region, Ogden, UT.

Baker, W. L. 1992. The landscape ecology of large disturbances in the design and management of nature reserves. Landscape Ecology **7**:181-194.

Baker, W. L. 2009. Fire ecology in Rocky Mountain landscapes. Island Press, Washington, D.C.

Baker, W. L. and D. Ehle. 2001. Uncertainty in surface-fire history: the case of ponderosa pine forests in the western United States. Canadian Journal of Forest Research **31**:1205-1226.

Baker, W. L., T. T. Veblen, and R. L. Sherriff. 2007. Fire, fuels and restoration of ponderosa pine-Douglas fir forests in the Rocky Mountains, USA. Journal of Biogeography **34**:251-269.

Cleland, D. T., P. E. Avers, W. H. McNab, M. E. Jensen, R. G. Bailey, T. King, and W. E. Russell. 1997. National hierarchical framework of ecological units. *in* M. S. Boyce and A. Haney, editors. Ecosystem Management. Yale University Press, New Haven, CT.

Collins, B. M., M. Kelly, J. W. van Wagtendonk, and S. L. Stephens. 2007. Spatial patterns of large natural fires in Sierra Nevada wilderness areas. Landscape Ecology **22**:545-557.

Collins, B. M. and S. L. Stephens. 2010. Stand-replacing patches within a 'mixed severity' fire regime: quantitative characterization using recent fires in a long-established natural fire area. Landscape Ecology **26**:927-939.

Cwynar, L. C. 1987. Fire and the Forest History of the North Cascades Range. Ecology **68**:791-802.

Duffy, P. A., J. Epting, J. M. Graham, T. S. Rupp, and A. D. McGuire. 2007. Analysis of Alaskan burn severity patterns using remotely sensed data. International Journal of Wildland Fire **16**:277-284.

ECOMAP 2007. Delineation, peer review, and refinement of subregions of the conterminous United States. U.S. Department of Agriculture, Forest Service, Washington, DC.

Everett, R. L., R. Schellhaas, D. Keenum, D. Spurbeck, and P. Ohlson. 2000. Fire history in the ponderosa pine/Douglas-fir forests on the east slope of the Washington Cascades. Forest Ecology and Management **129**:207-225.

Fahnestock, G. R. 1976. Fires, fuel, and flora as factors in wilderness management: The Pasayten case. Pages 33-69 *in* Tall Timbers Fire Ecology Conference. Tall Timbers Research Station.

Finney, M. A., C. W. McHugh, and I. C. Grenfell. 2005. Stand- and landscape-level effects of prescribed burning on two Arizona wildfires. Canadian Journal of Forest Research-Revue Canadienne De Recherche Forestiere **35**:1714-1722.

Franklin, J. F. and C. T. Dyrness. 1988. Natural Vegetation of Oregon and Washington. Oregon State University Press, Corvallis.

French, N. H. F., E. S. Kasischke, R. J. Hall, K. A. Murphy, D. L. Verbyla, E. E. Hoy, and J. L. Allen. 2008. Using Landsat data to assess fire and burn severity in the North American boreal forest region: an overview and summary of results. International Journal of Wildland Fire **17**:443-462.

Hadndcock, M. S. and M. Morris. 2003. Relative Distribution Methods in Social Science. Springer, New York.

Haire, S. L. and K. McGarigal. 2009. Changes in fire severity across gradients of climate, fire size, and topography: a landscape ecology perspective. Fire Ecology **5**:86-103.

Hemstrom, M. A. and J. F. Franklin. 1982. Fire and Other Disturbances of the Forests in Mount Rainier National-Park. Quaternary Research **18**:32-51.

Hessburg, P. F., J. K. Agee, and J. F. Franklin. 2005. Dry forests and wildland fires of the inland Northwest USA: Contrasting the landscape ecology of the pre-settlement and modem eras. Forest Ecology and Management **211**:117-139.

Hessburg, P. F., R. B. Salter, and K. M. James. 2007. Re-examining fire severity relations in pre-management era mixed conifer forests: inferences from landscape patterns of forest structure. Landscape Ecology **22**:5-24.

Heyerdahl, E. K., L. B. Brubaker, and J. K. Agee. 2001. Spatial controls of historical fire regimes: A multiscale example from the interior west, USA. Ecology **82**:660-678.

Heyerdahl, E. K., D. McKenzie, L. D. Daniels, A. E. Hessl, J. S. Littell, and N. J. Mantua. 2008. Climate drivers of regionally synchronous fires in the inland Northwest (1651-1900). International Journal of Wildland Fire **17**:40-49.

Keane, R. E., J. K. Agee, P. Fule, J. E. Keeley, C. Key, S. G. Kitchen, R. Miller, and L. A. Schulte. 2008. Ecological effects of large fires on US landscapes: benefit or catastrophe? International Journal of Wildland Fire **17**:696-712.

Keeley, J. E., T. Brennan, and A. H. Pfaff. 2008. Fire severity and ecosystem responses following crown fires in California shrublands. Ecological Applications **18**:1530-1546.

Kellogg, L. K. B., D. McKenzie, D. L. Peterson, and A. E. Hessl. 2008. Spatial models for inferring topographic controls on historical low-severity fire in the eastern Cascade Range of Washington, USA. Landscape Ecology **23**:227-240.

Kennedy, M. C. and D. McKenzie. 2010. Using a stochastic model and cross-scale analysis to evaluate controls on historical low-severity fire regimes. Landscape Ecology **25**:1561-1573.

Key, C. H. and N. C. Benson. 2006. Landscape Assessment (LA). In Pages LA-1-55 *in* D. C. Lutes, R. E. Keane, J. F. Caratti, C. H. Key, N. C. Benson, S. Sutherland, and G. L.J., editors. FIREMON: Fire Effects Monitoring and Inventory System. USDA Forest Service, Rocky Mountain Research Station, Fort Collins, CO.

Kopper, K. E. 2009. Personal communication.

Kutner, M. C., C. J. Nachtsheim, J. Neter, and W. Li. 2005. Applied Linear Statistical Models, 5th ed.:1396.

Lentile, L. B., Z. A. Holden, A. M. S. Smith, M. J. Falkowski, A. T. Hudak, P. Morgan, S. A. Lewis, P. E. Gessler, and N. C. Benson. 2006. Remote sensing techniques to assess active

fire characteristics and post-fire effects. International Journal of Wildland Fire **15**:319-345.

Lentile, L. B., P. Morgan, A. T. Hudak, M. J. Bobbitt, S. A. Lewis, A. M. Smith, and P. R. Robichaud. 2007. Post-fire burn severity and vegetation response following eight large wildfires across the western United States. Fire Ecology **3**:91-101.

Lentile, L. B., F. W. Smith, and W. D. Shepperd. 2005. Patch structure, fire-scar formation, and tree regeneration in a large mixed-severity fire in the South Dakota Black Hills, USA. Canadian Journal of Forest Research **35**:2875-2885.

Littell, J. S., D. McKenzie, D. L. Peterson, and A. L. Westerling. 2009. Climate and wildfire area burned in western U. S. ecoprovinces, 1916-2003. Ecological Applications **19**:1003-1021.

Littell, J. S., E. E. Oneil, D. McKenzie, J. A. Hicke, J. A. Lutz, R. A. Norheim, and M. M. Elsner. 2010. Forest ecosystems, disturbance, and climatic change in Washington State, USA. Climatic Change **102**:129-158.

Lorenz, M. O. 1905. Methods for measuring the concentration of wealth. American Statistical Association **9**:209-219.

Lutz, J. A., J. W. van Wagtendonk, A. E. Thode, and J. D. Miller. 2009. Climate, lightning ignitions, and fire severity in Yosemite National Park, California, USA. International Journal of Wildland Fire **19**:765-774.

McGarigal, K. S., A. Cushman, M. C. Neel, and E. Ene. 2002. FRAGSTATS: Spatial Pattern Analysis Program for Categorical Maps. Computer software program produced by the authors at the University of Massachusetts, Amherst. http://www.umass.edu/landeco/research/fragstats/fragstats.html.

McKenzie, D., C. Miller, and D. A. Falk. 2011. Synthesis: landscape ecology and changing fire regimes. Chapter 12 in D. McKenzie, C. Miller, and D. A. Falk, eds. The Landscape Ecology of Fire. Springer, Dordrecht, The Netherlands.

Miller, J. D., E. E. Knapp, C. H. Key, C. N. Skinner, C. J. Isbell, R. M. Creasy, and J. W. Sherlock. 2009. Calibration and validation of the relative differenced Normalized Burn Ratio (RdNBR) to three measures of fire severity in the Sierra Nevada and Klamath Mountains, California, USA. Remote Sensing of Environment **113**:645-656.

Miller, J. D. and A. E. Thode. 2007. Quantifying burn severity in a heterogeneous landscape with a relative version of the delta Normalized Burn Ratio (dNBR). Remote Sensing of Environment **109**:66-80.

Monitoring Trends in Burn Severity. 2008. Individual Fire-Level Geospatial Data - Monitoring Trends in Burn Severity (MTBS). <http://mtbs.gov/dataquery/individualfiredata.html> accessed: 3-01-2008.

Morgan, P. 2008. Multi-season climate synchronized forest fires throughout the 20th century, Northern Rockies, USA. Ecology **89**:717-728.

Morgan, P., C. C. Hardy, T. W. Swetnam, M. G. Rollins, and D. G. Long. 2001. Mapping fire regimes across time and space: Understanding coarse and fine-scale fire patterns. International Journal of Wildland Fire **10**:329-342.

National Park Service, US Department of the Interior. 2007. Wildland Fire Management Plan: North Cascades National Park Service Complex.

Odion, D. C., E. J. Frost, J. R. Strittholt, H. Jiang, D. A. Dellasala, and M. A. Moritz. 2004. Patterns of fire severity and forest conditions in the western Klamath Mountains, California. Conservation Biology **18**:927-936.

Peterson, G. D. 2002. Contagious disturbance, ecological memory, and the emergence of landscape pattern. Ecosystems **5**:329-338.

Prichard, S. J. 2003. Spatial and temporal dynamics of fire and vegetation change in Thunder Creek watershed, North Cascades National Park, Washington. University of Washington, Seattle.

Prichard, S. J., D. Peterson, and K. Jacobson. 2010. Fuel treatments reduce the severity of wildfire effects in dry mixed conifer forest, Washington, USA. Canadian Journal of Forest Research **40**:1615-1626.

R Development Core Team. 2010. R: A language and environment for statistical computing. R Foundation for Statistical Computing, Vienna, Austria. ISBN 3-900051-07-0, URL http://www.R-project.org/.

Roberts, S. L., J. W. van Wagtendonk, A. K. Miles, D. A. Kelt, and J. A. Lutz. 2008. Modeling the effects of fire severity and spatial complexity on small mammals in Yosemite National Park, California. Fire Ecology Special Issue **4**:83-104.

Rodriguez, J. T. 2005. A remote sensing method of quantifying patch characteristics of post fire landscapes in the Crown of the Continent ecosystem, Montana, USA. University of Montana, Missoula.

Rollins, M. G., T. W. Swetnam, and P. Morgan. 2001. Evaluating a century of fire patterns in two Rocky Mountain wilderness areas using digital fire atlases. Canadian Journal of Forest Research **31**:2107-2123.

Romme, W. H., M. G. Turner, L. L. Wallace, and J. S. Walker. 1995. Aspen, elk, and fire in Northern Yellowstone National Park. Ecology **76**:2097-2106.

Saab, V. A., J. Dudley, and W. L. Thompson. 2004. Factors influencing occupancy of nest cavities in recently burned forests. Condor **106**:20-36.

Soverel, N. O., D. D. B. Perrakis, and N. C. Coops. 2010. Estimating burn severity from Landsat dNBR and RdNBR indices across western Canada. Remote Sensing of Environment **114**:1896-1909.

Thode, A. E. 2005. Quantifying the fire regime attributes of severity and spatial complexity using field and imagery data. PhD Dissertation, University of California, Davis, CA.

Turner, M. G. 2010. Disturbance and landscape dynamics in a changing world. Ecology **91**:2833-2849.

Turner, M. G., W. W. Hargrove, R. H. Gardner, and W. H. Romme. 1994. Effects of fire on landscape heterogeneity in Yellowstone National Park, Wyoming. Journal of Vegetation Science **5**:731-742.

Turner, M. G. and W. H. Romme. 1994. Landscape dynamics in crown fire ecosystems. Landscape Ecology **9**:59-77.

Turner, M. G., W. H. Romme, and R. H. Gardner. 1999. Prefire heterogeneity, fire severity, and early postfire plant reestablishment in subalpine forests of Yellowstone National Park, Wyoming. International Journal of Wildland Fire **9**:21-36.

Turner, M. G., W. H. Romme, R. H. Gardner, and W. W. Hargrove. 1997. Effects of fire size and pattern on early succession in Yellowstone National Park. Ecological Monographs **67**:411-433.

van Wagtendonk, J. W. and J. A. Lutz. 2007. Fire regime attributes of wildland fires in Yosemite National Park, USA. Fire Ecology Special Issue **3**:34-52.

van Wagtendonk, J. W., R. R. Root, and C. H. Key. 2004. Comparison of AVIRIS and Landsat ETM+ detection capabilities for burn severity. Remote Sensing of Environment **92**:397-408.

Weiner, J. and O. T. Solbrig. 1984. The meaning and measurement of size hierarchies in plant populations. Oecologia **61**:334-336.

Weiner, J. and S. C. Thomas. 1986. Size variability and competition in plant monocultures. Oikos **47**: 211-222.

Westerling, A. L., H. G. Hidalgo, D. R. Cayan, and T. W. Swetnam. 2006. Warming and earlier spring increase western US forest wildfire activity. Science **313**:940-943.

Zhu, Z., C. H. Key, D. Ohlen, and N. C. Benson. 2006. Evaluate sensitivities of burn severity mapping algorithms for different ecosystems and fire histories in the United States. Final Report to the Joint Fire Science Program. Project: JFSP 01-1-4-12.

TABLES

Table 9. Federal land management designation and protected status

Land management designation	Agency	Additional protected status	Area (ha)
North Cascades National Park	NPS	Stephen Mather Wilderness	203,000
Ross Lake National Recreation Area	NPS	Stephen Mather Wilderness	47,282
Lake Chelan National Recreation Area	NPS	Stephen Mather Wilderness	25,458
Mt. Baker-Snoqualmie National Forest	USFS	Glacier Peak Wilderness	48,368
Okanogan-Wenatchee National Forest	USFS	Glacier Peak Wilderness	116,992
Okanogan-Wenatchee National Forest	USFS	Henry M. Jackson Wilderness	11,112
Okanogan-Wenatchee National Forest	USFS	Chelan-Sawtooth Wilderness	61,911
Okanogan-Wenatchee National Forest	USFS	Pasayten Wilderness	215,106
Okanogan-Wenatchee National Forest	USFS		716,315
Study area			1,445,545

Table 10. Ecological subsections and subsection groups

Grouped ecological subsections	Ecological subsections	Subsection area (ha)	Percentage study area	Flammable area (ha)	Non-flammable area (ha)*	Percentage non-flammable area
North Cascades	North Cascades Lowland Forests	596449	41.3	535839	60610	10.2
	North Cascades Highland Forests					
Okanogan-Chelan Hills	Chelan Tephra Hills	326895	22.6	319469	7426	2.3
	Chiwaukum Hills and Lowlands					
	Okanogan Pine-Fir Hills					
	Okanogan Valley					
	Missoula Flood Channeled Scablands					
Pasayten-Sawtooth Highlands	Pasayten-Sawtooth Highland Forests	352172	24.4	345148	7023	2.0
Wenatchee-Chelan Highlands	Wenatchee-Chelan Highland Forests	170029	11.8	158622	11407	6.7
Study Area		1445545	100.0	1359079	86466	6.0

*Classified in the FIREMON existing vegetation layer as water, ice, or barren

Table 11. "Landscape level" spatial metrics

Metric	Landscape structure measured by metric	Spatial grain of calculation	Formula
Total Area	Area		$TA = A\left(\frac{1}{10000}\right)$ A = total landscape area (m^2)
Contagion Index	Spatial Aggregation	Pixel	$CONTAG = \left[1 + \frac{\sum_{i=1}^{m}\sum_{k=1}^{m}\left[(P_i)\left(\frac{g_{ik}}{\sum_{k=1}^{m} g_{ik}}\right)\right] * \left[\ln(P_i)\left(\frac{g_{ik}}{\sum_{k=1}^{m} g_{ik}}\right)\right]}{2\ln(m)}\right](100)$ P_i = proportion of the landscape occupied by patch type i. g_{ik} = number of adjacencies between pixels of patch types i and k based on the double count method m = number of patch types present in the landscape, including landscape border if present
Aggregation Index	Spatial Aggregation	Pixel	$AI = \left[\sum_{i=1}^{m}\left(\frac{g_{ii}}{\max \rightarrow g_{ii}}\right)P_i\right](100)$ g_{ii} = number of like adjacencies between pixels of patch type i based on the single-count method max-g_{ii} = maximum number of like adjacencies between pixels of patch type i based on the single-count method. P_i = proportion of landscape in patch type i.

Table 11 (extended)

Description	Strengths	Limitations
Total area (*TA*) equals the total area (in square meters) of the landscape divided by 10000 to convert to hectares. In this study it is equal to the size of the fire.	Easy to interpret	
The Contagion Index measures spatial aggregation based on the number of pixel adjacencies that involve the same class. Pixel adjacencies are tallied using a double count method and a 4-neighbor rule. Values range from 0 to 100, with high disaggregation and high interspersion at low values, and high aggregation (contagion) at high values.	Contagion Index is normalized by dividing the observed contagion by the maximum possible contagion for a given number of classes.	Not normalized based on the minimum and maximum values possible for a given class area.
The Aggregation Index measures spatial aggregation based on the number of pixel adjacencies that involve the same class. In the calculation of this metric pixel adjacencies are tallied using a single count method, (2) landscape boarder is ignored, and (3) normalization is based on the maximum possible aggregation for a given class if the class were to be clumped into a single, compact patch. Values range from 0 to 100, with high disaggregation at low values, and greater aggregation at high values.	Aggregation Index is normalized based on the maximum possible aggregation for a given class if the class were to be clumped into a single compact patch.	Landscape boarder is ignored. Not normalized by the number of classes.

Table 12. "Class level" spatial metrics

Metric	Landscape structure measured by metric	Spatial grain of calculation	Formula
Class Area	Area		$CA = \sum_{j=1}^{a} a_{ij}\left(\frac{1}{10000}\right)$ a_{ij} = area (m^2) of patch ij
Proportion	Composition		$P_i = \frac{\sum_{j=1}^{n} a_{ij}}{A}(100)$ P_i = proportion of landscape occupied by patch type i. a_{ij} = area (m^2) of patch ij A = total landscape area (m^2)
Core Area	Composition and Spatial Aggregation	Patch	$CORE = a_{ji}^{c}\left(\frac{1}{10000}\right)$ a_{ig}^{c} = core area (m^2) of patch if based on specific edge depths (m)
Clumpiness Index	Spatial Aggregation	Pixel	$G_i = \left(\frac{g_{ii}}{(\sum_{i-1}^{m} g_{ii}) - \min e_i}\right)$ g_{ii} = number of like adjacencies between pixels of type i g_{ik} = number of adjacencies between pixels of types i and k $CLUMPY = \begin{bmatrix} \frac{G_i - P_i}{P_i} \text{ for } G_i < P_i \ \& \ P_i < .5, \text{ else} \\ \frac{G_i - P_i}{1 - P_i} \end{bmatrix}$ min e_i = minimum perimeter (in terms of the number of cell surfaces of patch type i for a maximally clumped class) P_i = proportion of the landscape in type i
Normalized Landscape Shape Index	Spatial Aggregation	Pixel	$nLSI = \frac{e_i - \min e_i}{\max e_i - \min e_i}$ e_i = total length of edge of class i in terms of the number of cell surfaces min e_i = minimum perimeter of class i in terms of the number of cell surfaces max e_i = maximum perimeter of class i in terms of the number of cell surfaces
Gini Coefficient	Patch Size Distribution	Patch	$G = \frac{\sum_{i=1}^{n}\sum_{j=1}^{n}\lvert x_i - x_j\rvert}{2n^2\bar{x}}$ x_i = the area of patch i n = number of patches $\bar{x}$ = mean patch size

Table 12 (extended)

Description	Strengths	Limitations
The class area is the sum of the area of all patches of the corresponding patch type divide by 10000.	Easy to interpret	
The sum of all the areas of a corresponding class type divided by the total landscape area, multiplied by 1000 to convert to a percentage, i.e. the percentage of the landscape made up of a given severity class	Easy to interpret	
The area in hectares of a severity class that is greater than 100m from the edge of a different severity class	Easy to interpret	Edge depth is inherently subjective
A metric of spatial aggregation computed based on the number of like pixel adjacencies for a given class. Pixel adjacencies are tallied using a double count method and a 4-neighbor rule. Values range from -1 to 1, with maximum disaggregation at 1, random distribution at 0, and maximum aggregation at 1.	Normalized to the number of classes.	
A metric of spatial aggregation computed based on the *length of edge* of a given class. Values range from 0 to 1, with maximum aggregation at 0, and maximum dispersion at 1.	Normalized to both the maximum and minimum number of like adjacencies.	
The Gini Coefficient measures the inequality in the size distribution of patches. A Gini Coefficient ranges from 0-1, and values close to 1 indicate that a small proportion of large patches make up most of the class area.	Is not influenced by the abundance of small patches on the landscape.	

Table 13. Area burned by subsection. The top table is based on mosaic raster calculated by year, and then summed over the whole subsection.

Ecological Subsection	Number of Fires	Total area of fires (ha)	Area burned twice or more (ha)	Area affected by fire at least once (ha)	Percentage of flammable area affected by fire at least once
North Cascades	51	10582	115	10467	2
Okanogan-Chelan Hills	30	99878	1133	98745	31
Pasayten-Sawtooth Highlands	32	126412	3840	122572	36
Wenatchee-Chelan Highlands	12	60918	1081	59838	38
Study Area	125	297790	6169	291622	21

Table 14. Burn severity by subsection, using three different methods to summarize data. Difference in the distribution of burn severity were less than one percent between yearly mosaic (a) and a mosaic with all years (b). Differences ranged from 0-4 percent when fires were not clipped to the study area boundary (c) and when they were (a and b).

a. Burn severity calculated based on annual burn severity images clipped to the study area boundaries

Ecological Subsection	Area burned at severity (ha)				Percentage area burned at severity level			
	High	Moderate	Low	Unchanged	High	Moderate	Low	Unchanged
North Cascades	2854	2981	1768	2979	27	28	17	28
Okanogan-Chelan Hills	28777	34500	17650	18951	29	35	18	19
Pasayten-Sawtooth Highlands	70550	25400	14176	16286	56	20	11	13
Wenatchee-Chelan Highlands	21702	16436	9682	13099	36	27	16	22
Study Area	123883	79317	43277	51314	42	27	15	17

b. Burn severity calculated based on a mosaic of all years, with burn severity from most recent fire year used in cases of overlapping fires.

Ecological Subsection	Area burned at severity (ha)				Percentage area burned at severity level			
	High	Moderate	Low	Unchanged	High	Moderate	Low	Unchanged
North Cascades	2837	2953	1748	2929	27	28	17	28
Okanogan-Chelan Hills	28533	34272	17400	18539	29	35	18	19
Pasayten-Sawtooth Highlands	69432	24699	13565	14669	57	20	11	12
Wenatchee-Chelan Highlands	21570	16120	9391	12757	36	27	16	21
Study Area	122372	78045	42103	48893	42	27	14	17

c. Burn severity calculated by individual fire, including areas outside the study area boundary.

Ecological Subsection	Area burned at severity (ha)				Percentage area burned at severity level			
	High	Moderate	Low	Unchanged	High	Moderate	Low	Unchanged
North Cascades	2329	2569	1696	2896	25	27	18	31
Okanogan-Chelan Hills	29887	33435	18495	23878	28	32	17	23
Pasayten-Sawtooth Highlands	80972	34625	18725	19593	53	22	12	13
Wenatchee-Chelan Highlands	16050	13552	7125	9353	35	29	15	20
Study Area	129238	84181	46041	55720	41	27	15	18

Table 15. Spatial pattern metrics based on "study-wide" and "subsection-wide" images.

Metric	Severity Class	Subsection				
		North Cascades Forests	Okanogan-Chelan Hills	Pasayten-Sawtooth Highlands	Wenatchee-Chelan Highlands	Study Area
Gini coefficient	High	0.88	0.91	0.97	0.93	
	Moderate	0.76	0.85	0.78	0.82	
	Low	0.57	0.62	0.61	0.59	
	Unchanged	0.84	0.88	0.82	0.85	
	All	0.79	0.84	0.87	0.83	
Maximum patch size (ha)	High	173	2721	18268	2842	
	Moderate	80	844	968	605	
	Low	21	88	116	51	
	Unchanged	341	2003	802	1560	
Percentage of burned area made up of the largest patch	High	1.63	2.72	14.45	4.67	
	Moderate	0.76	0.85	0.77	0.99	
	Low	0.2	0.09	0.09	0.08	
	Unchanged	3.22	2.01	0.63	2.56	
Mean patch size	High	2.2	1.9	5.7	2.1	3.3
	Moderate	0.8	1.1	0.7	0.9	0.9
	Low	0.3	0.4	0.3	0.3	0.3
	Unchanged	1.3	1.3	0.9	1	1
Total core area (ha)	High	394	4621	29008	6655	
	Moderate	0	0	0	0	
	Low	3	29	7	15	
	Unchanged	175	779	588	1706	
Core area percentage of landscape	High	4	5	24	11	
	Moderate	0	0	0	0	
	Low	0	0	0	0	
	Unchanged	2	1	0	3	
Normalized Landscape Shape Index	High	0.2	0.21	0.12	0.15	0.14
	Moderate	0.4	0.36	0.45	0.4	0.4
	Low	0.61	0.56	0.58	0.57	0.57
	Unchanged	0.3	0.31	0.33	0.27	0.3
Clumpiness Index	High	0.73	0.7	0.78	0.76	0.77
	Moderate	0.44	0.45	0.44	0.45	0.46
	Low	0.27	0.32	0.35	0.32	0.33
	Unchanged	0.58	0.62	0.62	0.65	0.63
Aggregation Index	All	65	66	75	69	70
Contagion Index	All	20	20	35	23	25

FIGURES

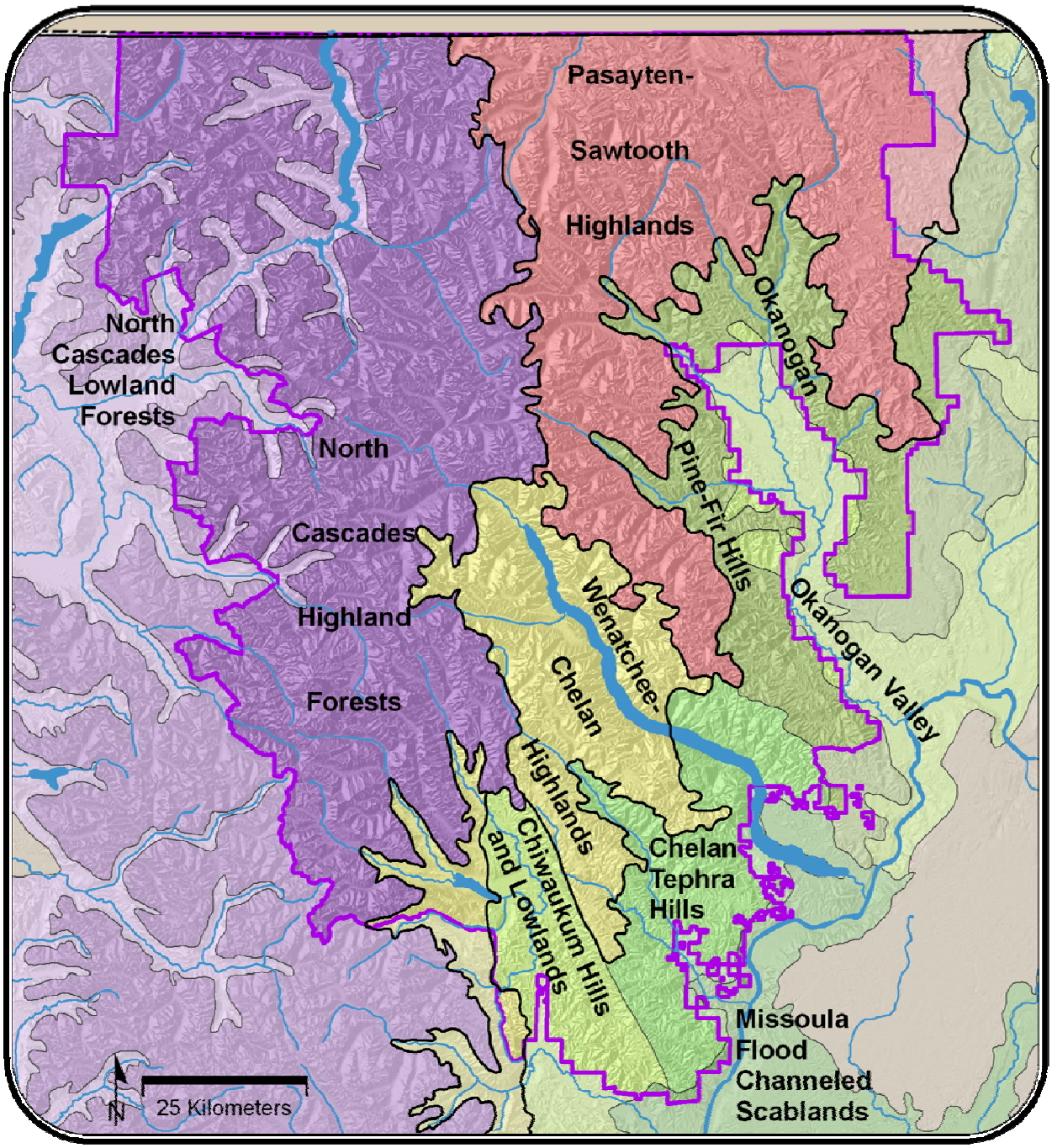

Figure 8. Ecological subsections. Grouped subsections are shown in similar colors, with the Okanogan-Chelan Hills in green, and the North Cascades in purple.

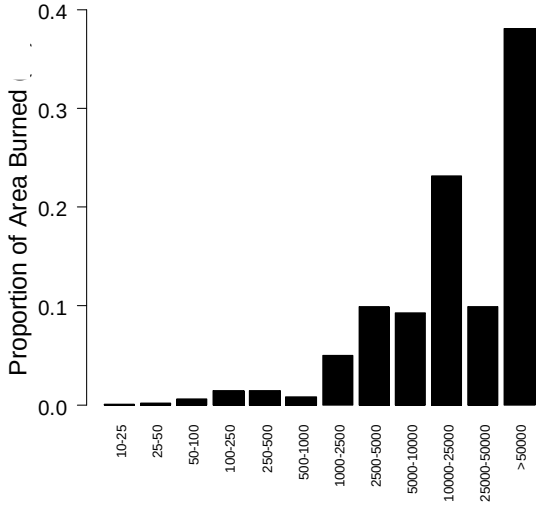

Figure 9. Proportion of area burned by fire size (ha) class.

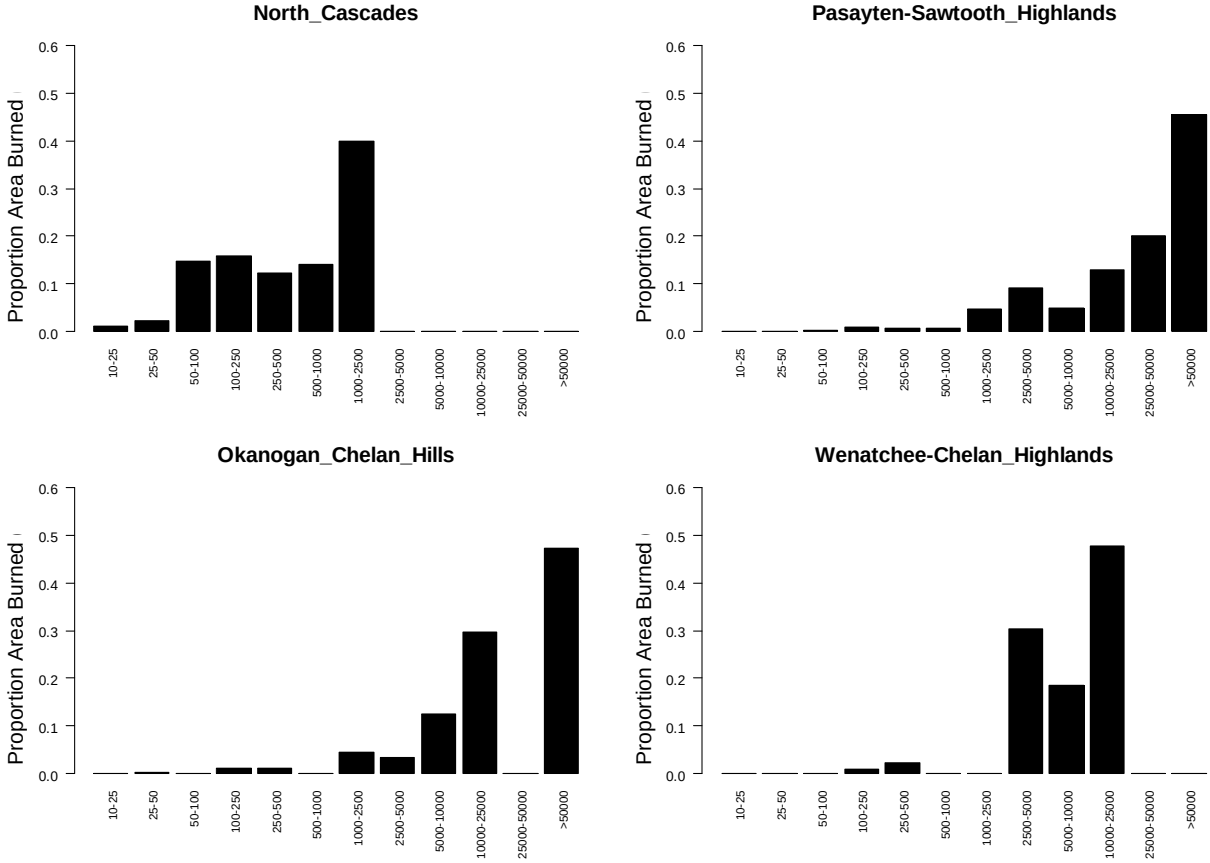

Figure 10. Proportion of area burned by fire size (ha) in each subsection.

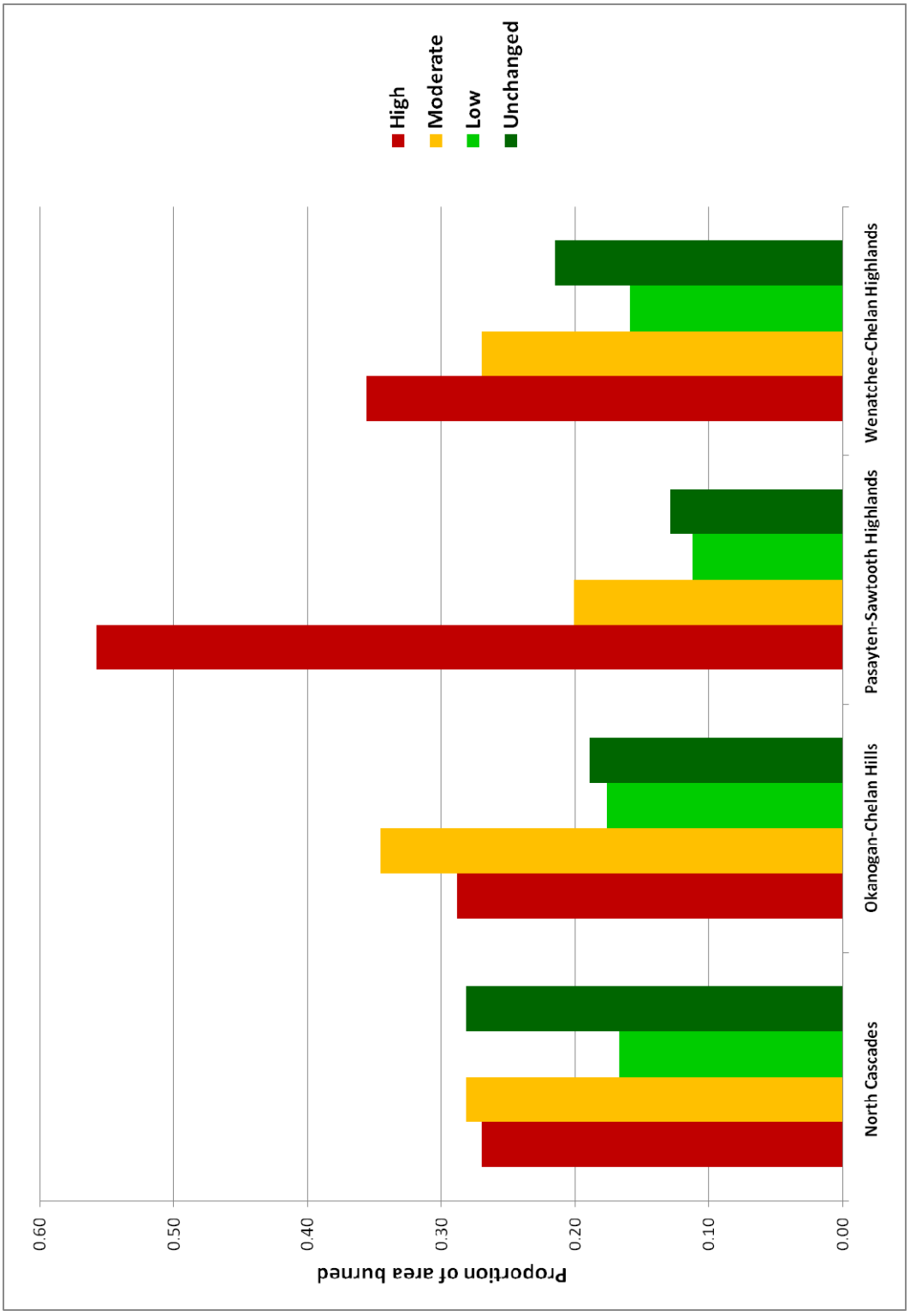

Figure 11. Burn severity by subsection. Graph is based on burn-severity totals calculated by year, and then summed over the subsection.

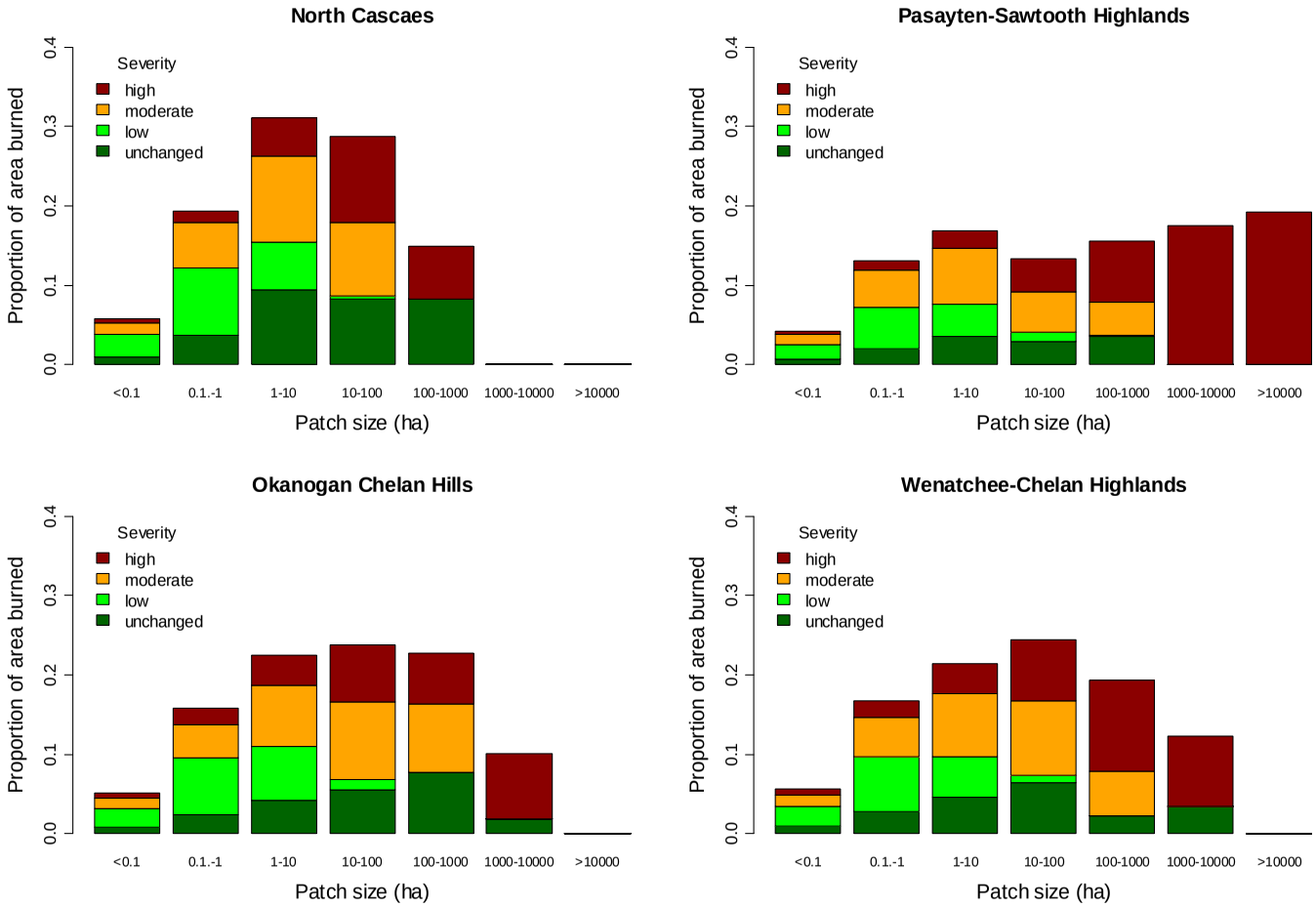

Figure 12. Proportion of total area burned in each subsection by severity patches of a given size class, based on the individual fire data. Severity patch size classes are in $\log_{10}$ bins from <0.1 ha to >10,000 ha.

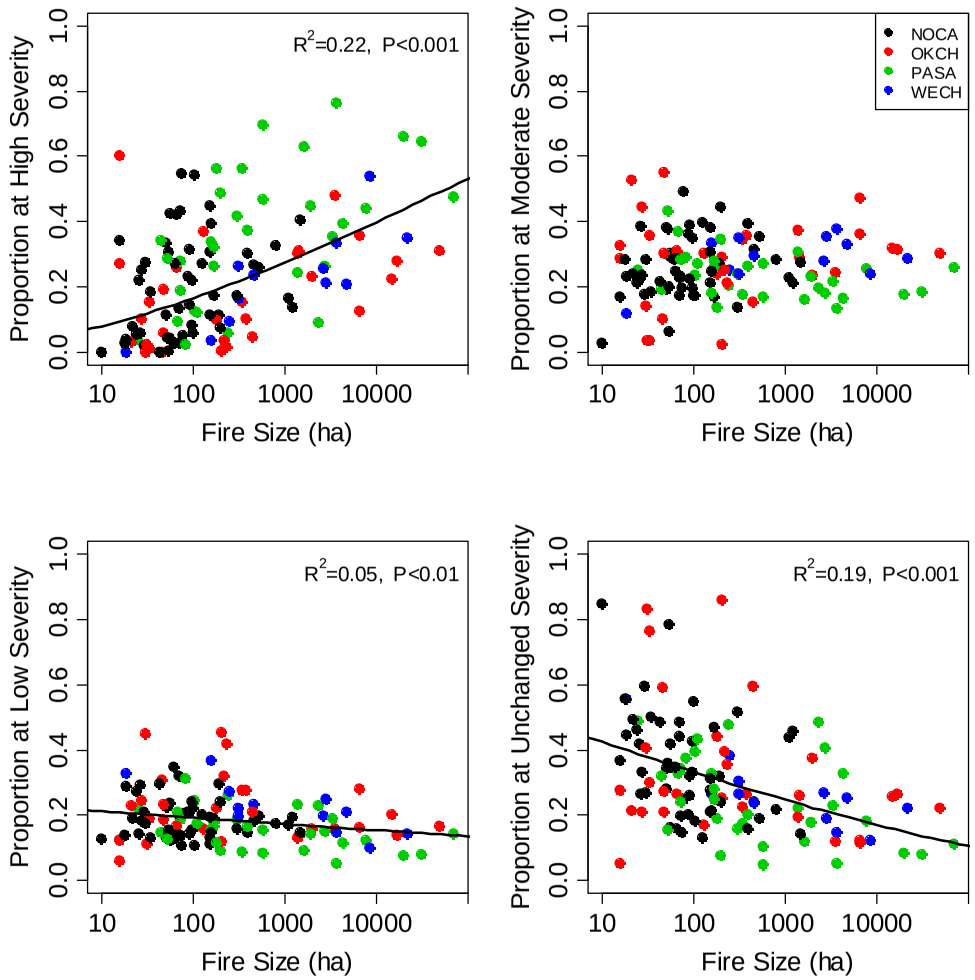

Figure 13. Regression plots for fire size and proportion burned at a given severity: high severity (upper left), moderate severity (upper right), low severity (lower left) and unchanged severity (lower right). Regression lines are for all subsections combined. Subsections are shown by color, with North Cascades (black), Okanogan-Chelan Hills (red), Pasayten-Sawtooth Highlands (green), and Wenatchee-Chelan Highlands (blue).

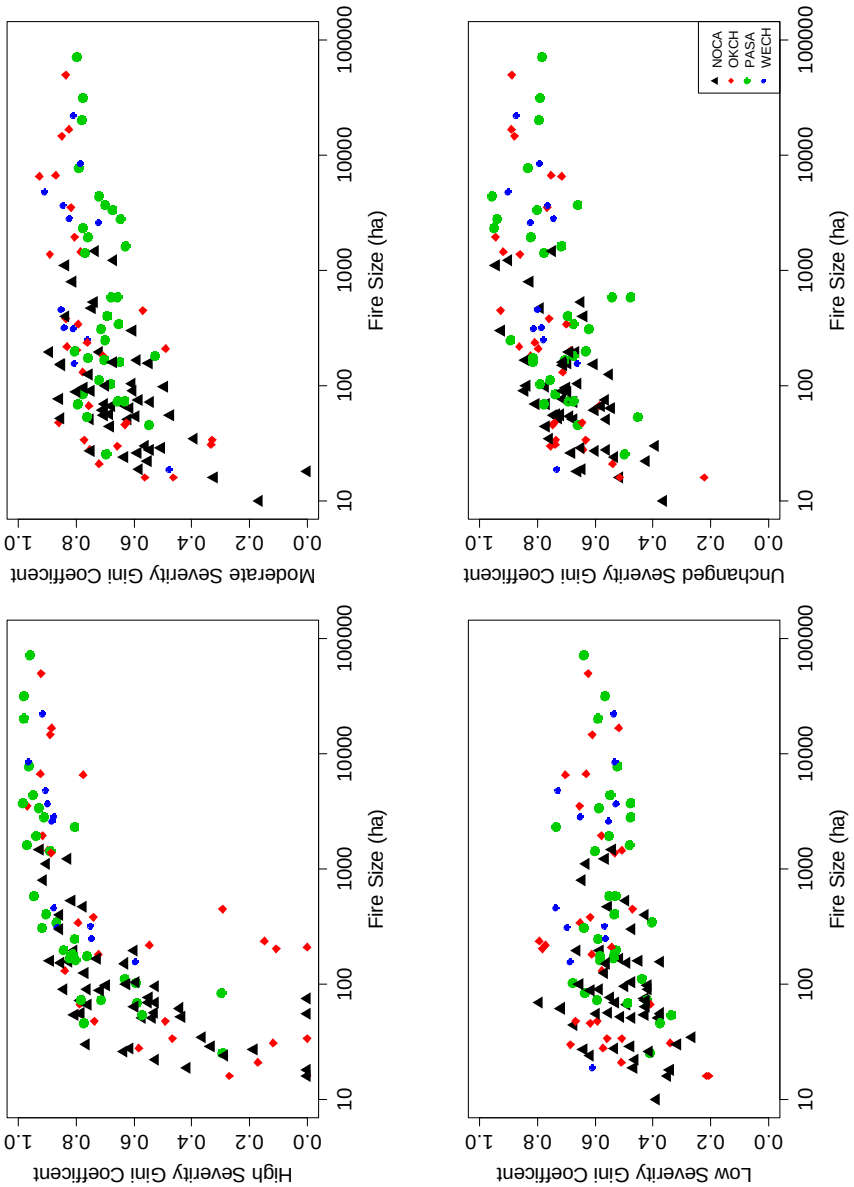

Figure 14. The Gini coefficient plotted against fire size, for high severity (top left), moderate severity (top right), low severity (bottom left), and unchanged severity (bottom right).

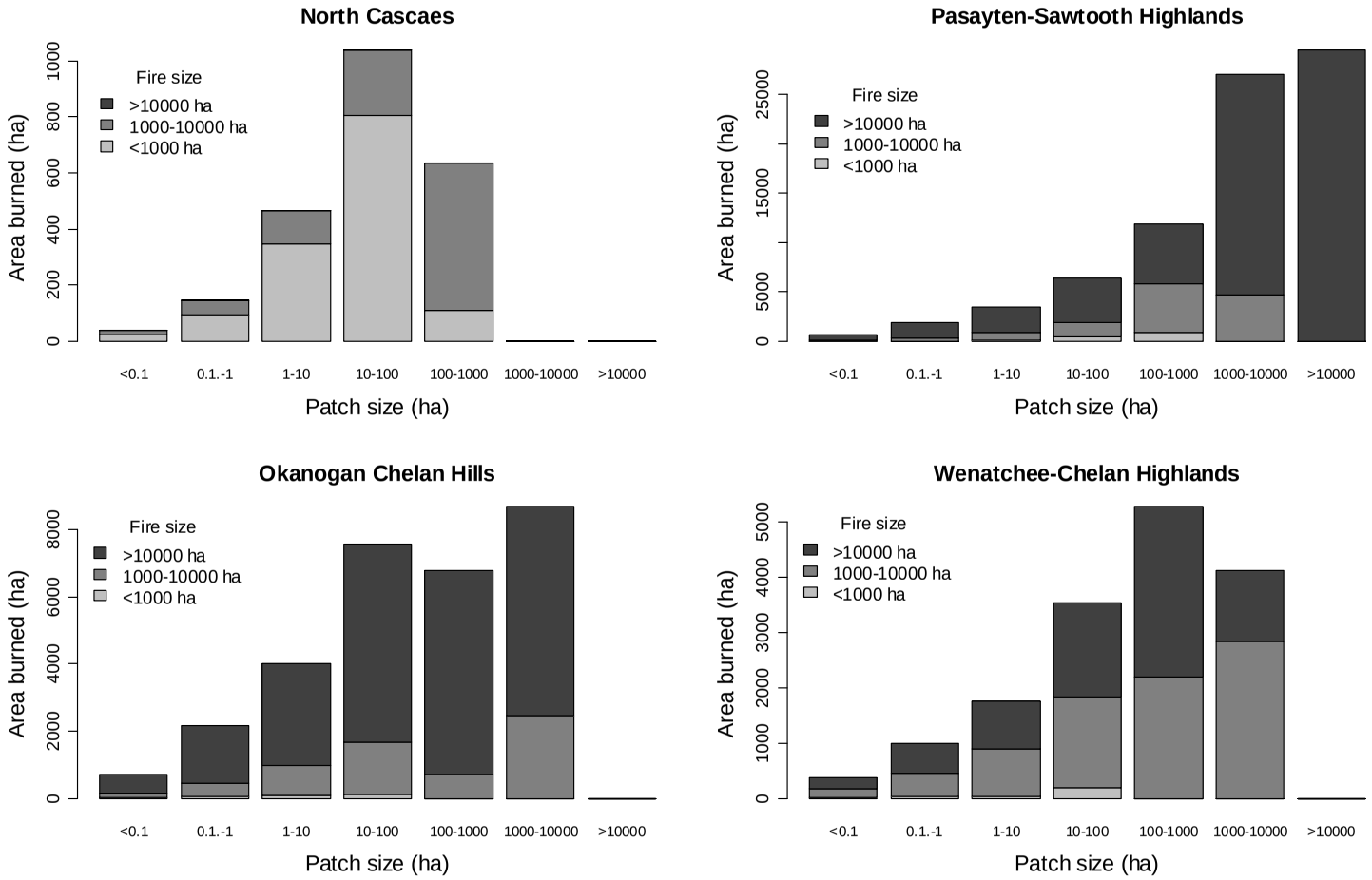

Figure 15. The total area burned in each subsection by high severity patches in a given size class. Shading shows patches that were created by fires of different sizes: under 1000 ha, 1000-10,000 ha, and over 10,000 ha. The y-axis is the total area burned by all fires in a subsection; note that the y-axes differ between plots.

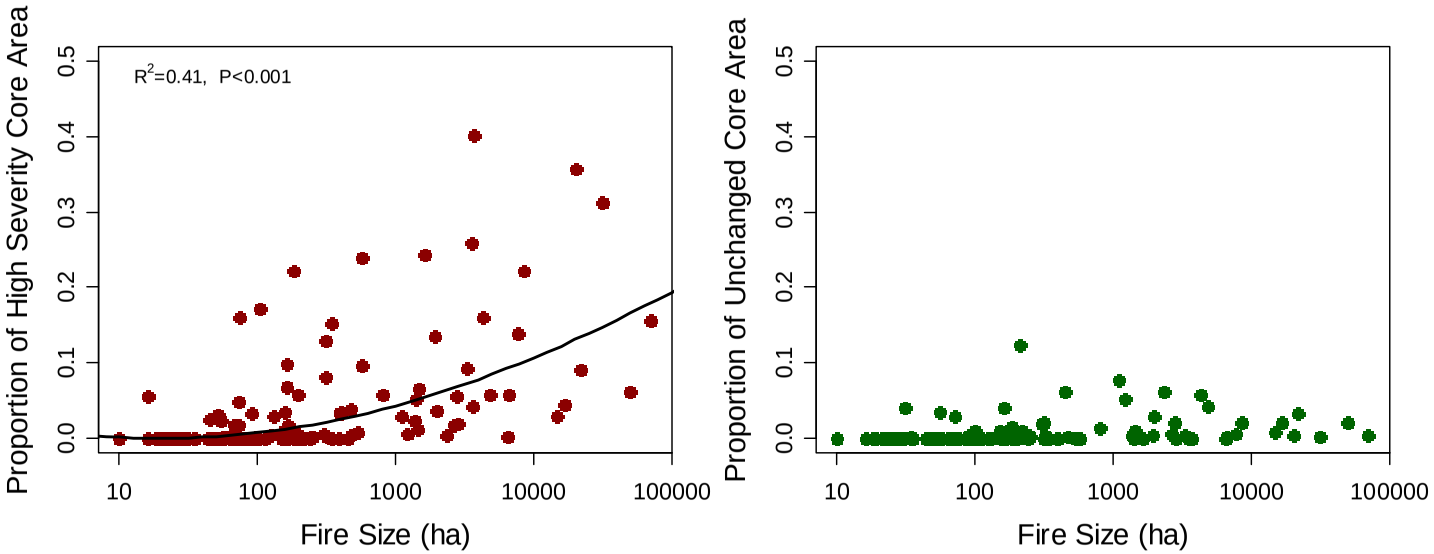

Figure 16. High severity core area increases with fire size (left), whereas unchanged severity core area was not significantly related to fire size.

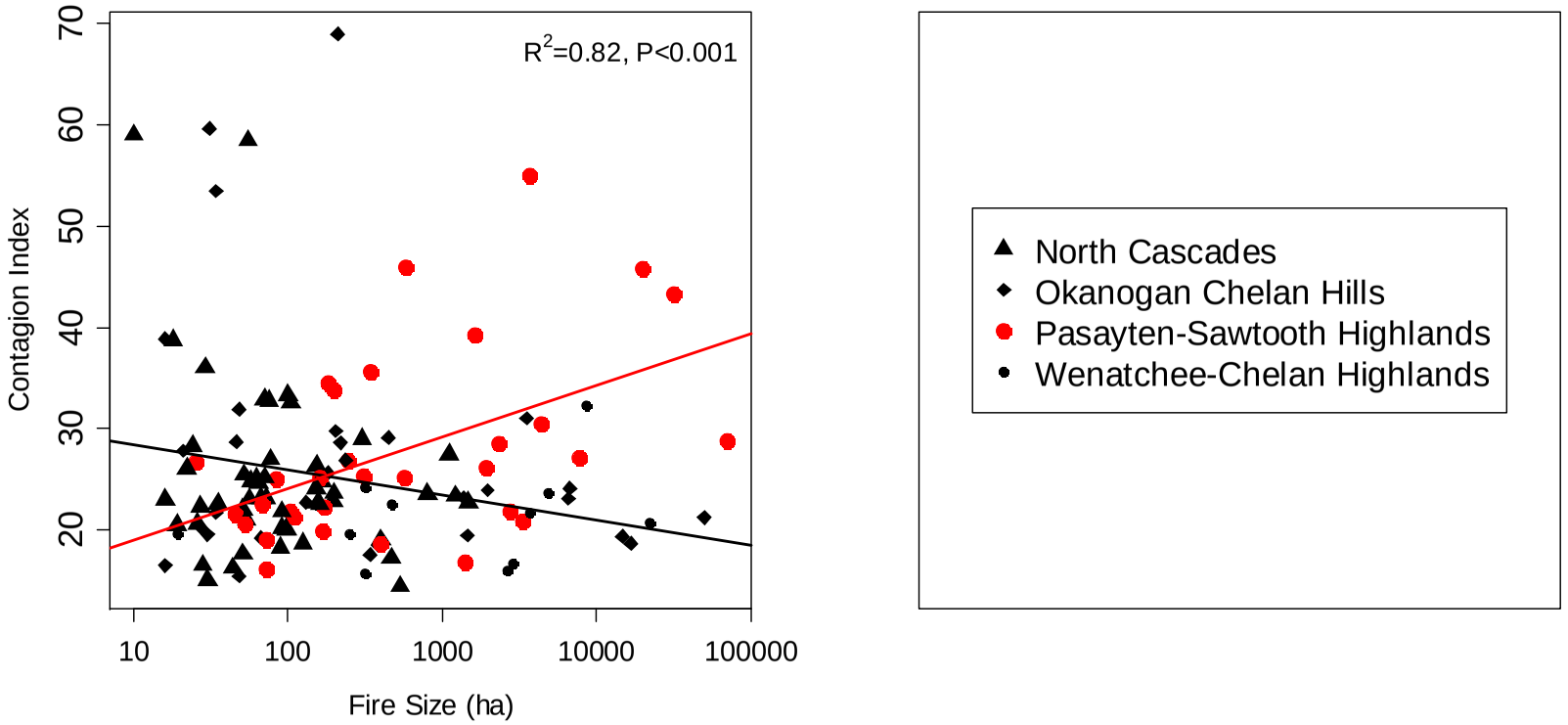

Figure 17. Contagion index calculated across all severity classes, plotted against fire size. Contagion increased in the Pasayten-Sawtooth Highlands as fire size increased ($P < 0.001$). In other subsections contagion decreased with fire size ($P < 0.001$), but also was heteroscedastic; note the high variance at small fire sizes, and decreasing variance at large fire sizes. The regression for the Pasayten-Sawtooth Highlands is shown in red, and the regression line for all other subsections combined is shown in black. The R^2 and P-value are shown for the full model (Pasayten-Sawtooth as one group, and all other subsections combined as a second group.)

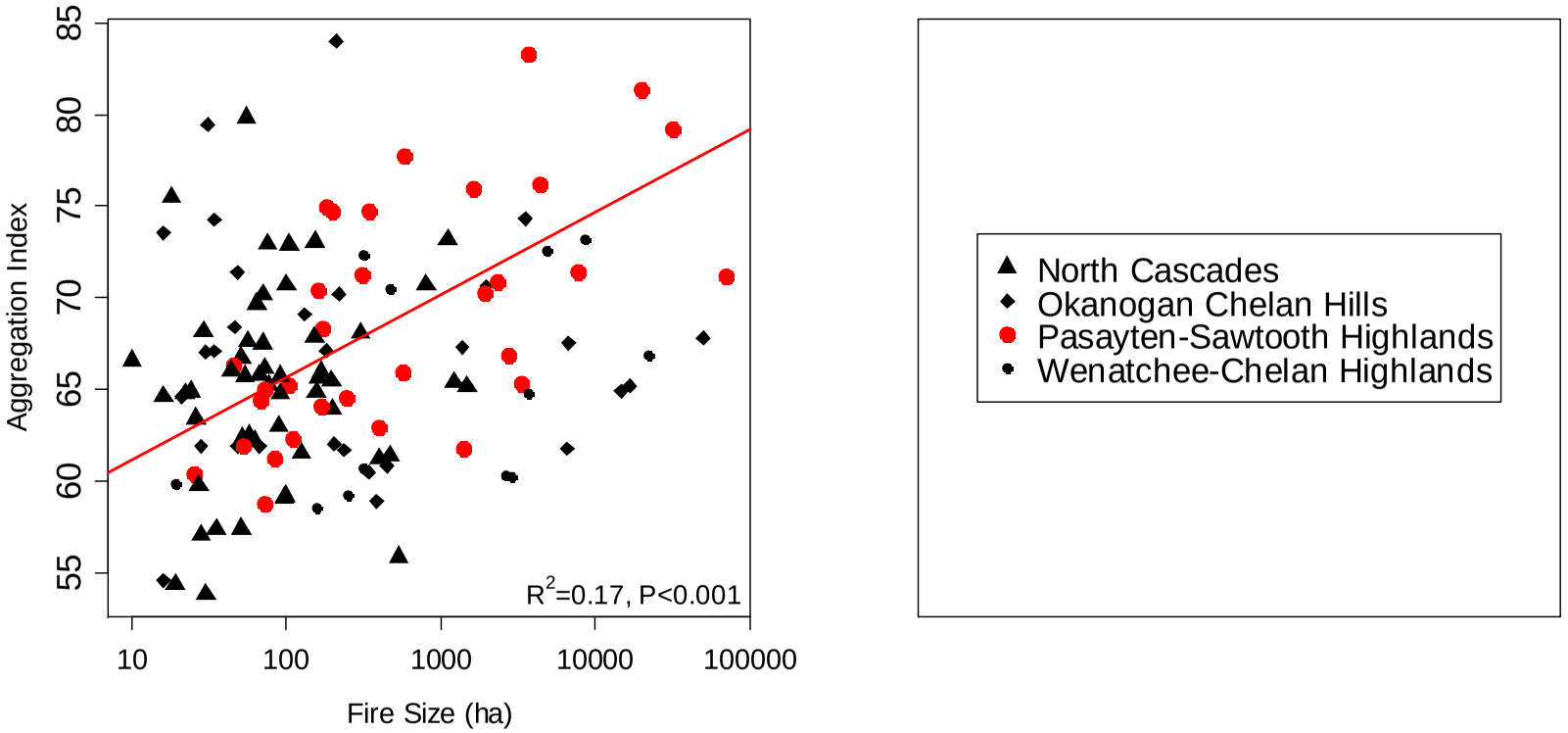

Figure 18. Aggregation index calculated across all severity classes, plotted against fire size. In other subsections there was no significant trend with fire size. Aggregation increased in the Pasayten-Sawtooth Highlands as fire size increased (red line, P = 0.005), but other subsections, either combined as a group or individually, did not have a significant relationship with fire size. The R^2 and P-value are shown for the full model (Pasayten-Sawtooth as one group, and all other subsections combined as a second group.)

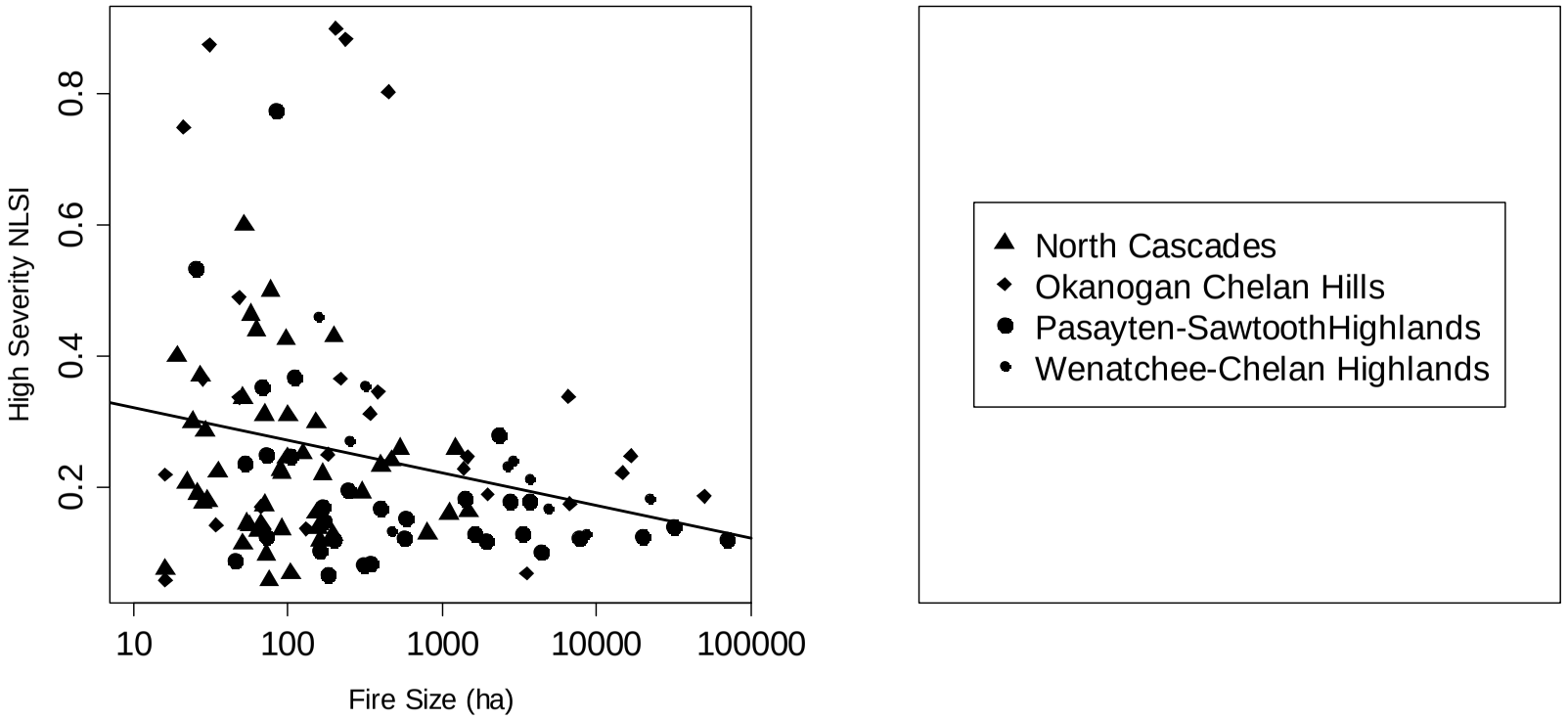

Figure 19. High severity NLSI plotted against fire size. NLSI decreases with fire size (solid black line, $P = 0.009$, $R^2 = 0.06$), indicating decreased spatial complexity. Based on ANCOVA, NLSI values for the Okanogan-Chelan Hills were significantly higher than the North Cascades ($P < 0.001$) and the Pasayten-Sawtooth Highlands. There is also a trend of decreasing variance as fire size increases.

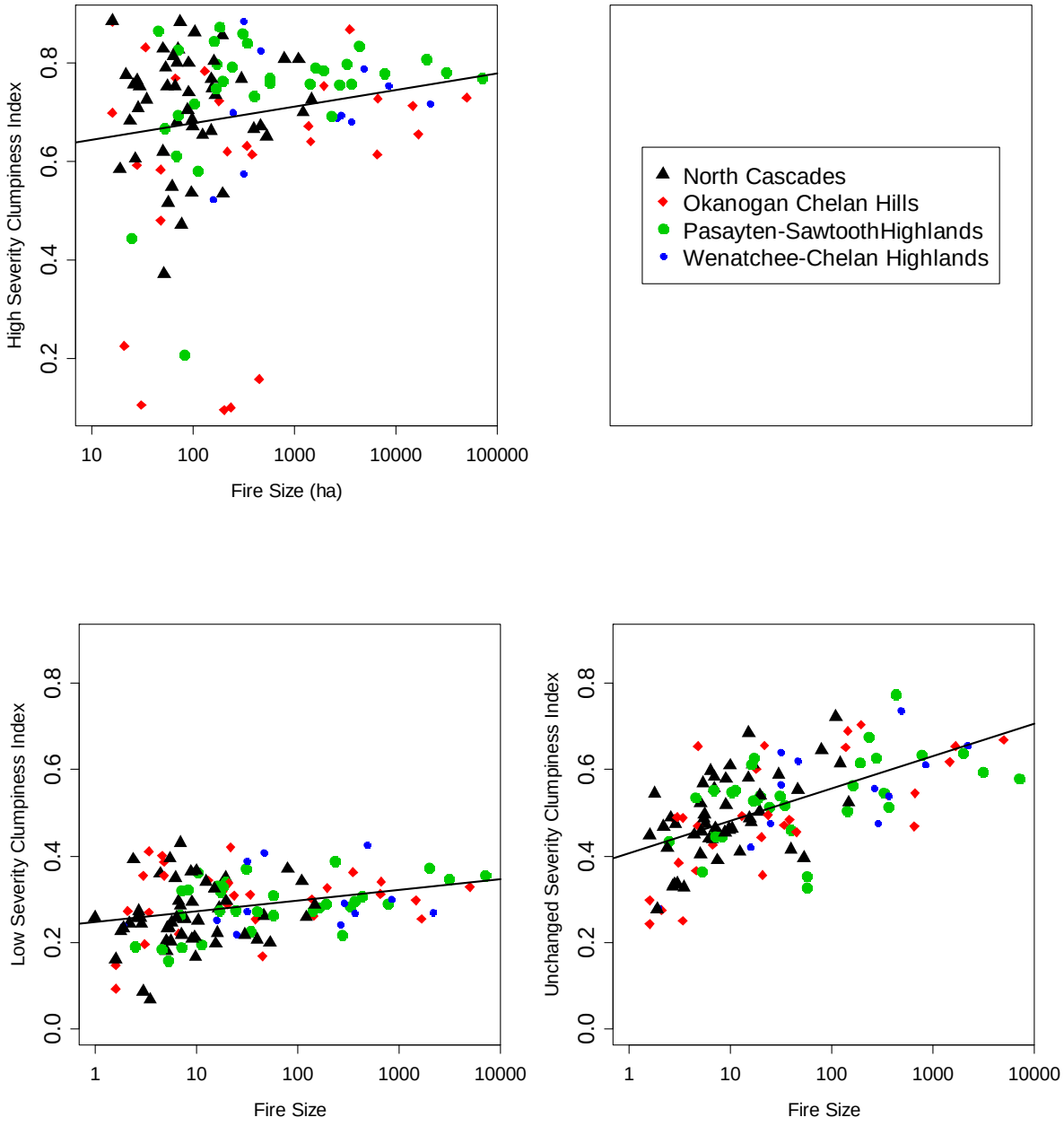

Figure 20. Clumpiness index plotted against fire size for high severity (top left), low severity (bottom left) and unchanged severity (bottom right). The solid black line indicates the regression for all subsections combined. Based on ANCOVA, the Okanogan-Chelan Hills had significantly lower high severity clumpiness values than the North Cascades. There was no significant difference between subsections, and for both high severity and low severity variance decreased as fire size increased.

CHAPTER 3: CLIMATE AND TOPOGRAPHICAL INFLUENCES ON BURN SEVERITY IN THE NORTHERN CASCADE RANGE, WASHINGTON, USA

ABSTRACT

I examined the influence of annual climate and topographical complexity on the occurrence, size, severity, and within-fire severity pattern of fires in the northern Cascade Range of Washington, USA. Landsat Thematic Mapper (LTM) data were used to quantify fire severity for all fires greater than 10 ha (n = 125) that occurred during a 25-year period (1984-2008). Categorical burn-severity images were developed from an index of burn severity (Relative differenced Normalized Burn Ratio) derived from LTM data and parameterized with data from 639 field plots.

My results show that the fire regime of the northern Cascade Range responds to annual climatic variation. Spring snowpack and summer temperature were negatively and positively correlated, respectively, with fire occurrence, and summer temperature was positively correlated with annual area burned, the proportion of landscape burned at high severity, and spatial aggregation of the high-severity class. Nevertheless, the within-fire severity mosaic reflects the underlying topographic complexity. Fires in areas with greater topographical complexity had increased spatial complexity of burn severity.

Several recent studies in the western United States have documented a positive relationship between warm and dry climate and annual area burned. The relationship between climate drivers and fire-regime attributes identified in this study—a positive relationship between warm and dry conditions and the proportion of area burned at high severity and spatial aggregation of high severity patches—adds nuance to the climate-area burned relationship documented in previous studies.

INTRODUCTION

Regional studies in western North America have shown that climate has a strong influence on fire occurrence and annual area burned (Heyerdahl et al. 2002, McKenzie et al. 2004, Schoennagel et al. 2005, Westerling et al. 2006, Kitzberger et al. 2007, Brown et al. 2008, Heyerdahl et al. 2008, Morgan et al. 2008, Littell et al. 2009), but which aspects of climate drive fire occurrence and area burned vary with the location and scale of the study. For example, climate drivers of annual area burned vary regionally, with climate drivers in mountainous ecosystems exhibiting strong relationships with growing-season precipitation, temperature, and the Palmer Drought Severity Index (PDSI), and climate drivers in grass-dominated regions showing a positive relationship between area burned and winter or spring precipitation as well as PDSI (Littell et al. 2009).

The association between climate and annual area burned is of interest because climate change will influence fire regimes. Numerous studies worldwide have projected an increase in fire occurrence and area burned in boreal and temperate regions (Flannigan et al. 2009). Regional studies have also projected increases in area burned with future climate. Based on statistical relationships with annual area burned and a number of climate drivers, Littell et al. (2010) projected that annual area burned in forest ecosystems in the Pacific Northwest will increase by a factor of 3.8 by the 2040s compared to 1980-2006 reference conditions. Because individual climate variables, such as temperature and precipitation, are likely to change at different rates, understanding which climate variables are most closely associated with fire-regime attributes for a given geographic location is important.

Under warmer and dryer future climate, fires may not only be more frequent and larger in size, but may also burn with higher severity and a more aggregated spatial pattern (Duffy et al. 2007, Holden et al. 2007, Keane et al. 2008, Haire and McGarigal 2009, Lutz et al. 2009b). Burn severity is of interest because it is a more direct indication of the ecological impact of fire than area burned. Burn severity influences the composition and structure of post-fire vegetation (Romme et al. 1995, Turner et al. 1997, Turner et al. 1999, Saab et al. 2004, Baker et al. 2007, Lentile et al. 2007, Keane et al. 2008). The spatial pattern of severity influences post-fire seed dispersal, succession (Turner et al. 1994), and wildlife habitat quality (Romme et al. 1995, Saab et al. 2004, Roberts et al. 2008).

Increased burn severity is associated with warmer and dryer climate in some systems. Haire and McGargal (2009) examined twenty fires in the southwestern USA, and found that ENSO was weakly correlated with proportion of area burned at high severity and spatial aggregation of high-severity fire. Other studies have used fire size as a surrogate for climate, in order to make inferences about how severity and spatial pattern may change. In Yosemite National Park, CA, the proportion of area burned at high severity increased with the annual area burned (Lutz et al. 2009a). Keane et al. (2008) examined burn severity on 11 large fires (>10500 ha) and 25 small fires (<2200 ha) in the northern Rocky Mountains and found that on average large fires burned with higher severity and had lower patch density (i.e. larger patches) and less edge than small fires, but that the spatial complexity of burn-severity classes within fires did not vary significantly with fire size.

Topography, i.e. slope and aspect, influences fire behavior and spread (Agee 1993), and can be strongly correlated with burn severity (Lentile et al. 2006b, Collins et al. 2007, Holden et al. 2009). When Sierra mixed-conifer forests have high fuel moisture, little of the landscape

burns at high severity, but under dryer conditions burns are more heterogeneous (Collins et al. 2007). In the Gila National Forest of New Mexico, USA, high burn severity occurred more frequently at higher elevations, on north-facing steep slopes, and at wet cool sites, and the occurrence of high burn severity could be predicted with 80% accuracy from topographic attributes (Holden et al. 2009).

The influence of climate on fire occurrence is moderated by the complexity of topography. In the Blue Mountains of OR, USA, regional variation in the frequency of fire was correlated with regional climate, but within individual watersheds, the frequency of fire occurrence was related to topography except in the watershed with few barriers to fire spread (Heyerdahl et al. 2001). Topographic complexity is associated with longer mean fire-return intervals pre-European settlement in forested systems in the Ozark Highlands. (Guyette et al. 2002). Kellogg et al. (2008) found that in complex terrain, synchrony of fire occurrence took place at smaller spatial scales, whereas regional climate synchronized fire occurrence over larger spatial scales in gentler terrain. In an analysis of burn severity in Alaskan boreal forests, Duffy et al. (2007) found that burn severity is more variable in areas of higher topographic complexity, and the burn severity is significantly correlated with vegetation type in flat landscapes but not in topographically complex landscapes. Using burn-severity data from 20 fires in the southwestern US, Haire and McGarigal (2009) found that small changes in topography, specifically a shift from low to moderate complexity, significantly decreased burn severity.

My research provides an empirical basis for predicting fire-related landscape pattern under current and future climate by examining the influences of climate and topography on burn severity and its spatial pattern in the northern Cascade Range of Washington, USA. I used a 25-year record of fire occurrence, area burned, satellite-derived burn severity, and climate during

1984-2008. I analyzed spatial aggregation of burn severity with spatial statistics. I examined the relationship between individual climate variables—temperature, relative humidity, precipitation, and spring snowpack—and fire regime attributes—fire occurrence, area burned, burn severity, and burn severity spatial pattern. I also examined the relationship between topographic complexity and fire size, burn severity, and burn severity spatial pattern for individual fires.

The overarching motivation for this research is to understand how climate and topography influence burn severity and burn-severity patterns in mixed- and high-severity fire regimes. First, I test the hypothesis that increased summer temperature and decreased summer relative humidity, summer precipitation, and spring snow water equivalent area positively correlated with: (1) increased fire occurrence, (2) increased area burned, (3) increased burn severity, and (4) decreased spatial complexity of burn severity. Second, I test the hypothesis that topographic complexity (1) limits fire size, (2) limits high burn severity, and (3) is positively correlated with increased spatial complexity of burn severity.

METHODS

STUDY AREA

The northern Cascade Range has steep climatic (summer temperature and annual precipitation) and topographic (complex to more rolling) gradients. The study area includes a large contiguous section of federally managed land, including all of North Cascades National Park and portions of the Okanogan-Wenatchee National forests from the southern edge of Glacier Peak Wilderness east to the southern portions of the Lake Chelan watershed, and north to the Canada border (Figure 21). Higher summer drought due to decreasing precipitation occurs from west to east in the study area (Franklin and Dyrness 1988). Terrain near the Cascade Crest,

which lies in the western portion of the study area, is steep and highly dissected due to past uplifts and glaciations (Franklin and Dyrness 1988, Tabor and Haugerud 1999). The northeastern and eastern parts of the study area have more open rolling terrain.

DATA SOURCES

Fire occurrence, area burned, and burn severity

Fire locations were determined from geospatial fire-occurrence data from federal land management agencies. Burn severity was measured with the Relative differenced Normalized Burn Ratio (RdNBR) (Miller and Thode 2007) one year after the fire for all fires over ten hectares in the study area from 1984 through 2008 (n = 125). RdNBR is based on the Normalized Burn Ratio (NBR), an index of burn severity based on the near- and mid-infrared bands of Landsat Thematic Mapper (LTM) data. RdNBR is calculated by taking the difference between the pre-fire and post-fire NBR, normalized by the square root of the pre-fire NBR. Unclassified RdNBR images and fire perimeters were developed by the US Geological Survey National Center for Earth Resources Observation and Science (EROS), using quality controls of the Monitoring Trends in Burn Severity project (Zhu et al. 2006, Severity 2008). Burn severity was classified into high severity, moderate severity, low severity, and unchanged (unburned or no difference detectable by satellite), and calibrated with field data from 639 field plots located in four fires within the study area (Chapter 1).

Burn-severity pattern

The spatial pattern of the categorical burn-severity data was analyzed in FRAGSTATS (McGarigal et al. 2002). The composition of the burned area was measured by the proportion of area in each severity class. The spatial pattern of burn severity was measured across all burn severity classes (the "landscape level" described in the FRAGSTATS user's manual) and for

individual burn severity classes (the "class level" described in the FRAGSTATS user's manual) (McGarigal et al. 2002). I calculated spatial aggregation of patches (patch density, and mean patch size) and pixels (Aggregation Index and Normalized Landscape Shape Index), and core area, defined as the area greater than 90 meters from the edge of a patch. Core area is a measure of both the size and shape of patches and the composition (amount of "patch interior") of the landscape. For the climate analysis, I used the landscape pattern of all fires in the study area. For the analysis of topographic complexity, I calculated spatial metrics for each individual fire.

Climate

I used climate observations from Remote Automated Weather Stations (RAWS) and snow telemetry stations (SNOTEL). RAWS stations provide monthly observations of temperature, precipitation, and relative humidity (RH). Eight RAWS stations are located in or near the study area. After reviewing station records for quality and completeness, I identified two stations that had high-quality complete records for summer months during 1986-2008: the Douglas Ingram RAWS station for July and August and the Camp Four RAWS station for June.

The Washington State SNOTEL network uses snow pillows to measure the water content of snow per unit area, or snow water equivalent (SWE). Spring SWE reflects both the total precipitation in the winter and the rate of snowmelt in the spring, so it is indicative of the length of the summer fire season. Of the 14 SNOTEL stations in or near the study area, only 6 measured SWE for the whole study period. I used the average annual peak SWE from these stations in the analysis.

All climate observations were converted to annual anomalies for analysis, by subtracting each observation from the 1984-2008 mean, and then dividing by the standard deviation.

Exploratory data analysis indicated that RAWS observations from July and August were more strongly correlated with fire regime attributes than those from June, so I used July and August as climate predictors in regressions. The relationship between fire-regime attributes and peak SWE anomalies was tested for each of the six stations. Due to high correlation between observations at different stations, only 1 station was used as a predictor. The most easterly stations, Pope Ridge and Salmon Meadows, were weakly correlated with the other stations, likely reflecting their consistently low SWE levels, early snow-free dates (often by the first of March), and lower variation in peak SWE between years. Observations from the other 4 stations were strongly correlated, so I used SWE from the station that was most centrally located in the study area, the Lyman Lakes station.

To test the relationship between fire occurrence (count data) and climate variables, I used a generalized linear model of the Poisson family. Area burned and burn-severity spatial pattern were modeled as a function of the climate variables using both simple and multiple linear regression. A $\log_{10}$ transformation was applied to the total area burned and the total core area. To model the proportion of area burned at a given severity an arcsine/square-root transformation was applied to the response variable, following the formula given in (Kutner et al. 2005):

$$2 * arcsine\sqrt{proportional\ severity}$$

I used backward elimination to find the most parsimonious model without a significant loss of explanatory power. All statistical tests were performed in the statistical program R (R Core Development Team 2010).

Topography

I calculated two metrics of topographical complexity from 30-m digital elevation models (DEMs) for each fire: topographic fractal dimension (Kellogg et al. 2008) and the surface-to-area ratio ("Jenness topographic roughness") (Jenness 2004). Linear regression was used to predict fire size and spatial pattern metrics from topographic complexity. The fractal dimension is a cross-scale measure of topographic complexity. It is based on the Hurst exponent, or the slope of the logarithm of the standard deviation of elevation within a varying-size window regressed against the logarithm of the window lengths. For a 3-dimensional surface, the fractal dimension is 3 – the Hurst exponent:

$$D = 3 - H$$

where: $H = \beta \log(\sigma) = a + \beta \log(\tau)$

D= Fractal Dimension

H = Hurst exponent

σ = average standard deviation of elevation

τ = window length

Window lengths started at 60 m (2 pixels) and increased by a factor of 2 over 6 window sizes to a maximum of 1920 meters (6 pixels). I computed the fractal dimension in ArcGIS using the spatial analyst extension, and a script written in the PYTHON programming language. Moving windows that overlapped by one pixel were used as samples. Fractal dimension was calculated only on the 47 fires over 300 hectares, which were large enough to fit 6 window lengths within their perimeters.

The surface area is calculated by generating 8 3-dimensional triangles connecting each cell center point with the center points of the 8 surrounding cells, summing the area of each triangle. The surface-to-area ratio for this cell is simply this surface area divided by the planar area of the cell. The ratio is then calculated over the entire fire. The surface-to-area ratio was

calculated with an extension for ArcGIS freely available at http://www.jennessent.com/arcview/surface_areas.htm.

RESULTS

CLIMATE

Fire occurrence and area burned

Fire occurrence was significantly correlated with spring SWE, July maximum average temperature, and July RH (Figure 22). The best GLM used both spring SWE and July maximum average temperature, and explained 54.8% of the deviance ($P < 0.001$). Area burned was significantly correlated with July temperature and July RH, but not with spring SWE (Figure 22). The best linear regression model used only July maximum average temperature, and explained 46.6% of the variance ($P < 0.001$). Interestingly, despite being correlated with fire occurrence, spring SWE was not significantly correlated with annual area burned.

Burn severity

Climate (July temperature) was correlated with the proportion of area burned at high severity ($R^2 = 0.27$, $P = 0.012$) and the proportion of unchanged area ($R^2 = 0.36$, $P = 0.003$), but not the proportions of low and moderate severity (Figure 23). The proportion of unchanged area was weakly positively correlated with August RH ($R^2 = 0.19$, $P = 0.038$).

Burn severity pattern

Across the entire landscape, mean patch size was positively correlated with July temperature ($R^2 = 0.37$, $P = 0.003$) (Figure 24). Patch density, Contagion Index and Aggregation

Index were not correlated with any climate variables. High-severity "patch density" showed the opposite relationship from that I expected: it was weakly positively correlated with July temperature ($R^2 = 0.18$, $P = 0.050$) and negatively correlated with July RH ($R^2 = 0.28$, $P = 0.011$) (Figure 25). Although the relationship with patch density indicates that patch sizes decreased with increased summer temperature, high-severity mean patch size was not correlated with any climate variables, and the proportion of high-severity core area was significantly positively correlated with July temperature ($R^2 = 0.36$, $P = 0.003$). This observed relationship between July temperature and high-severity core area follows the expected relationship of increased spatial aggregation with high severity. Of the two indices of pixel-based spatial aggregation, Clumpiness index was not correlated with any climate variables, but NLSI was weakly negatively correlated with spring SWE ($R^2 = 0.24$, $P = 0.017$) and August precipitation ($R^2 = 0.18$, $P = 0.047$). Observations from one year were very influential outliers, however, driving and neither model was significant at $\alpha=0.05$ if that year was dropped.

In the unchanged severity class, Clumpiness index was weakly positively correlated with August RH ($R^2 = 0.17$, $P = 0.049$), but no other significant correlations between unchanged severity pattern and climate variables were found. There were no significant correlations between the spatial patterns of the moderate and low burn severity classes and climate variables.

TOPOGRAPHY AND WITHIN-FIRE SPATIAL PATTERN

The results for the two measures of topographical complexity were different. The fractal dimension of topography was not significantly correlated with fire size, burn severity, or spatial pattern metrics, but surface-to-area ratio was significantly correlated with burn-severity pattern. The lack of correlation for fractal dimension may be because of its smaller sample size and high

variability, limiting statistical power, or because the fractal dimension of topography is a cross-scale method of assessing topographic complexity whereas the spatial metrics were calculated at the scale of the fire.

Based on the surface-to-area ratio, burn-severity spatial complexity increased with topographical complexity. As surface-to-area ratio increased overall patch sizes decreased, as can be seen by the positive correlation with patch density ($R^2 = 0.08$ $P = 0.001$) and negative correlation with mean patch size ($R^2 = 0.08$, $P = 0.049$) (Figure 26). As surface-to-area ratio increased spatial complexity of burn severity at the landscape level also increased. Surface-to-area ratio was positively correlated (though weakly) with the contagion index ($R^2 = 0.09$, $P < 0.001$) and aggregation index ($R^2 = 0.13$, $P < 0.001$) (Figure 26). Of the within-class spatial metrics, only the proportion of high-severity core area was significantly correlated with surface-to-area ratio, and that correlation was also weak ($R^2 = 0.05$, $P = 0.013$). Despite the weak correlation, visual inspection indicates that there are reasonably well defined domains in this bivariate relationship (Figure 27), and that high topographic complexity may still limit the fire size, the proportion of area at high severity, and proportion of high severity core area.

DISCUSSION

In the northern Cascade Range fire-season climate (July temperature) is more important than antecedent climate (winter snowpack) for predicting fire occurrence and area burned. This differs from the strong relationship between area burned and spring SWE found in Yosemite, CA, where and SWE explained 69% of the variance in fire occurrence ($P<0.001$) (Lutz et al. 2009c), and from the observed climate-area burned relationship for the Coast Range and Cascade

Range of Oregon and Washington, in which the best model for predicting area burned included growing season precipitation, winter precipitation, winter temperature, the previous year's winter precipitation, and previous year's summer precipitation (Littell et al. 2009).

The relative lack of importance of spring SWE in predicting area burned in the northern Cascade Range suggests that summer climate is more important than winter climate, in that summers may stay cool enough that fuels do not dry out. This differs from the Southwest, the Sierra Nevada, and the southern Cascade Range, where fuels almost always become dry enough during the summer to burn. In these other locations, spring SWE, which influences the overall length of the fire season (Westerling et al. 2006), is more clearly associated with area burned and fire occurrence. This implies that the primary climate variable associated with area burned for a given region may change as the climate changes. For example, if summer climate in the northern Cascade Range changes so that fuels are almost always dry enough to burn, a stronger relationship between spring SWE and annual area burned may develop.

I expected increased spatial aggregation under warmer and dryer climate, but found decreased spatial aggregation based on patch size, and increased spatial aggregation based on core area and NLSI. Observed relationships explained only 12-32 percent of the variance in the relationship between climate and the spatial aggregation of the high-severity fire; unexplained variance is likely due to unmeasured variables such fuel continuity and fire weather.

High-severity patch density increased with July temperature and decreased with July RH, which was opposite from the expected relationship. The observed increase in patch density may be because of this analysis was conducted based on study-wide burn-severity images. Warm dry climate increases the number of both very small high-severity patches (within all fires) and

extremely large high-severity patches (within very large fires). This pattern is related to the higher frequency of fires in warmer dryer years. On a per-fire basis, larger fires have lower patch density (Chapter 2) but when analyzed across the whole study area patch density increases with July temperature, presumably because the increased number of small fires with high patch density compensates for the increased fire sizes. In warm dry years, large fires may have extensive patches of high severity (i.e. increased proportion of high-severity core area), but spatially heterogeneous areas within the large fires area also created. There are also more spatially complex small and mid-sized fires in dry years. Overall, the relationship between climate and spatial pattern indicates that warm dry conditions create large patches of uniformly high severity, but these may be embedded in larger areas of mixed severity within individual fires, or may be offset by the creation of spatially complex burn severity patterns in other fires.

The analysis of topographical complexity showed consistent results, although the amount of variance explained by the regressions was low, and may have been limited by both the metrics used and the scale at which the analysis was conducted. Surface-to-area ratio may be a poor metric of topographic complexity in that it explained only 8-13% of the variation of selected burn-severity metrics (Figure 26). Better characterization of this complexity, or additional factors such as the heterogeneity of fuels and fire weather, may explain the variation within the burn-severity mosaic. Future research should examine topographic complexity across large regions (i.e. western North America) or within individual fires, such as was done with uncategorized burn-severity data, using variograms, by Duffy (2007). Lastly, relating burn severity directly with topography (*sensu* Holden et al. 2007), and then examining the climate and weather when those relationship do not hold, may be informative.

The influence of climate on fire size is more limited in topographically complex landscapes (Heyerdahl et al. 2001, Guyette et al. 2002, Kellogg et al. 2008), which have permanent barriers to fire spread, such as talus fields and cliff faces, and temporary barriers, such as slopes and aspects with fuel types and conditions that limit fire behavior. Based on the severity of the 1988 Yellowstone fires and simulation modeling, Turner and Romme (1994) proposed that under moderate climate, fuels mediate burn-severity pattern, but under very dry conditions all fuel types are available to burn, increasing landscape connectivity and making high-intensity fire likely.

My study suggests that climate and topographical complexity may be influencing different aspects of burn severity. Topographical complexity influences the interspersion and complexity of all burn-severity classes, whereas climate drivers mainly influenced the spatial aggregation of the high burn severity class. I can therefore propose that topography accentuates the interspersion of different burn-severity levels, whereas climate regulates the proportion of area burned at high severity, independently of spatial pattern, but by doing so increases the aggregation metrics within that class. Topography modifies the top-down effects of climate (Heyerdahl et al. 2001, Kellogg et al. 2008, Kennedy and McKenzie 2010), and the propensity for climate to override local controls (*sensu* Turner and Romme 1994) may depend on the local ecological context and the local physiographic setting; the greatest increases in fire size, severity, and spatial aggregation with climate change may occur in systems with less complex topography.

Given that larger and more severe fires are likely in the Pacific Northwest under future climate (Littell et al. 2010), burn-severity patterns found in this study can provide a baseline for estimating the degree of change in future landscape pattern. Examining the spatial patterns created by fire is also important because those patterns influence ecosystem processes, such as

the severity and timing of future disturbances, wildlife habitat suitability, and the composition and timing of post-fire succession. My results show that fires in the northern Cascade Range respond both to topographical controls and to large-scale annual climatic variation. A warmer and dryer future climate may override local controls, however, causing the size of fires and the spatial pattern of burn severity not to reflect endogenous controls (Kennedy and McKenzie 2010), but instead to be more homogeneous, with larger contiguous areas of high severity. These changes would in turn affect other ecosystem processes. The propensity for climate to override local controls is dependent on the local ecological context and the local physiographic setting; the greatest increases in fire size, high severity, and the spatial aggregation of high severity may occur in systems with more homogeneous fuel patterns and less complex topography. Continued investigation of how climate interacts with fuels and topography to influence within-fire spatial pattern of burn severity will allow better prediction of how landscape patterns may change under future climate.

REFERENCES

Baker, W. L., T. T. Veblen, and R. L. Sherriff. 2007. Fire, fuels and restoration of ponderosa pine-Douglas fir forests in the Rocky Mountains, USA. Journal of Biogeography **34**:251-269.

Brown, P. M., E. K. Heyerdahl, S. G. Kitchen, and M. H. Weber. 2008. Climate effects on historical fires (1630-1900) in Utah. International Journal of Wildland Fire **17**:28-39.

Duffy, P. A., J. Epting, J. M. Graham, T. S. Rupp, and A. D. McGuire. 2007. Analysis of Alaskan burn severity patterns using remotely sensed data. International Journal of Wildland Fire **16**:277-284.

Flannigan, M. D., M. A. Krawchuk, W. J. de Groot, B. M. Wotton, and L. M. Gowman. 2009. Implications of changing climate for global wildland fire. International Journal of Wildland Fire **18**:483-507.

Guyette, R. P., R. M. Muzika, and D. C. Dey. 2002. Dynamics of an anthropogenic fire regime. Ecosystems **5**:472-486

Haire, S. L. and K. McGarigal. 2009. Changes in fire severity across gradients of climate, fire size, and topography: a landscape ecology perspective. Fire Ecology **5**:86-103.

Heyerdahl, E. K., L. B. Brubaker, and J. K. Agee. 2001. Spatial controls of historical fire regimes: A multiscale example from the interior west, USA. Ecology **82**:660-678.

Heyerdahl, E. K., L. B. Brubaker, and J. K. Agee. 2002. Annual and decadal climate forcing of historical fire regimes in the interior Pacific Northwest, USA. Holocene **12**:597-604.

Heyerdahl, E. K., D. McKenzie, L. D. Daniels, A. E. Hessl, J. S. Littell, and N. J. Mantua. 2008. Climate drivers of regionally synchronous fires in the inland Northwest (1651-1900). International Journal of Wildland Fire **17**:40-49.

Holden, Z. A., P. Morgan, M. A. Crimmins, R. K. Steinhorst, and A. M. S. Smith. 2007. Fire season precipitation variability influences fire extent and severity in a large southwestern wilderness area, United States. Geophysical Research Letters **34**:1-5.

Holden, Z. A., P. Morgan, and J. S. Evans. 2009. A predictive model of burn severity based on 20-year satellite-inferred burn severity data in a large southwestern US wilderness area. Forest Ecology and Management **258**:2399-2406.

Jenness, J. S. 2004. Calculating landscape surface area from digital elevation models. Wildlife Society Bulletin **32**:829-839.

Keane, R. E., J. K. Agee, P. Fule, J. E. Keeley, C. Key, S. G. Kitchen, R. Miller, and L. A. Schulte. 2008. Ecological effects of large fires on US landscapes: benefit or catastrophe? International Journal of Wildland Fire **17**:696-712.

Kellogg, L. K. B., D. McKenzie, D. L. Peterson, and A. E. Hessl. 2008. Spatial models for inferring topographic controls on historical low-severity fire in the eastern Cascade Range of Washington, USA. Landscape Ecology **23**:227-240.

Kennedy, M. C. and D. McKenzie. 2010. Using a stochastic model and cross-scale analysis to evaluate controls on historical low-severity fire regimes. Landscape Ecology **25**:1561-1573.

Kitzberger, T., P. M. Brown, E. K. Heyerdahl, T. W. Swetnam, and T. T. Veblen. 2007. Contingent Pacific-Atlantic Ocean influence on multicentury wildfire synchrony over western North America. Proceedings of the National Academy of Sciences of the United States of America **104**:543-548.

Kutner, M. C., C. J. Nachtsheim, J. Neter, and W. Li. 2005. Applied Linear Statistical Models, 5th ed.:1396. McGraw-Hill, Boston.

Lentile, L. B., P. Morgan, A. T. Hudak, M. J. Bobbitt, S. A. Lewis, A. M. Smith, and P. R. Robichaud. 2007. Post-fire burn severity and vegetation response following eight large wildfires across the western United States. Fire Ecology **3**:91-101.

Littell, J. S., D. McKenzie, D. L. Peterson, and A. L. Westerling. 2009. Climate and wildfire area burned in western U. S. ecoprovinces, 1916-2003. Ecological Applications **19**:1003-1021.

Littell, J. S., E. E. Oneil, D. McKenzie, J. A. Hicke, J. A. Lutz, R. A. Norheim, and M. M. Elsner. 2010. Forest ecosystems, disturbance, and climatic change in Washington State, USA. Climatic Change **102**:129-158.

Lutz, J. A., J. W. van Wagtendonk, and J. F. Franklin. 2009a. Twentieth-century decline of large-diameter trees in Yosemite National Park, California, USA. Forest Ecology and Management **257**:2296-2307.

Lutz, J. A., J. W. van Wagtendonk, A. E. Thode, and J. D. Miller. 2009b. Climate, lightning ignitions, and fire severity in Yosemite National Park, California, USA. International Journal of Wildland Fire **19**:765-774.

Lutz, J. A., J. W. van Wagtendonk, A. E. Thode, J. D. Miller, and J. F. Franklin. 2009c. Climate, lightning ignitions, and fire severity in Yosemite National Park, California, USA. International Journal of Wildland Fire **18**:765-774.

McGarigal, K. S., A. Cushman, M. C. Neel, and E. Ene. 2002. FRAGSTATS: Spatial Pattern Analysis Program for Categorical Maps. Computer software program produced by the authors at the University of Massachusetts, Amherst. Available at the following web site: http://www.umass.edu/landeco/research/fragstats/fragstats.html.

McKenzie, D., Z. Gedalof, D. L. Peterson, and P. Mote. 2004. Climatic change, wildfire, and conservation. Conservation Biology **18**:890-902.

Miller, J. D. and A. E. Thode. 2007. Quantifying burn severity in a heterogeneous landscape with a relative version of the delta Normalized Burn Ratio (dNBR). Remote Sensing of Environment **109**:66-80.

Morgan, P., E. K. Heyerdahl, and C. E. Gibson. 2008. Multi-season climate synchronized forest fires throughout the 20th century, northern Rockies, USA. Ecology **89**:717-728.

Monitoring Trends in Burn Severity. 2008. Individual Fire-Level Geospatial Data - Monitoring Trends in Burn Severity (MTBS)<http://mtbs.gov/dataquery/individualfiredata.html> accessed: 3-01-2008.

R Development Core Team. 2010. R: A language and environment for statistical computing. R Foundation for Statistical Computing, Vienna, Austria. ISBN 3-900051-07-0, URL http://www.R-project.org/.

Roberts, S. L., J. W. van Wagtendonk, A. K. Miles, D. A. Kelt, and J. A. Lutz. 2008. Modeling the Effects of Fire Severity and Spatial Complexity on Small Mammals in Yosemite National Park, California. Fire Ecology Special Issue **4**:83-104.

Romme, W. H., M. G. Turner, L. L. Wallace, and J. S. Walker. 1995. Aspen, elk, and fire in Northern Yellowstone National Park. Ecology **76**:2097-2106.

Saab, V. A., J. Dudley, and W. L. Thompson. 2004. Factors influencing occupancy of nest cavities in recently burned forests. Condor **106**:20-36.

Schoennagel, T., T. T. Veblen, W. H. Romme, J. S. Sibold, and E. R. Cook. 2005. Enso and pdo variability affect drought-induced fire occurrence in Rocky Mountain subalpine forests. Ecological Applications **15**:2000-2014.

Turner, M. G., W. W. Hargrove, R. H. Gardner, and W. H. Romme. 1994. Effects of fire on landscape heterogeneity in Yellowstone National Park, Wyoming. Journal of Vegetation Science **5**:731-742.

Turner, M. G., W. H. Romme, and R. H. Gardner. 1999. Prefire heterogeneity, fire severity, and early postfire plant reestablishment in subalpine forests of Yellowstone National Park, Wyoming. International Journal of Wildland Fire **9**:21-36.

Turner, M. G., W. H. Romme, R. H. Gardner, and W. W. Hargrove. 1997. Effects of fire size and pattern on early succession in Yellowstone National Park. Ecological Monographs **67**:411-433.

Westerling, A. L., H. G. Hidalgo, D. R. Cayan, and T. W. Swetnam. 2006. Warming and earlier spring increase western US forest wildfire activity. Science **313**:940-943.

Zhu, Z., C. H. Key, D. Ohlen, and N. C. Benson. 2006. Evaluate sensitivities of burn severity mapping algorithms for different ecosystems and fire histories in the United States. Final Report to the Joint Fire Science Program. Project: JFSP 01-1-4-12.

FIGURES

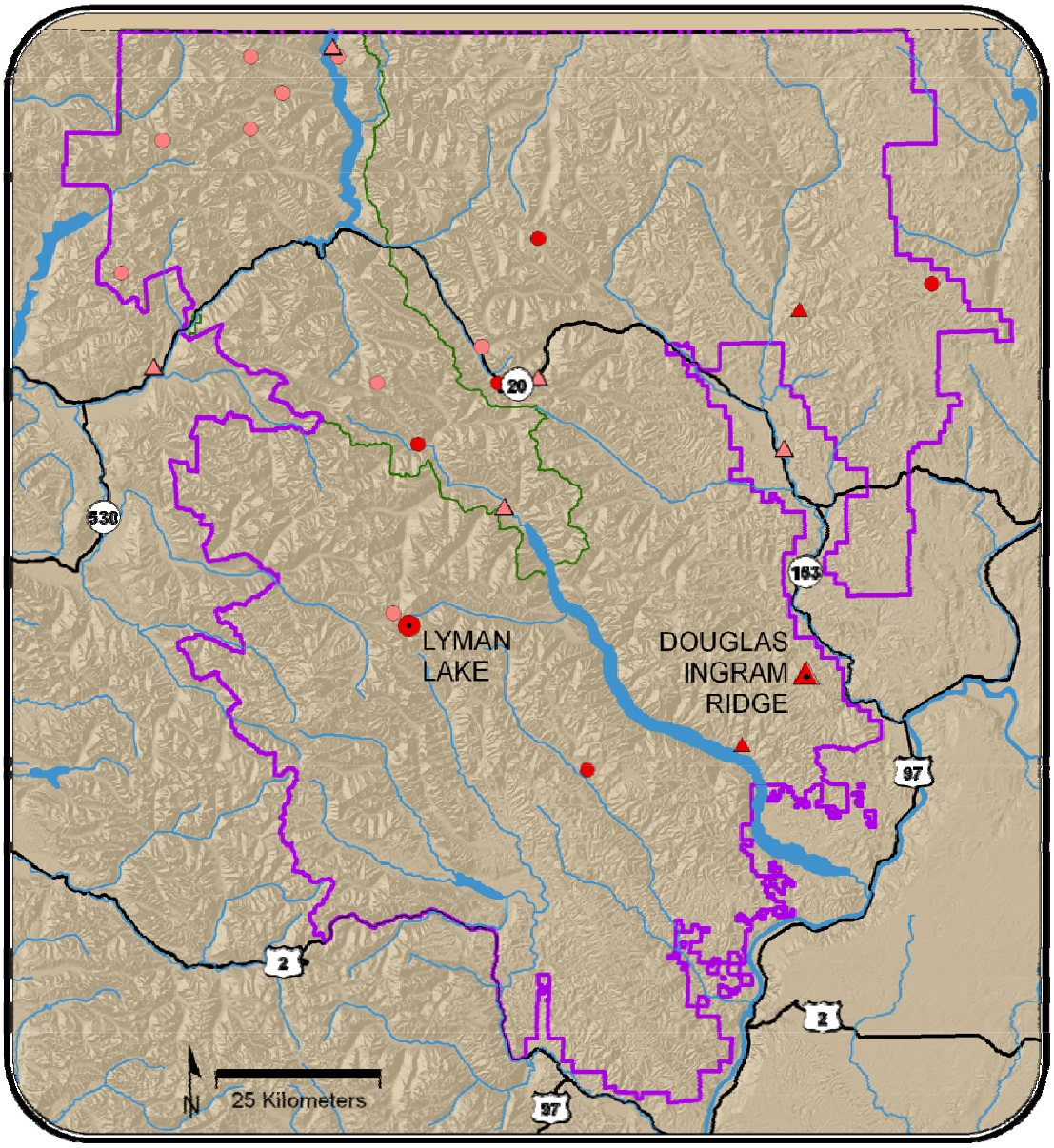

Figure 21. Climate stations within the study area.

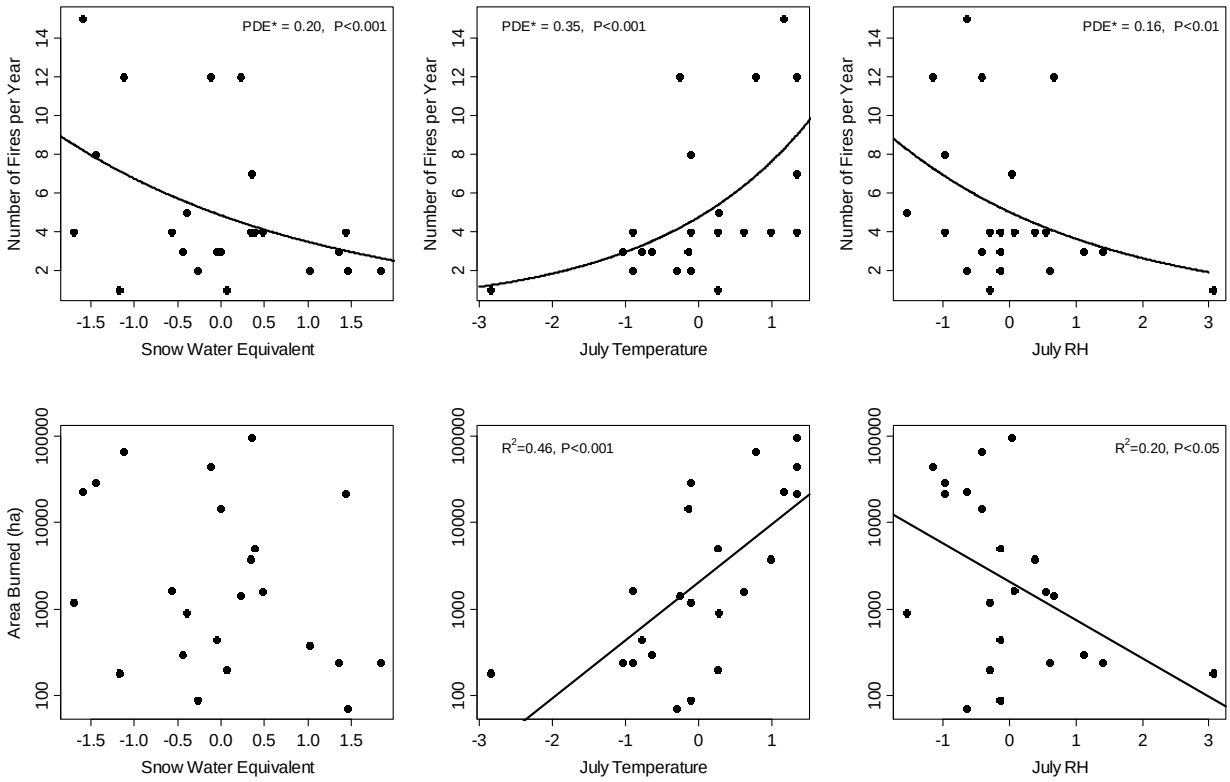

*PDE = Proportion of deviance explained in generalized linear models

Figure 22. Fire occurrence (top) and annual area burned (bottom) as functions of climate variables.

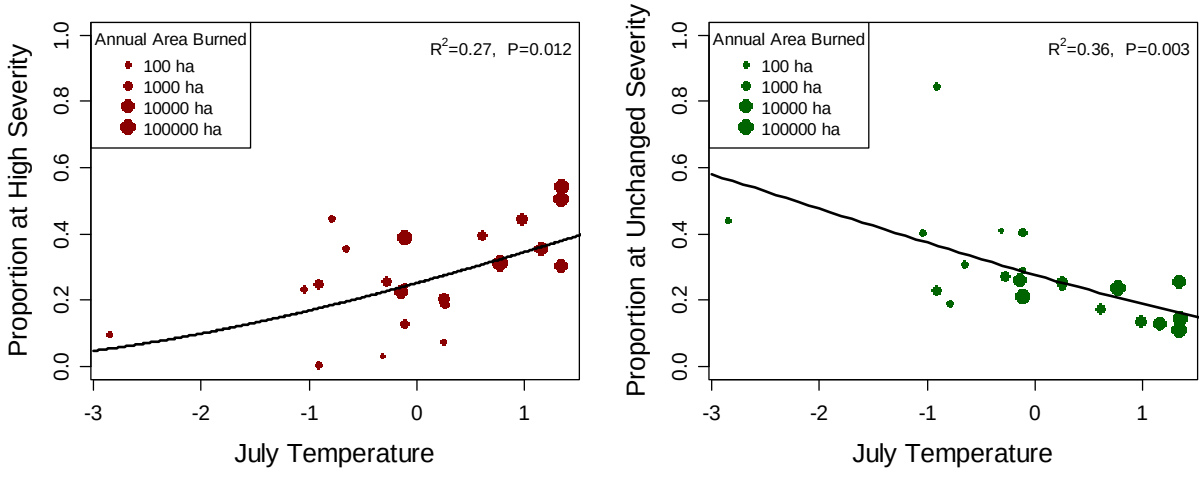

Figure 23. The proportion of area burned at high severity (left) and the proportion of unchanged area (right) as functions of July temperature.

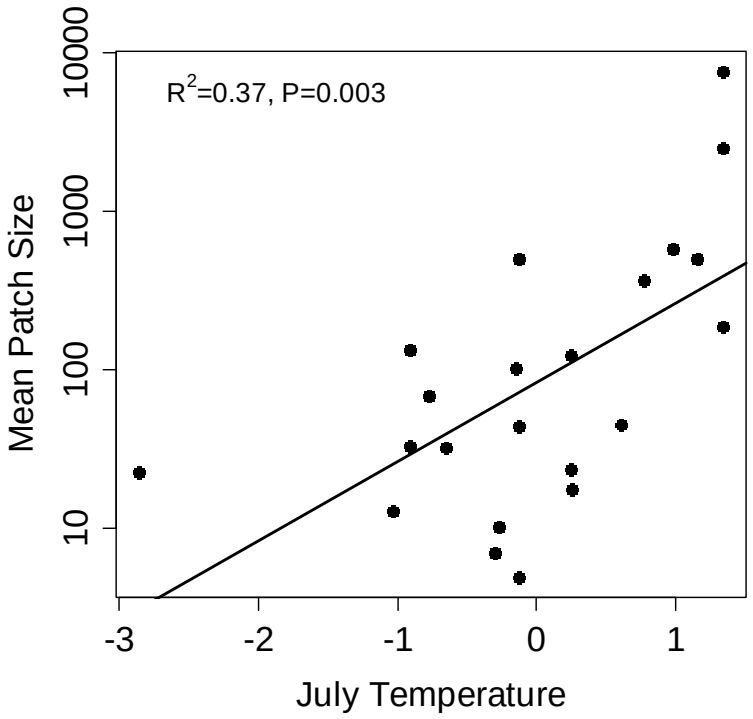

Figure 24. Mean patch size was positively correlated with July temperature.

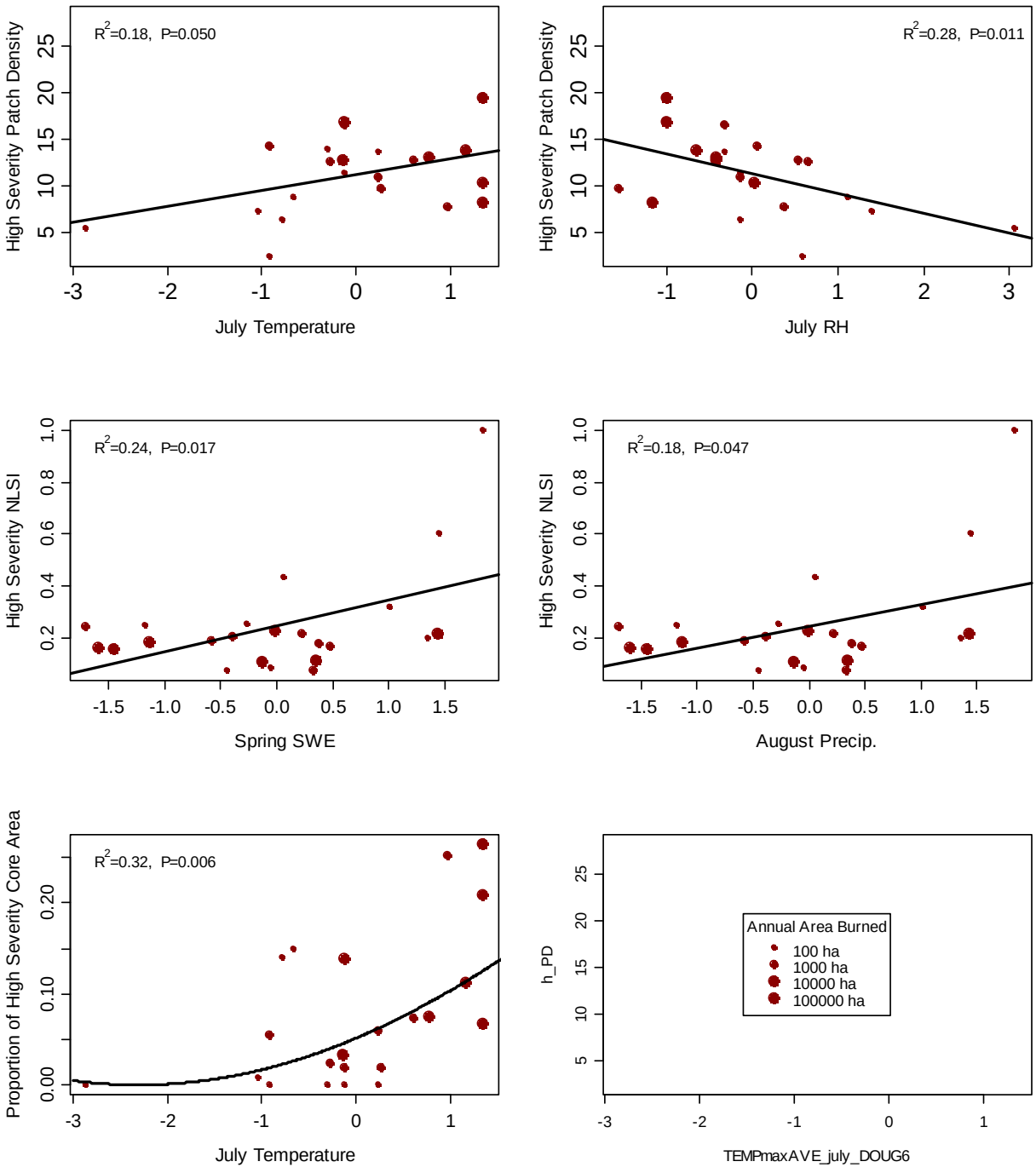

Figure 25. High-severity spatial pattern metrics as functions of climate variables.

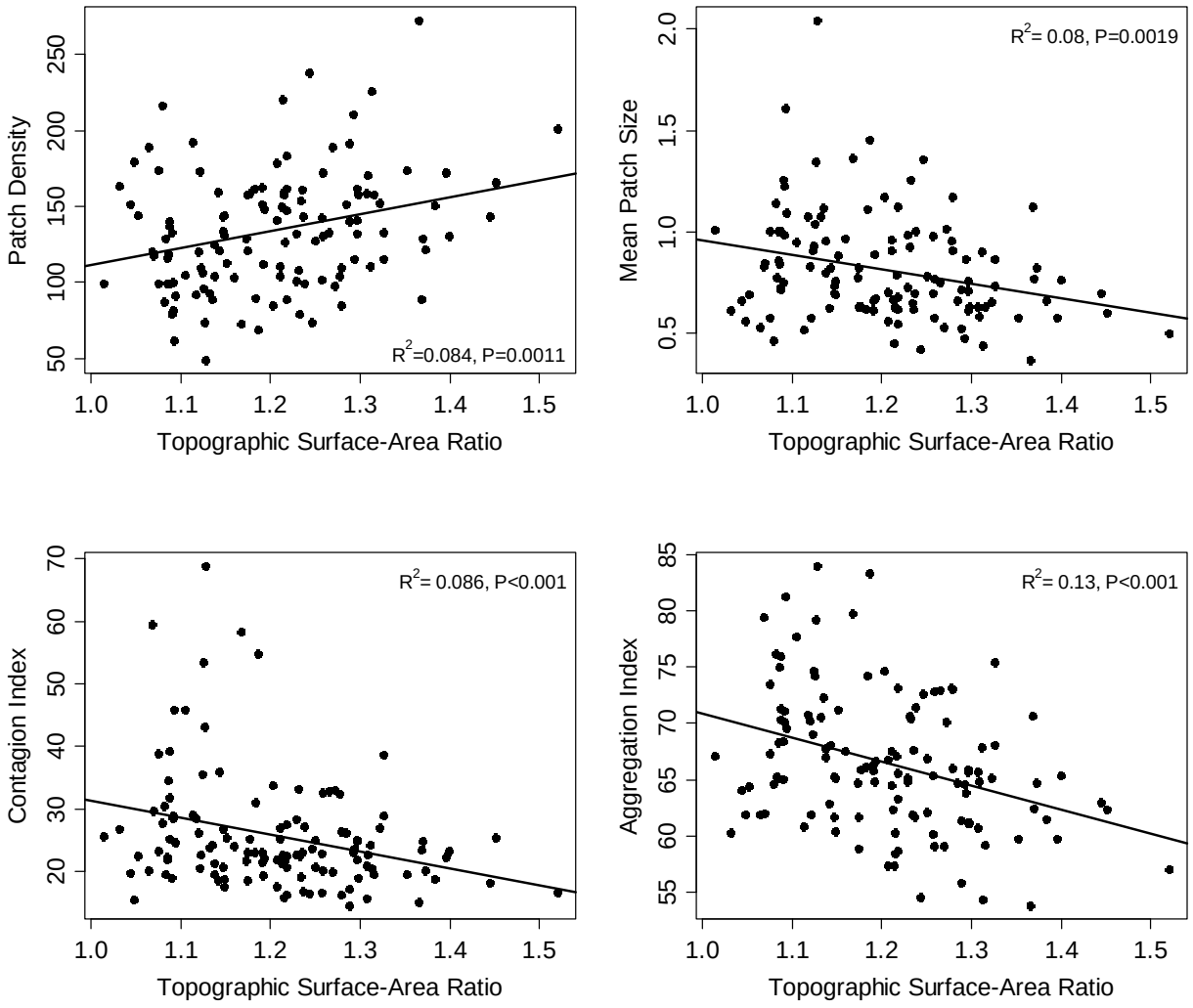

Figure 26. Landscape-level spatial-pattern metrics as a function of topographic complexity, as measured by the surface-to-area ratio in individual fires.

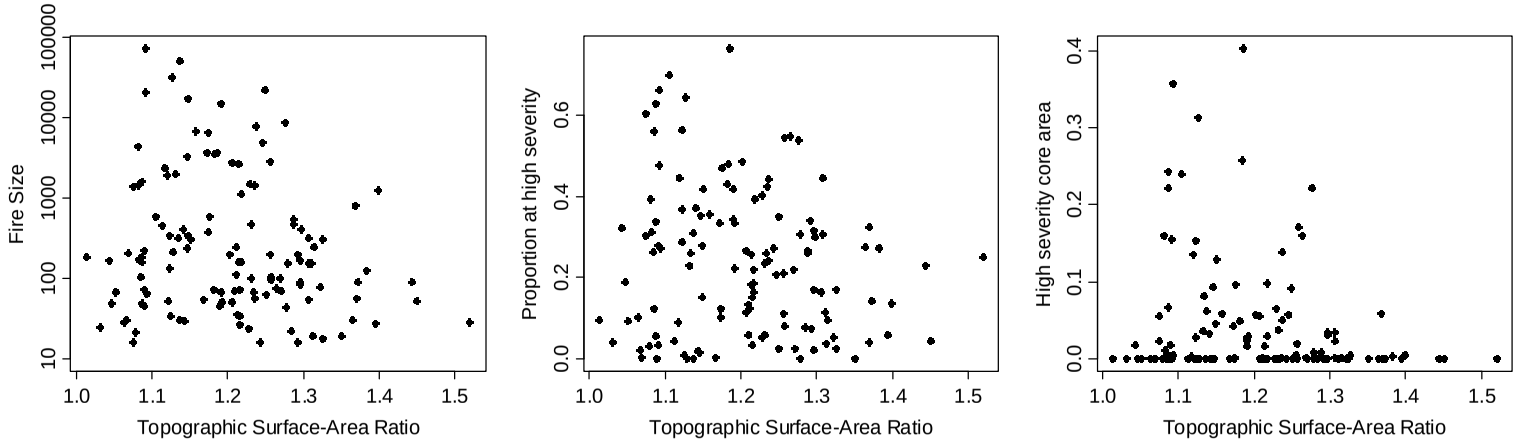

Figure 27. Fire size (left), proportion of high severity (center), and proportion of high-severity core area (right) plotted against topographical complexity. Visual examination (triangular pattern in scatterplot) suggests that high topographical complexity may limit maximum fire size, maximum proportion of high severity, and high-severity core area, even though linear relationships are weak.

APPENDIX I

Year	Name	Path	Row	Date of pre-fire image	Date of post-fire image	Ecological subsection	Fire size (ha)
1984	Maple Creek	45	26	7/28/1984	7/15/1985	North Cascades Highland Forests	62
1984	Swamp Creek	45	26	7/28/1984	7/15/1985	North Cascades Highland Forests	98
1984	Wellie	45	26	7/28/1984	7/15/1985	Pasayten-Sawtooth Highlands	245
1985	Butte Creek	45	26	7/28/1984	8/3/1986	Okanogan Pine-Fir Hills	46
1985	Cascade	45	26	7/28/1984	8/3/1986	Wenatchee-Chelan Highlands	158
1985	Hubbard CR	45	26	7/15/1985	8/3/1986	Pasayten-Sawtooth Highlands	2751
1985	Minie Mine	45	26	7/15/1985	8/3/1986	Okanogan Valley	1450
1985	Unnamed	45	27	8/13/1984	8/3/1986	Missoula Flood Channeled Scablands	203
1986	Blue	45	26	8/16/1985	8/22/1987	Okanogan Pine-Fir Hills	131
1986	Chance	45	26	8/16/1985	8/22/1987	Pasayten-Sawtooth Highlands	111
1986	Eureka	45	26	8/16/1985	8/22/1987	Pasayten-Sawtooth Highlands	1407
1986	Pelican Creek	45	26	8/16/1985	8/22/1987	Okanogan Pine-Fir Hills	16
1987	Dutton Creek	45	26	8/3/1986	7/23/1988	Pasayten-Sawtooth Highlands	103
1987	Mill Creek	45	26	8/3/1986	7/23/1988	North Cascades Highland Forests	195
1987	Reynolds	45	26	8/3/1986	7/23/1988	Pasayten-Sawtooth Highlands	197
1987	Sunny	45	26	8/3/1986	7/23/1988	Pasayten-Sawtooth Highlands	25
1987	Van Creek	45	27	6/19/1987	7/7/1999	Chelan Tephra Hills	383
1988	Dinkelman	45	27	7/23/1988	8/11/1989	Chelan Tephra Hills	14668
1988	Indian Creek	45	27	8/3/1986	8/3/1989	North Cascades Highland Forests	70
1988	Little Giant	45	27	8/3/1986	8/3/1989	North Cascades Highland Forests	51
1989	Hunter	45	27	8/7/2023	8/14/1990	Okanogan Valley	28
1989	Lodgepole	46	26	8/31/1988	9/6/1990	Pasayten-Sawtooth Highlands	343
1989	Unnamed	46	26	8/31/1988	9/6/1990	North Cascades Highland Forests	77
1990	Big Face	46	26	9/19/1989	9/25/1991	North Cascades Highland Forests	26
1990	Canoe Creek	45	27	9/12/1989	9/2/1991	Wenatchee-Chelan Highlands	249
1990	Devils Club	45	27	9/12/1989	9/2/1991	North Cascades Highland Forests	57
1990	Fisher Peak	46	26	9/19/1989	9/25/1991	North Cascades Highland Forests	16
1990	Freezeout	46	26	9/19/1989	9/25/1991	North Cascades Highland Forests	75
1990	McAllister	46	26	9/19/1989	9/25/1991	North Cascades Lowland Forests	153
1990	Meadows	46	26	9/19/1989	9/25/1991	North Cascades Highland Forests	29
1990	Pistol	46	26	9/19/1989	9/25/1991	Pasayten-Sawtooth Highlands	72
1990	Swamp Creek	46	26	9/19/1989	9/25/1991	North Cascades Highland Forests	156
1990	Unnamed	45	27	9/12/1989	9/2/1991	North Cascades Highland Forests	22
1990	West Joke	46	26	9/19/1989	9/25/1991	North Cascades Highland Forests	51

1990	White River	45	27	8/11/1989	8/1/1991	North Cascades Highland Forests	534
1991	Unnamed1	45	27	8/14/1990	8/3/1992	Chelan Tephra Hills	34
1991	Unnamed2	45	27	8/14/1990	8/3/1992	Chelan Tephra Hills	209
1992	McCay	45	26	9/2/1991	9/7/1993	Pasayten-Sawtooth Highlands	182
1992	McFarland	45	26	9/18/1991	9/7/1993	Okanogan Valley	31
1992	War Creek	45	26	9/2/1991	9/7/1993	Pasayten-Sawtooth Highlands	83
1993	Unknown	45	27	8/3/1992	7/24/1994	Chiwaukum Hills and Lowlands	181
1994	Butte Creek	45	26	7/18/1992	7/27/1995	Wenatchee-Chelan Highlands	2625
1994	Falls Creek	45	26	9/7/1993	9/13/1995	North Cascades Highland Forests	56
1994	Gold Creek	45	26	9/7/1993	9/13/1995	Okanogan Pine-Fir Hills	30
1994	Poorman	45	26	9/7/1993	9/13/1995	Okanogan Pine-Fir Hills	341
1994	Round Mountain	46	27	7/15/1994	7/18/1995	Chiwaukum Hills and Lowlands	1376
1994	Stub Creek	45	26	9/2/1991	9/13/1995	Pasayten-Sawtooth Highlands	308
1994	Threemile	45	26	9/7/1993	9/13/1995	Pasayten-Sawtooth Highlands	45
1994	Thunder	45	26	7/8/1994	7/27/1995	Pasayten-Sawtooth Highlands	4339
1994	Tommy Creek	45	27	9/7/1993	9/13/1995	Chelan Tephra Hills	48
1994	Tyee Creek	45	27	7/24/1994	7/25/1995	Chelan Tephra Hills	50027
1994	Unnamed	45	27	9/7/1993	9/13/1995	Chelan Tephra Hills	34
1994	Whiteface	46	26	7/18/1992	7/18/1995	Pasayten-Sawtooth Highlands	1614
1995	Pot Peak	45	27	7/24/1994	7/13/1996	Chelan Tephra Hills	67
1995	Prince Creek	45	27	7/24/1994	7/13/1996	Wenatchee-Chelan Highlands	317
1996	Elbow Basin	46	26	7/18/1995	9/25/1997	North Cascades Highland Forests	1477
1996	Myrtle	45	27	9/13/1995	9/2/1997	North Cascades Highland Forests	70
1996	Old Guard	45	26	9/13/1995	9/2/1997	North Cascades Highland Forests	30
1996	Preston	45	27	9/13/1995	9/2/1997	Chelan Tephra Hills	16
1997	Borealis	46	26	8/21/1996	8/27/1998	North Cascades Highland Forests	10
1997	Fools	46	26	8/21/1996	8/27/1998	North Cascades Highland Forests	67
1997	Redoubt	46	26	8/21/1996	8/27/1998	North Cascades Lowland Forests	167
1998	Cinnamon	45	26	9/2/1997	9/8/1999	North Cascades Highland Forests	72
1998	Corral	45	27	8/4/1998	8/23/1999	Chelan Tephra Hills	21
1998	North 25 mile	45	27	8/1/1997	7/22/1999	Chelan Tephra Hills	3517
1998	Unnamed	45	27	8/4/1998	8/23/1999	Chelan Tephra Hills	236
1999	McMillan	46	26	8/27/1998	8/16/2000	North Cascades Highland Forests	52
1999	Miner	45	27	8/4/1998	8/1/2000	Wenatchee-Chelan Highlands	19
2000	Flat Creek	46	26	8/22/1999	8/11/2001	North Cascades Highland Forests	198
2001	Thirtymile	45	26	7/16/2000	7/14/2002	Pasayten-Sawtooth Highlands	3692
2001	Boundary	45	26	7/16/2000	7/14/2002	Pasayten-Sawtooth Highlands	172

2001	Glory Mountain	45	26	8/8/2000	8/14/2002	North Cascades Highland Forests	399
2001	Libby South	45	26	5/24/2001	8/20/2001	Okanogan Pine-Fir Hills	1960
2001	Long Swamp	45	26	7/16/2000	7/14/2002	Pasayten-Sawtooth Highlands	161
2001	Rex Creek Complex	45	27	7/22/1999	7/14/2002	Wenatchee-Chelan Highlands	22036
2001	Tommy Creek	45	27	8/1/2000	7/22/2002	Wenatchee-Chelan Highlands	314
2001	Windy Peak	45	26	7/16/2000	7/14/2002	Pasayten-Sawtooth Highlands	167
2002	Deer Point	45	27	7/27/2001	7/12/2003	Chelan Tephra Hills	16734
2002	Middle Mountain	46	26	8/14/2002	7/24/2003	Pasayten-Sawtooth Highlands	3307
2002	Mount David	45	27	8/12/2001	8/18/2003	North Cascades Highland Forests	24
2002	Quartz Creek	46	26	8/14/2002	7/24/2003	Pasayten-Sawtooth Highlands	1909
2003	Big Beaver	46	26	8/14/2002	8/11/2004	North Cascades Highland Forests	802
2003	Bottle Springs	45	26	8/31/2002	8/20/2004	Pasayten-Sawtooth Highlands	68
2003	Dome Creek	45	26	8/31/2002	8/20/2004	North Cascades Highland Forests	125
2003	Farewell	46	26	7/27/2001	8/11/2004	Pasayten-Sawtooth Highlands	31338
2003	Isabel	45	26	7/16/2000	8/20/2004	Pasayten-Sawtooth Highlands	2328
2003	Maple 2	45	27	7/14/2002	8/20/2004	North Cascades Highland Forests	1105
2003	Mineral Park	46	26	7/24/2003	7/26/2004	North Cascades Highland Forests	1220
2003	Needles	46	26	7/24/2003	7/26/2004	Pasayten-Sawtooth Highlands	7743
2003	No Name	46	26	7/24/2003	7/26/2004	North Cascades Highland Forests	301
2003	Sonny Boy	46	26	8/14/2002	8/11/2004	North Cascades Highland Forests	100
2003	Sweetgrass	45	26	9/8/1999	9/21/2004	Pasayten-Sawtooth Highlands	72
2003	Tricouni	46	26	8/14/2002	8/11/2004	North Cascades Highland Forests	89
2004	Deep Harbor	45	27	7/17/2003	8/7/2005	Wenatchee-Chelan Highlands	8537
2004	Dirtyface	45	27	8/18/2003	8/7/2005	North Cascades Highland Forests	91
2004	Downy	46	26	7/24/2003	7/29/2005	North Cascades Highland Forests	91
2004	Fisher	45	27	7/17/2003	8/7/2005	Chiwaukum Hills and Lowlands	6553
2004	Freezout	46	26	7/24/2003	7/29/2005	North Cascades Highland Forests	467
2004	Little Beaver	46	26	7/24/2003	7/29/2005	North Cascades Lowland Forests	28
2004	McMillan	46	26	7/24/2003	7/29/2005	North Cascades Highland Forests	54
2004	Mebee	46	26	7/24/2003	7/29/2005	North Cascades Highland Forests	104
2004	New Halem	46	26	7/24/2003	7/29/2005	North Cascades Lowland Forests	27
2004	Papoose	45	27	8/18/2003	8/7/2005	North Cascades Highland Forests	44
2004	Perry	46	26	7/24/2003	7/29/2005	North Cascades Lowland Forests	18
2004	Pot Peak	45	27	7/17/2003	8/7/2005	Chelan Tephra Hills	6685
2004	Sisi Ridge	46	26	7/24/2003	7/29/2005	North Cascades Highland Forests	161
2004	Trinity	45	27	8/18/2003	8/7/2005	North Cascades Highland Forests	19
2004	Williams Butte	45	27	8/18/2003	8/7/2005	Pasayten-Sawtooth Highlands	398
2005	Dirtyface	45	27	8/18/2003	8/26/2006	Wenatchee-Chelan Highlands	466

2005	Pearrygin Lake	45	26	8/20/2004	8/26/2006	Okanogan Pine-Fir Hills	218
2005	Shady	45	26	8/20/2004	8/26/2006	North Cascades Highland Forests	64
2005	Squaw Creek	45	27	7/17/2003	7/25/2006	Okanogan Valley	449
2006	Cedar Creek	45	26	8/7/2005	7/25/2007	Pasayten-Sawtooth Highlands	573
2006	Flick Creek	46	26	8/7/2005	7/28/2007	Wenatchee-Chelan Highlands	2856
2006	Tatoosh Complex	46	26	8/7/2005	7/28/2007	Pasayten-Sawtooth Highlands	20072
2006	Tin Pan	45	27	8/7/2005	9/14/2001	Wenatchee-Chelan Highlands	3660
2006	Tripod Complex	46	26	8/7/2005	7/28/2007	Pasayten-Sawtooth Highlands	70754
2006	Unnamed	45	27	8/7/2005	8/13/2007	North Cascades Highland Forests	55
2006	Van Peak	46	26	8/7/2005	7/28/2007	Pasayten-Sawtooth Highlands	578
2007	Domkey Lake	45	27	7/25/2006	7/14/2008	Wenatchee-Chelan Highlands	4842
2007	Glory	45	26	7/25/2006	7/14/2008	Okanogan Valley	48
2007	Panther Creek	45	27	8/26/2006	8/15/2008	North Cascades Highland Forests	97
2007	Tolo	45	26	7/25/2006	7/14/2008	North Cascades Highland Forests	152
2008	Arctic Creek	46	26	9/2/2006	9/10/2009	North Cascades Highland Forests	35
2008	Camel Humps	46	26	9/2/2006	9/10/2009	Pasayten-Sawtooth Highlands	53